

**PREPARATION AND CHARACTERIZATION OF
POLYMERIC SCAFFOLDS FOR NERVE TISSUE
ENGINEERING APPLICATIONS**

**A Thesis Submitted to
the Graduate School of Engineering and Sciences of
İzmir Institute of Technology
in Partial Fulfillment of the Requirements for the Degree of**

DOCTOR OF PHILOSOPHY

in Bioengineering

**by
Melda BÜYÜKÖZ**

**December 2014
İZMİR**

We approve the thesis of **Melda BÜYÜKÖZ**

Examining Committee Members:

Prof. Dr. Sacide ALSOY ALTINKAYA

Department of Chemical Engineering, Izmir Institute of Technology

Prof. Dr. Neşe ATABEY

Department of Medical Biology, Dokuz Eylul University

Prof. Dr. Volga BULMUŞ

Department of Chemical Engineering, Izmir Institute of Technology

Prof. Dr. Şermin GENÇ

Department of Neuroscience, Dokuz Eylul University

Assist. Prof. Dr. Ayben TOP

Department of Chemical Engineering, Izmir Institute of Technology

17 December 2014

Prof. Dr. Sacide ALSOY ALTINKAYA

Supervisor, Department of Chemical Engineering, Izmir Institute of Technology

Prof. Dr. Esra ERDAL

Co-Supervisor, Department of Medical Biology, Dokuz Eylul University

Prof. Dr. Volga BULMUŞ

Head of Department of Biotechnology and Bioengineering

Prof. Dr. Bilge KARAÇALI

Dean of the Graduate School of Engineering Science

ACKNOWLEDGEMENTS

I am especially grateful to my advisor Prof. Dr. Sacide Alsoy Altınkaya and my co-advisor Prof. Dr. Esra Erdal for their guidance, support, motivation and encouragement during my thesis.

I want to thank my laboratory colleagues, Filiz Yaşar Mahlıçlı, Metin Uz, Bahar Başak Pekşen, Pelin Oymacı from Izmir Institute of Technology; Sanem Tercan Avcı, Emine Kandemis, Evin Özen, Eren Şahin, Deniz Balcı from Dokuz Eylul University for their support and help in lab experiences.

I would like to thank Alev Güneş Yerkesikli, İpek Erdoğan, Mehmet Emin Uslu, Özge Tuncel, Seda Güneş, Sedef Tamburacı for their frendship during long working hours.

I am eternally grateful for the unconditionally support and encouragement of my family. I would like to express my special thank to my husband Mustafa İlker Büyüköz for him endless support and encouragement during my education and thesis.

This thesis was supported by The Scientific and Technological Research Council of Turkey (Grant # 112M568).

ABSTRACT

PREPARATION AND CHARACTERIZATION OF POLYMERIC SCAFFOLDS FOR NERVE TISSUE ENGINEERING APPLICATIONS

The major goal in tissue engineering is to develop three-dimensional biomimetic scaffolds which can provide an optimal environment for cell adhesion, proliferation, differentiation and guide new tissue formation. In this study macroporous, nanofibrous gelatin scaffolds in the form of a disc and channeled conduit were prepared for nerve tissue engineering applications. Alginate microspheres have been integrated into the scaffolds to deliver nerve growth factor (NGF) to differentiate PC12 cells. Methods combining thermally induced phase separation technique with porogen leaching and injection molding were used to manufacture disc shaped and channeled nanofibrous scaffolds, respectively. Microcarriers loaded with NGF were fabricated by water-in-oil emulsification technique and attached in the scaffold by chemical crosslinking with carbodiimide reaction. The relationship among processing parameter, porosity, pore size, interpore connectivity and the mechanical properties were investigated. In addition release kinetics of NGF from the particles were determined and viability, proliferation and differentiation of PC12 cells in the scaffolds were evaluated. The fiber sizes of nanofibrous scaffolds were found similar to the size of natural collagen fiber bundles. In nanofibrous scaffolds, the dimensional stability and in vitro degradation rates improved when compared to solid walled scaffolds. The release rate of NGF from the particles was controlled by the alginate concentration and poly(L-lysine) coating. Integrating NGF into the nanofibrous gelatin scaffold in encapsulated form reduced amount of NGF and time required for the differentiation of PC12 compared to free NGF directly added to the cells.

ÖZET

SİNİR DOKU MÜHENDİSLİĞİ UYGULAMALARINDA KULLANILMAK ÜZERE POLİMERİK DOKU İSKELELERİNİN HAZIRLANMASI VE KARAKTERİZASYONU

Doku mühendisliği çalışmalarında hedef; hücre tutunması, çoğalması, farklılaşması ve yeni doku oluşumunda hücrelerin yönlendirilmesini sağlayacak üç boyutlu ve biyolojik yapıyı taklit eden doku iskelelerinin geliştirilmesidir. Bu çalışmada sinir doku mühendisliği uygulamalarında kullanılmak üzere 2 farklı formda nanolifli jelatin doku iskeleleri üretilmiştir. Birinci tip doku iskelesi beyin doku mühendisliği çalışmalarında kullanılmak üzere disk şeklinde, ikinci tip ise çevresel sinir sistemi hasarlarında kullanılmak üzere kanallı yapıda ve boru şeklinde üretilmiştir. Model hücre hattı PC12 hücrelerinin farklılaşmasını sağlamak için sinir büyüme faktörü (NGF) yüklü alginat mikroküreler doku iskelelerine tutturulmuştur. Isı etkili faz ayrımı ve parçacık uzaklaştırma tekniği ile ısı etkili faz ayrımı ve kalıplama tekniği sırasıyla, disk ve kanallı yapıdaki doku iskelelerinin üretiminde kullanılan tekniklerdir. NGF yüklü kürelerin üretiminde yağ içinde su emülsiyonu tekniği kullanılmış ve bu küreler karbodiimid reaksiyonu ile doku iskelelerine tutturulmuştur. Hazırlanan doku iskeleleri üretim parametreleri, gözenekliliği, gözenek boyutu, gözenekler arası bağlantısı ve mekanik özellikleri açısından incelenmiştir. Ayrıca NGF' in mikrokürelerden salım kinetiği belirlenmiş, PC12 hücrelerinin doku iskelesi üzerinde çoğalması ve farklılaşması incelenmiştir. Üretilen nanolifli yapıdaki doku iskelelerinin doğal kollajen dokunun sahip olduğu lifler ile benzer lif çapına sahip olduğu belirlenmiştir. Katı duvarlı doku iskeleleri ile karşılaştırıldığında nanolifli doku iskelelerinde bütünlüğün ve *in vitro* parçalanma oranlarının geliştirildiği gözlenmiştir. NGF' in alginat küreciklerden salımının polimer konsantrasyonu ve kürelerin poly(L-lisin) kaplanması ile sağlanabildiği belirlenmiştir. NGF, enkapsule edilmiş bir şekilde nanolifli doku iskelesine tutturulduğunda PC12 hücrelerinin farklılaşması için gerekli olan miktarının serbest olarak eklenen NGF miktarına göre daha az olduğu ve farklılaşma süresinin de daha kısa olduğu belirlenmiştir.

TABLE OF CONTENTS

LIST OF FIGURES.....	ix
LIST OF TABLE.....	xiv
CHAPTER 1. INTRODUCTION.....	1
CHAPTER 2. TISSUE ENGINEERING.....	5
2.1. Tissue Engineering Scaffold.....	5
2.1.1. Thermally Induced Phase Separation.....	6
2.1.2. Other Methods Used for Fabricating Scaffolds.....	8
2.1.3. Materials Used For Fabricating Scaffolds.....	10
2.2. Biologically Active Molecules.....	11
2.2.1. Emulsification-Solidification Method Used for Encapsulating Biologically Active Agents.....	14
2.2.2. Other Methods Used for Encapsulating Biologically Active Agents.....	15
2.3. Cells.....	16
2.4. Nerve Tissue Engineering.....	19
CHAPTER 3. EXPERIMENTAL.....	24
3.1. Materials.....	24
3.2. Molding.....	24
3.3. Preparation of Paraffin Spheres.....	25
3.4. Preparation of Gelatin Scaffolds.....	26
3.4.1. Preparation of Nanofibrous Scaffolds.....	26
3.4.2. Preparation of Solid-Walled (SW) Scaffolds.....	27
3.5. Preparation of Channeled Nanofibrous Scaffolds.....	27
3.6. Chemical Crosslinking of 3D NF and SW Gelatin Scaffolds.....	27
3.6.1. Ninhydrin Assay.....	28
3.6.2. Determination of Swelling Ratio.....	29
	vi

3.7. Characterization.....	29
3.7.1. Surface Morphology Examination.....	29
3.7.2. Porosity.....	30
3.7.3. Swelling Volume Ratio Measurement.....	30
3.7.4. Mechanical Test.....	30
3.8. In vitro Degradation of Scaffolds with MMP-9 Enzyme.....	31
3.9. Preparation of Alginate Microspheres.....	31
3.10. Determination of NGF Loading and Release from Alginate Microspheres.....	32
3.11. Attachment of Alginate Microspheres onto Gelatin Scaffold and Release of NGF from the Scaffolds.....	32
3.12. In vitro Cell Culture.....	34
3.12.1. Determination of Growth Curve for PC12 Cells.....	34
3.12.2. Determination of NFG Amount for the Differentiation of PC12 Cells.....	34
3.12.3. Determination of Attachment and Proliferation of PC12 Cell onto Gelatin Scaffold.....	35
3.13. Determination Bioactivity of Released NGF from Alginate Microspheres.....	36
3.14. Determination of PC12 Cell Differentiation on the NGF Loaded Alginate Microspheres Attached Nanofibrous Gelatin Scaffold....	36
3.15. Statistical Analysis.....	36
 CHAPTER 4. RESULTS AND DISCUSSIONS.....	 37
4.1. Preparation and Characterization of Macroporous Nanofibrous and Solid-Walled Scaffolds.....	37
4.1.1. Preparation of Porogen Agent.....	37
4.1.2. Preparation of Nanofibrous and Solid Walled Scaffolds.....	40
4.1.3. Chemical Crosslinking of Nanofibrous and Solid Walled Scaffolds.....	44
4.1.4. Characterization of Macroporous Solid Walled and Nanofibrous Scaffolds.....	46
4.1.4.1. Porosity.....	46
	vii

4.1.4.2. Fiber Length and Diameter.....	47
4.1.4.3. Swelling Volume Ratio.....	49
4.1.4.4. Mechanical Properties.....	50
4.1.4.5. <i>In vitro</i> Degradation of Scaffolds.....	52
4.2. Preparation and Characterization of Channeled Nanofibrous Gelatin Scaffolds.....	53
4.3. Preparation of NGF Loaded Alginate Microspheres.....	59
4.3.1. NGF Loading to the Ca-alginate Microspheres.....	63
4.3.2. Attachment of NGF Loaded Alginate Microspheres into Macroporous Gelatin Scaffold.....	64
4.3.3. NGF Release from Alginate Microspheres.....	65
4.4. PC12 Cell Culture.....	68
4.4.1. Growth Curve of PC12 Cells.....	69
4.4.2. Determination Amount of Free NGF Required for Differentiation of PC12 Cell.....	71
4.4.3. Cell Attachment.....	74
4.4.4. PC12 Cell Proliferation onto Alginate Microspheres Attached NF Gelatin Scaffolds.....	75
4.4.5. Determination of NGF Bioactivity.....	76
4.4.6. Determination of PC12 Cell Differentiation onto NGF Loaded Alginate Microspheres Attached Nanofibrous Gelatin Scaffold.....	77
 CHAPTER 5. CONCLUSION.....	 82
 REFERENCES.....	 84
 APPENDICES	
APPENDIX A. CALCULATION OF EDC, NHS, COOHFREE AND ACETONE AMOUNTS REQUIRED FOR CROSSLINKING REACTION.....	94
APPENDIX B. PROCEDURE FOR COATING CA-ALGINATE MICROSPHERES WITH POLY(L-LYSINE).....	97

LIST OF FIGURES

<u>Figure</u>	<u>Page</u>
Figure 2.1. The general perspective of tissue engineering (Source: Stamatialis 2008).....	5
Figure 2.2. Binary phase diagram of a polymer solution with TIPS properties (Source: Yang et al. 2004).....	7
Figure 2.3. Different forms of polymeric scaffolds for tissue engineering (Source: Chung and Park 2007).....	11
Figure 2.4. Model of biomimetic nanoscaffold system with interconnected macropores, nanofiber matrix structure and growth factor loaded micro/nanospheres (Source: Ma 2004).....	13
Figure 2.5. Water soluble polymer and protein in the form of microspheres after solidification in W/O emulsion process (Source: Wang et al. 2013).....	15
Figure 2.6. Structural repair strategies used for improving existing hollow nerve guidance conduits (Source: Daly et al. 2012).....	23
Figure 3.1. Custom made 20 well Teflon mold.....	25
Figure 3.2. Appearance of the teflon molds with different number of needles.....	27
Figure 3.3. Crosslinking reaction of gelatin (I) with EDC (II) and NHS (III), (IV is isourea byproduct).....	28
Figure 3.4. Crosslinking of alginate and gelatin in the presence of EDC (Source: Hermanson 1996).....	33
Figure 4.1. SEM micrographs of paraffin particles prepared with 578 rpm stirring rate and different concentration of PVA. a- 0.5 %, b- 0.75 %, c- 1.0 %.....	38
Figure 4.2. SEM pictures of paraffin spheres with a magnification of A-150X, B- 400X and C- Phase contrast microscope images of paraffin spheres produced in 600 ml solution containing 1% PVA and stirred at a rate of 578 rpm.....	39
Figure 4.3. Particle size distribution of paraffin spheres obtained from the three different batches.....	40

Figure 4.4. SEM images of the solid walled scaffolds with different pre-heat treatment times; a- 20 min, b-50 min, c-200 min, d-400 min at 37°C.....	41
Figure 4.5. General appearance of NF(left) and SW(right) scaffolds.....	42
Figure 4.6. SEM micrographs of SW-gelatin and NF-gelatin scaffolds, a-Solid-walled gelatin scaffold, x500; b- pore wall morphology of solid-walled scaffold, x5,000; c- NF-gelatin scaffold, x500; d- NF-gelatin scaffold, x2500.....	43
Figure 4.7. NF scaffolds prepared with 10% gelatin concentration and a-c; 250-425 μm , d-f; 425-600 μm paraffin spheres. Preheating times; 400 min.....	43
Figure 4.8. a- Cross-linked nanofibrous scaffold according to EDC: gelatin (5: 1) (w/w), b- Cross-linked NF-scaffold according to EDC: $\text{COOH}_{\text{gelatin}}$ (2: 1) (mole/mole).....	44
Figure 4.9. Effect of increasing ratio of EDC/ $\text{COOH}_{\text{free}}$ (mol/mol) on absorbance value.....	45
Figure 4.10. Swelling ratio of crosslinked gelatin scaffolds in phosphate buffer at room temperature. The molar ratio of NHS to EDC was 0.2.....	46
Figure 4.11. Schematic phase diagram for temperature induced phase separation (Source: Yang et al. 2004).....	48
Figure 4.12. Scaffold prepared with TIPS a- 5% gelatin solution X5000, b- Schematic phase diagram of polymer solution (Source: Yang et al. 2004), c- 10% gelatin solution X5000, d- 10% gelatin solution X20000 preheating times 200 min.....	48
Figure 4.13. Swelling volume ratio of NF and SW scaffolds after crosslinking in acetone: water ratio of 90/10 (v/v) solution and EDC: $\text{COOH}_{\text{gelatin}}$ (mole/mole) ratio of 2:1.....	49
Figure 4.14. Stress-strain curves from the mechanical test A; Solid-walled, B; Nanofibrous scaffolds.....	50
Figure 4.15. The effects of interconnection time on compressive modulus of solid walled and nanofiber scaffolds prepared with 10% gelatin solution.....	51

Figure 4.16. Degradation percent of solid walled and nanofibrous scaffold in PBS and MMP-9 included PBS.....	52
Figure 4.17. General appearance of mold and prepared scaffold.....	53
Figure 4.18. SEM micrograph of four channel solid walled gelatin scaffold prepared from 5% (w/v) gelatin solution at -80°C a; vertical crosssection, b; horizontal cross-section with channel structure, c; tubular microchannels structures.....	54
Figure 4.19. Nano-fibrous scaffold prepared from different concentration of gelatin solution at +4 °C.....	55
Figure 4.20. Gelatin scaffolds prepared with a; 40/60 (v/v), b; 30/70, c; 20/80, d; 10/90 ethanol/water solution. All examples gelatin concentration was 5% (w/v) and phase separation was -20°C.....	56
Figure 4.21. Mechanical properties of nanofiber gelatin matrix in terms of a; Young's Modulus, b; Ultimate tensile strength.....	58
Figure 4.22. Nanofibrous gelatin conduit with a-c; one channeled, d; 4 channeled and e; 7 channeled prepared from 5% gelatin solution in 70/30 water/ethanol and phase separated at -20°C.....	59
Figure 4.23. Diameter of alginate microspheres.....	61
Figure 4.24. Microspheres prepared with a-b; 0.1 % (w/v) alginate and c-d; 1 % (w/v) alginate.....	62
Figure 4.25. Diameters of NGF loaded and nonloaded microspheres.....	63
Figure 4.26. Chemical crosslinking of alginate and RGD (gelatin) in the presence of EDC (Source: Hermanson 1996).....	64
Figure 4.27. a; General appearance of scaffolds (SW and NF) and NGF loaded microspheres attached scaffolds (MS-SW and MS-NF), SEM images of microsphere attached scaffolds b; MS-SW and NF.....	65
Figure 4.28. Release profiles of NGF from a- 1.0% and b-0.1% alginate microspheres.....	67
Figure 4.29. Release profile of NGF from 0.1% alginate particles incorporated nanofibrous gelatin scaffold.....	68
Figure 4.30. Behaviour of PC12 cells in the concentration of 500 cell/well in different cell culture media during 13 days in CM; complete medium, SM; starvation medium, SM+NGF; NGF added starvation medium....	70

Figure 4.31. Behaviour of PC12 cells in the concentration of 1000 cell/well in different cell culture media during 13 days in CM; complete medium, SM; starvation medium, SM+NGF; NGF added starvation medium....	71
Figure 4.32. 7 th day images of PC12 cells in SM with a; 25 ng/ml, b; 50 ng/ml, c;100 ng/ml, d; no NGF.....	72
Figure 4.33. 10 th day images of PC12 cells in SM with A; 25 ng/ml, B; 50 ng/ml, C;100 ng/ml, D; no NGF.....	73
Figure 4.34. Measurement of neurite length of PC12 cells at 7 th and 10 th day after treatment of different concentrations of NGF.....	74
Figure 4.35. PC 12 cells onto the cross-linked NF and SW scaffolds prepared with 425-600 μ m of paraffin spheres.....	74
Figure 4.36. Fluorescent images of 50 ng/ml of NGF treated PC12 cells into gelatin scaffold a; dyed with DAPI (blue), b; Phalloidin (red), c; merged form of a and b.....	75
Figure 4.37. Absorbance value of PC12 cells cultured on macroporous nanofibrous gelatin scaffold with/without of attached alginate microspheres (A-MS) measured by XTT proliferation assay.....	76
Figure 4.38. Appearance of PC12 cells at the 5 th day in a; SM, b; NGF loaded alginate microspheres destroyed medium and SM.....	77
Figure 4.39. 4 th day SEM images of PC12 cells seeded on a; gelatin scaffold b; gelatin scaffold and treated with 50 ng/ml of NGF, c; NGF loaded 1.0% alginate microspheres attached gelatin scaffold, d-f; NGF loaded 0.1% alginate microspheres attached nano-fibrous gelatin scaffold (Yellow arrow is indicate PC12 cells onto scaffolds).....	78
Figure 4.40. 10 th day SEM images of PC12 cells seeded on a, b- 0.1% A-MS attached gelatin scaffold; c, d- 1.0% A-MS attached gelatin scaffold.....	79
Figure 4.41. a- Model of biomimetic nanoscaffold system with interconnected macropores scaffold and growth factor loaded microspheres, b- NGF loaded alginate microspheres attached gelatin scaffold, c- 0.1% NGF loaded alginate microspheres attached gelatin scaffold with PC12 cells cultured for 10 days x250, d- x1000, e- x 5000.....	81

Figure A.1. List of solid walled and nanofibrous scaffolds prepared to determine optimum preparation conditions..... 95

LIST OF TABLES

<u>Table</u>	<u>Page</u>
Table 4.1. The influences of volume of PVA solution, amount of paraffin and stirring rate on the shape of paraffin particle.....	38
Table 4.2. Maximum and minimum sizes of paraffin spheres.....	39
Table 4.3. The influence of preheating time on the porosity of the scaffolds.....	47
Table 4.4. Compressive modulus (kPa) of scaffolds prepared with 10% gelatin concentration.....	51
Table 4.5. Fiber length and diameter of gelatin scaffolds prepared at +4 °C.....	55
Table 4.6. Freezing point of ethanol based water solutions.....	56
Table 4.7. Fiber length, fiber diameter and porosity of gelatin scaffolds prepared at -20°C.....	57
Table 4.8. Volume of surfactants in water-oil emulsion system composed of 20 mL of iso-octane and 4 ml alginate solution.....	61
Table 4.9. Amount of NGF required at the end of 10 days for the observation of PC12 cell differentiation in 2D and 3D cell culture environment.....	80
Table 4.10. The prepared MS/NS incorporated macroporous nanofibrous system in literature and the place of current study among them.....	80
Table A.1. Compressive modulus value (kPa) of solid walled gelatin scaffolds.....	96
Table A.2. Compressive modulus value (kPa) of nanofibrous gelatin scaffolds.....	96

CHAPTER 1

INTRODUCTION

The generative and regenerative capabilities of nature is always magical in the history the idea of regeneration of living things started with the observation that animals especially amphibians have the capacity of regeneration. During the time the regeneration concept was progressed with the organ transplantation and the real foundations of regenerative medicine laid on using autograft and allograft. An autograph is tissue transplanted from one part of the body to another in the same individual and allografts are isolated from cadavers. Both approaches have limitations including short-age and host immune rejection, respectively. A new hope appeared with stem cells due to their regenerative capacity. Regenerative medicine includes genetic engineering, stem cell biology, tissue engineering, biomaterials, and biomedical devices. The term ‘tissue engineering’ was officially proposed at a National Science Foundation workshop in 1988 to mean ‘the application of principles and methods of engineering and life sciences toward the fundamental understanding of structure-function relationships in normal and pathological mammalian tissues and the development of biological substitutes to restore, maintain or improve tissue function’ (O’Brien 2011). Tissue engineering combines three important elements, scaffolds, cells and biologically active molecules, to improve or replace biological functions. Scaffolds provide appropriate environment for the regeneration of tissues and organs guiding neo-tissue formation and organization. They should have three dimensional (3D) highly porous structure for adequate diffusion of nutrients, expressed products and waste, mechanical rigidity or flexibility, should allow retention of biochemical factors and most importantly, they should mimic natural extracellular matrix (ECM). As a main component of natural ECM, collagen has fibers with a diameter of 50-500 nm. Studies have shown that nanofibrous structure has the advantages on cell proliferation (Venugopal et al. 2005), migration (Zhang et al. 2005), differentiation (Badami et al. 2006) and serum protein adsorption (Woo et al. 2003). Cells in tissue engineering are derived from donor tissue which is limited in supply or from stem or progenitor cells. Stem cells deserve considerable attention owing to their unique capability to

differentiate into desired cell lineage and to self renew. Another component of tissue engineered construct is growth factors. Growth factors are biologically active molecules, stimulate or inhibit cellular proliferation, differentiation, migration, adhesion and gene expression (Babensee et al 2000). Controlled release of the growth factor is critical to increase its longevity. Encapsulation of growth factor and other biologically active agents in small biodegradable particles and attaching these particles to the scaffold opens a new perspective in tissue engineering. This approach was first applied by Kim et al. (2003) for the cartilage tissue engineering. In this study, it was shown that scaffolds incorporated with transforming growth factor beta-1 (TGF- β 1) loaded microspheres significantly augmented the cell proliferation and production of extracellular matrix. Following this study, similar systems were studied in cartilage regeneration (Lee et al. 2004, Tan et al. 2009, Wu et al. 2011), bone regeneration (Niu et al. 2009) and nerve regeneration (Zeng et al. 2014). Wei et al. (2007) have shown that nanofibrous scaffold induced significant bone formation when bone morphogenic protein (BMP) was incorporated into the scaffold in encapsulated form compared to the case that BMP was directly adsorbed to the scaffold. *In vivo* performance of this microsphere immobilized scaffold was investigated in rat dorsal wound repair application (Wei et al. 2008) and results showed that cell migration and angiogenesis for soft tissue repair were enhanced when compared with controls.

Application of tissue engineering principles for treating injuries in brain and spinal cord has been receiving more attention than before since life-threatening injuries and diseases in brain frequently cause death or disability due to presence of inhibitor molecules like myelin and proteoglycan growth inhibiting components. In the case of peripheral nervous system, after an injury, regeneration is possible although such recovery is often limited by the long distance that regenerating peripheral axons must grow (Ferguson and Son, 2011). Attempts to improve axonal regeneration and functional recovery were tried by suppressing proteoglycan-based or myelin-based inhibitors through pharmacologic or genetic manipulations. However the results of these attempts were not sufficient (Bradbury et al. 2002, Lee et al. 2010, Lee et al. 2010). A new strategy which combines neural stem cells (NSCs) and scaffolds with specific factors or biomolecules seemed to be a promising approach for neural repair and regeneration (Wang et al. 2010). It has been reported that growth factors or cytokine factors are necessary to induce differentiation of NSCs *in vitro*. Genetically modified

brain derived growth factor (BDNF), nerve growth factor (NGF) and neurotrophin-3 (NT-3) have successfully increased the survival of NSCs and differentiated them into neurons. Among these factors, NGF promotes primarily survival and axonal outgrowth of sensory neurons, both *in vitro* and *in vivo* (Rich et al. 1987).

Scaffolds are generally produced from natural and synthetic polymers. Chitosan, collagen, gelatin and alginate are mostly used natural polymers. Synthetic polymers can be classified as non-degradable polymers (silicone), biodegradable polymers such as poly(lactic-co-glycolic acid (PLGA), poly (ϵ -caprolactone (PCL), poly L-lactic acid (PLLA) and conducting polymers (polypyrrole, polyaniline). Among natural polymers, gelatin is considered as a good candidate for production of scaffolds since it has good processability, transparency, and bioabsorbability (Ikada 2006). Gelatin is a denatured protein produced by acidic or basic hydrolysis of collagen and hydrolysis process eliminates the pathogens (Liu and Ma 2009). It has potential for guiding tissue in regeneration and also has the integrin binding domain consisting of arginine, glycine and aspartic acid (RGD) in its structure which improves adhesion of cells (Chen et al. 2006).

Another biopolymer commonly used in tissue engineering applications is alginate which is a linear polysaccharide derived from brown seaweed and bacteria. Alginate is a natural heteropolysaccharide composed of β -D-mannuronate (M) and α -L-guluronate (G), which is physically crosslinked with divalent ions such as calcium to form an anionic hydrogel. The presence of the carboxylate group within the G blocks rings bears a negative charge, at pH 7 usually compensated by sodium cations. Adding divalent ions like Ca^{2+} induces the crosslinking of the polymer and thus the formation of a gel (Alnaief et al. 2011). Because of these properties, alginate has significant interaction with high isoelectric point proteins (Wells et al. 2007) and was used for encapsulating the proteins. Bonds in calcium-crosslinked alginate are reversible, therefore, burst release of encapsulated proteins was observed (Wells et al. 2007). To decrease and control the release rate of proteins, alginate particles were coated with positively charged polymers like poly(L-lysine), poly(ethylene imine) or chitosan (Lemoine et al. 1998).

The advantages of using nanofibrous scaffolds with growth factor loaded microcarriers were not investigated in detail in the nerve tissue engineering. Based on this fact, in this thesis two new nanofibrous scaffolds, in disc shape and as a conduit

were prepared for nerve tissue engineering application. Disc shape, 3D macroporous nanofibrous scaffolds integrated with NGF loaded microspheres were prepared by a combination of thermally induced phase separation and porogen leaching process. with these scaffolds, brain tissue engineering applications were targetted. Nanofibrous and channeled gelatin conduits were manufactured with the modification of TIPS and molding technique for peripheral nerve tissue engineering applications. The influences of scaffold preparation conditions on the structure and mechanical properties of fabricated scaffolds were examined. NGF loaded alginate microspheres were fabricated by homogenization and crosslinking of alginate with calcium ions in a water-oil system. Parameters were systematically changed to obtain homogeneous particles with high loading capacities. Controlled and sustained release of NGF from microspheres were achieved by coating microspheres with poly(L-lysine). Immobilization of microspheres into nanofibrous scaffold was carried out by crosslinking with N-(3-Dimethylaminopropyl)-N'-ethylcarbodiimide hydrochloride (EDC) and N-Hydroxysuccinimide (NHS) system. The attachment and proliferation of model neural cell line; PC12, as well as the differentiation behaviour of PC12 cells in the disc shaped nanofibrous scaffolds integrated with NGF loaded microspheres were investigated.

This thesis consist of five chapters. After the introduction, in the second chapter three major components of tissue engineering; scaffolds, bioactive factors and cells are explained. In the third chapter, the detailed experimental methods used to prepare and characterize developed system are presented. Chapter 4 included a detailed discussion od all experimental results. In the chapter 5, gives the main conclusion and brief summary of the study and possible suggestions for further research are presented.

CHAPTER 2

TISSUE ENGINEERING

Organ transplantation seems to be a gold approach for the reconstruction of the devastated tissues or organs, however the shortage of donated organs, immune rejection, necessity of immunosuppressive therapy are problems in organ transplantation. An alternative approach to tissue and organ reconstruction is tissue engineering. Three elements; scaffolds, biologically active molecules and cells are important to improve or replace biological functions in tissue engineering.

2.1. Tissue Engineering Scaffold

A scaffold is a three dimensional (3D) construct which serves as temporary support for cells to grow into a new tissue (Figure 2.1). Prefabricated scaffold can either act as a supportive prosthetic material to regenerate tissue *in vivo*, or as a cell adhesive substratum to form engineered tissue *in vitro* (Chung and Park 2007). In 3D cell culture system, scaffolds provide appropriate environment for the regeneration of tissues and organs guiding neo-tissue formation and organization.

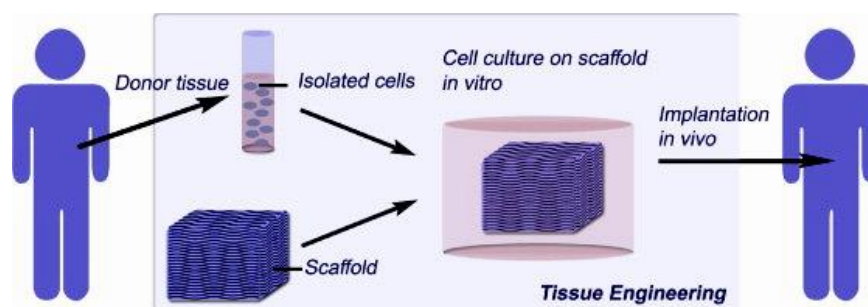


Figure 2.1. The general perspective of tissue engineering (Source: Stamatialis et al. 2008).

The functionality of the scaffold is greatly influenced by its design. Although the final requirements are dependent on the specific purpose of the scaffold, general characteristics of the scaffolds are similar (Stamatialis et al. 2008). The scaffold should be highly porous with good pore connectivity to ensure sufficient nutrient transport towards the cells and removal of waste products. An ideal scaffold should have also suitable mechanical properties comparable to *in vivo* tissue at the site of implantation and should be easily connected to the vascularization system of the host. The scaffold material should be biocompatible and degrade in tandem with tissue regeneration and remodeling of the extracellular matrix (ECM). Mimicking of natural extracellular matrix and surface should promote cell attachment and proliferation. The methods used for processing polymeric scaffolds can be classified as porogen (particulate) leaching, phase separation, gas foaming and electrospinning are discussed in the following section.

2.1.1. Thermally Induced Phase Separation (TIPS)

Recently, thermally induced phase separation (TIPS) technique has become popular for preparing porous scaffolds. The technique is based on decreasing the temperature of a homogenous polymer solution to induced a phase separation into two phases, polymer-rich phase (high polymer concentration) and polymer lean phase (low polymer concentration). Pores in the structure form once the solvent occupying the polymer-lean phase is removed by extraction, evaporation or sublimation and polymer in the polymer-rich phase forms the skeleton of the scaffold after solidification.

Figure 2.2 shows a typical phase diagram for a binary polymer-solvent mixture. At high temperatures, polymer solution is in one phase region and homogeneous. When the temperature is lowered below the critical point, either liquid-liquid or solid-liquid phase separation takes place. Binodal curve separates one phase from two phase region. The region between binodal and spinodal is metastable and liquid-liquid phase separation occurs by nucleation and growth. At low polymer concentrations, droplets of polymer rich phase are formed and dispersed in the polymer-lean phase. Consequently, a powder like polymer solid is obtained after removing of solvent (Figure 2.2, Inset A). At high polymer concentrations, droplets of polymer-lean phase are dispersed in a

matrix of polymer-rich phase leading to a closed pore structure (Figure 2.2, Inset C). In the spinodal region, polymer-rich and polymer-lean phases are completely interconnected, hence, a continuous pore structure is obtained (Figure 2.2, Inset B).

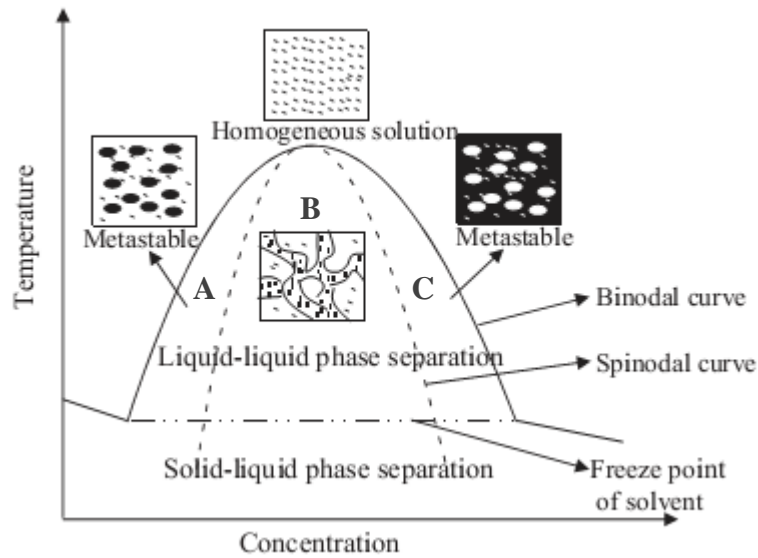


Figure 2.2. Binary phase diagram of a polymer solution with TIPS properties (Source: Yang et al. 2004).

To achieve liquid-liquid phase separation, a solvent with a freezing point lower than the phase separation temperature of the solution should be chosen. Final structure of the scaffold achieved with liquid-liquid phase separation depends on the concentration of the polymer solution, phase separation temperature and the molecular weight of the polymer. Scaffold obtained by liquid-liquid phase separation have pore sizes ranging from several microns to tens of microns (Chen and Ma, 2006). Phase separation time can be changed to control the increase in average size of the droplets which allows to control the pore size of the matrix.

In the solid-liquid phase separation technique, polymer solution is quenched below the freezing point of the solvent and then freeze dried, producing a porous (channeled) structure. When the temperature of the polymer solution is lower than the freezing point of the solvent, the crystallization of the solvent takes place and the polymer phase is expelled from the crystallization fronts as impurities. A continuous polymer-rich phase is formed by aggregation of polymer expelled from every single solvent crystal (Zhang and Ma, 1999). The solvent crystal structure reflects the scaffold

morphology therefore crystal growth is important. In this technique the freezing rate also greatly affects the resulting morphology of the scaffold. It was known that direction of channels in the structure is parallel to the direction of heat transfer. This technique has applications where guided regeneration is required, such as scaffolds for spinal cord injury (Park et al. 2002, Teng et al. 2002) and transplantation sheets for retina (Schugens et al. 1996, Tomita et al. 2005, Thomson et al. 2011).

TIPS has been used for several years to fabricate synthetic porous scaffolds for tissue engineering. Tissue engineering scaffolds formed by spinodal decomposition include in the form of poly(lactide- co -glycolide) (PLGA), poly(L-lactic acid) (PLLA) or poly(D-lactic acid) (PDLA) in tetrahydrofuran (THF) (Liu and Ma 2004) or dioxane/water (Nam and Park, 1999). In addition to porous scaffolds preparation with TIPS, fabrication of nanofibrous scaffold with TIPS can be achieved by nonsolvent washing after phase separation. This structure was first characterized by Ma and Zhang (1999). In this study, a solution of PLLA dissolved in THF was thermally induced phase separated and then the solvent was exchanged with water (nonsolvent) then freeze-dried and it yielded to nanofibrous PLLA matrices. In this study the fibers formed have diameters ranging from 50–500 nm, and have a porosity as high as 98%. In the another study water soluble natural polymer gelatin was used to prepare nanofibrous matrices. In this experiments gelatin was dissolved in 50/50 ethanol/water (v/v) solution and then phase separation was performed at -80°C for 5 hours. After solvent exchange with ethanol (nonsolvent) and then 1,4- dioxane, the nanofiber matrix with the fiber diameter of 177 nm was fabricated (Liu and Ma, 2009).

2.1.2. Other Methods Used for Fabricating Scaffolds

Porogen leaching is widely used to fabricate scaffolds for tissue engineering applications (Ma and Langer, 1999; Lu et al., 2000). The method starts with dispersing a template (particles, etc.) within a polymeric or monomeric solution, then continues with gelation or fixing the structure. Porous structure is obtained with the removal of the template. As a porogen salt, wax or sugars can be used. This technique is simple and inexpensive and pore size and geometry can be easily controlled by the amount of porogen added, the size and shape of the porogen (Plikk et al. 2009). In porogen

leaching technique small amount of polymer is required to fabricate the scaffold, however, controlling inter-pore openings are not easy. Ma and Choi (2001) have shown that well defined interconnected pores can be obtained with the heat treatment of spherical paraffin spheres. The surface of the scaffold obtained with this technique is not in nanofiber form, but, rather it is solid walled. Another technique used for preparing scaffolds is gas foaming. In this technique, formation of porous materials is achieved in solvent-free condition through gas bubbles where the size of bubbles can reach up to 100 μm . The scaffolds obtained with this technique do not contain interconnected pores and lack nanofiber structure.

Scaffolds prepared with electrospinning have nanometer and micron sized fibers in diameter. In this technique typically, a high (positive or negative) voltage is applied to a polymer solution or melt that is pumped through a small orifice or flat-tipped needle facing a target (collector) and scaffold is obtained in the form of sheets. Resulting fibers may have similar diameters to that of certain ECM microstructures (Hutmacher et al. 2008), on the other hand, it is difficult to generate appropriate pore sizes and pore connectivity for cellular ingrowth (Guan et al. 2008).

Among the above mentioned methods, electrospinning and thermally induced phase separation have been utilized to fabricate scaffolds with the nanoscale features necessary to mimic the extracellular matrix. The importance of mimicking of ECM comes from the role of architecture of natural ECM in the regulation of cellular behaviour (Abbott 2003, Schmeichel and Bissell, 2003). In literature, nanofibrous scaffolds have been shown to have advantageous effects on cellular behavior and tissue formation when compared to more traditional types of scaffolding (Ma 2008, Liu and Ma, 2009). In addition to nanofibers, to mimick natural ECM, the scaffold can be prepared with internal interconnected porous network, a common scaffold design requirement, to allow for cellular integration into the scaffold, transport of nutrients and waste product. It can even be designed to release growth factors to tailor tissue development (Wei et al., 2007).

2.1.3. Materials Used For Fabricating Scaffolds

Different types of materials can be used for production of scaffolds. In ‘soft’ tissue applications, e.g. skeletal muscle or cardiovascular substitutes, mainly polymers (synthetic or natural) are used whereas ceramics and metals are especially applied in ‘hard’ tissue replacements, e.g. bone substitutes. One of the natural polymers used for tissue engineering applications is fibrin which is a major constituent of blood clots, and it has been used in mixtures with thrombin to produce an *in-situ* forming gel. Type I collagen is capable of forming porous gel matrices which are already commercially available as skin replacements. Chitosan, a cationic polymer derived from chitin, can produce a scaffold with a hydrophilic surface, and cell adhesive/ differentiating characteristics, while its inherent osteoconductive nature endows its potential use for bone tissue engineering. Alginate, an anionic polysaccharide extracted from Brown algae, exhibits gel forming behavior when complexed with divalent cations such as Ca^{2+} . Hyaluronic acid, a non-sulfated glycosaminoglycan of repeating disaccharide units, is a major component of the natural ECM and forms crosslinkable hydrogels with various modifications (Chung and Park 2007). Synthetic polymeric scaffolds are also used in tissue engineering because they can be fabricated from a wide range of biodegradable polymers with easy processability, controlled degradation, and susceptibility to modification. The poly(α -hydroxyester)s such as polylactide (PLA), polyglycolide (PGA), and its copolymers are extensively used for preparing biodegradable scaffolds in the form of a solid foam. Especially, biodegradable devices made of poly(lactide-co-glycolide) (PLGA) copolymers are advantageous due to their controlled degradation behavior and tunable mechanical properties according to the specific requirements for the desired tissue. These hydrophobic polymers can be fabricated into microspheres as injectable matrices, or scaffolds with nanofibrous structure.

The forms of the polymeric scaffolds can be changed (Figure 2.3). These forms are; a solid foam, nanofibrous matrix, porous microsphere or hydrogel. A solid foam matrix has a 3D structure and pores while a nanofibrous matrix would provide a better resemblance of the physiological environment in the case of fiber size. Injectable matrices such as hydrogels and microspheres which are already widely utilized as sustained protein release formulations (Chung and Park 2007).

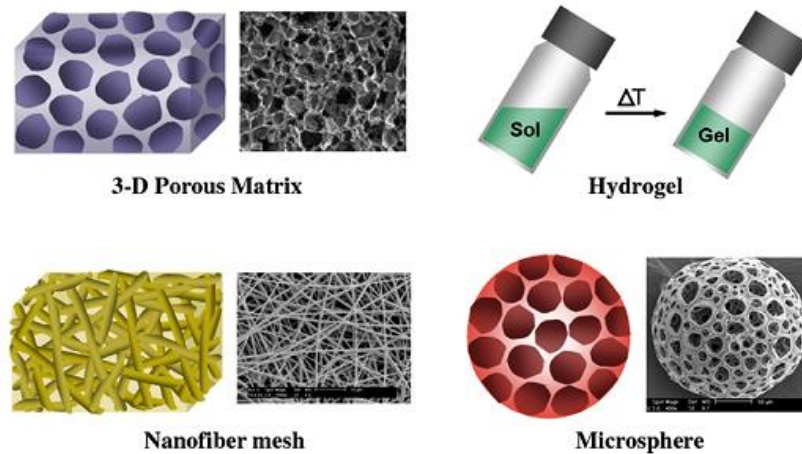


Figure 2.3. Different forms of polymeric scaffolds for tissue engineering (Source: Chung and Park 2007).

2.2. Biologically Active Molecules

Growth factors play an important role in developing tissue engineered constructs. They are biologically active molecules that stimulate or inhibit cellular proliferation, differentiation, migration, adhesion and gene expression (Babensee et al. 2000). The main challenge with the use of growth factors is their relatively short half-life within the body. Use of an appropriate delivery carrier, which can protect growth factor from enzymatic degradation and allow controlled release, is a promising approach for prolonged retention and biological activity of the drugs within the body. Polymers are attractive protein drug delivery carriers, as their properties, such as physical and chemical, can easily be modified and changed. A number of approaches have been reported on the controlled release of growth factors using polymeric carriers (Lee and Yuk, 2007). One of these approaches is the functionalization of the surface of a 3D scaffold by specific cell–matrix interactions to promote cell adhesion. In this approach growth factors can be encapsulated or embedded within the porous matrices and delivered in a sustained manner to enhance cell growth and morphogenesis, leading to a functionally organized tissue (Chung and Park 2007). Conventional synthetic biomaterials can not satisfy all required properties, therefore, the research recently condensed on natural biomaterials like proteins; collagen, elastin, silk, polysaccharides; hyaluronan, alginate, chitosan, some natural tissue derived materials and some engineered forms or derivatives of such substances. Bioactivity is provided to synthetic polymers by surface grafting of

molecules, such as peptide or amino acid sequences (Williams 2008). For example; Chen et al. (2006) used poly(l-lactide) and RGD modified microspheres as cell carriers for tissue engineering.

Another approach for the controlled release of growth factors is their encapsulation in small biodegradable particles and attaching these particles to the scaffold. This approach was first applied by Kim et al. (2003) for the cartilage tissue engineering. In this study, it was shown that scaffolds incorporated with transforming growth factor beta-1 (TGF- β 1) loaded microspheres significantly augmented the cell proliferation and production of extracellular matrix. Following this study, similar systems were studied in cartilage regeneration (Lee et al. 2004, Tan et al. 2009, Wu et al. 2011), bone regeneration (Niu et al. 2009) and nerve regeneration (Zeng et al. 2014). Wei et al. (2007) have shown that scaffold induced significant bone formation when bone morphogenic protein (BMP) was incorporated into the scaffold in encapsulated form compared to the case that BMP is directly adsorbed to the scaffold. *In vivo* performance of this microsphere immobilized scaffold was investigated in rat dorsal wound repair application (Wei et al. 2008) and results showed that cell migration and angiogenesis for soft tissue repair were enhanced when compared with controls.

Incorporation of protein loaded micro/nano spheres to the scaffold makes a new perspective to the tissue engineering and drug release studies. Scaffold serves as a 3D structure with porous matrix which provides adequate pore space and surface to support cell attachment, migration, proliferation, differentiation and neotissue genesis. Besides, controlled delivery of growth factor is important for the cellular activity and modulation of regeneration process (Hu and Ma 2011).

Incorporation of growth factor loaded microspheres into the macroporous nanofibrous scaffold opened a new perspective in the preparation of tissue engineered construct. The idea of combination of macroporous nanofibrous scaffold with protein loaded microspheres was first mentioned by Ma P.X. (2004) and this scaffold was called “biomimetic nano scaffold” (Figure 2.4). The suggested system was composed of nanofibrous architecture of a interconnected macropore network and microspheres for controlled release of regenerative factors. The nano-fibrous scaffolding design was used to provide a high surface area for cell attachment and new matrix deposition, and an open structure allowing an interactive environment for cell-cell, cell-nutrient, and cell-

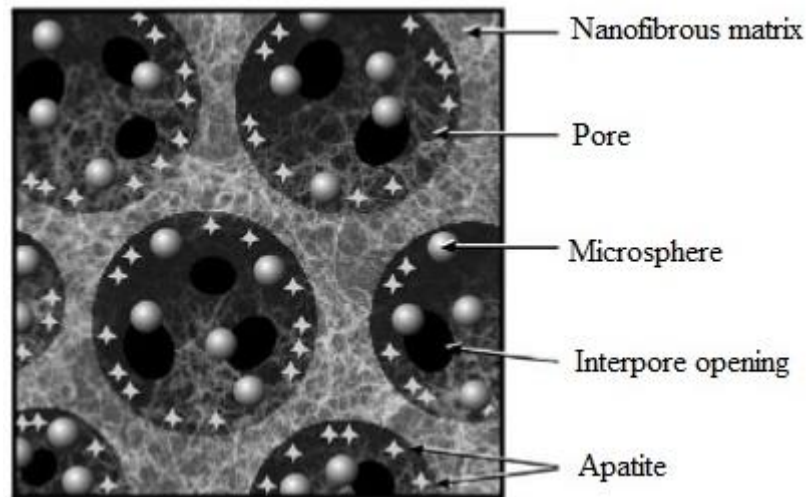


Figure 2.4. Model of biomimetic nanoscaffold system with interconnected macropores, nanofiber matrix structure and growth factor loaded micro/nanospheres (Source: Ma 2004).

signal molecule interactions. In this system, it was targeted that biodegradable microspheres release regenerative factors in a controlled fashion in a local environment.

The fabrication of biomimetic nanoscaffold system was first carried out in the bone tissue engineering application. This system was first made with the post seeding of platelet derived growth factor (PDGF) loaded poly(lactic-co-glycolic acid) (PLGA) microspheres to the nanofibrous poly(L-lactic acid) (PLLA) scaffold for periodontal tissue regeneration (Wei et al. 2006). Nanofibrous scaffolds were prepared with thermally induced phase separation technique. Prepared scaffold had the nanofiber which has the diameter of 50-150 nm similar size of collagen (50-500 nm) in the natural extracellular matrix. The PLGA microspheres were prepared with water-in-oil-in-water (w/o/w) double emulsion method. Same system was also used for loading of bone morphogenic factor-7 (BMP-7) protein to PLGA nanospheres and this nanosphere immobilized nanofibrous scaffold induced a significant bone formation when compared with the adsorption of free BMP into the scaffold (Wei et al. 2007). *In vivo* performance of this system was investigated in rat dorsal wound repair application (Wei et al. 2008). Results have shown that this system enhanced cell migration and angiogenesis for soft tissue repair *in vivo* when compared with controls.

Review of literature studies clearly indicate that biomimetic nanofibrous scaffold should be integrated with an ideal carrier capable of controlled and sustained release of bioactive molecules such as growth factor. Because of short half-life of these bioactive

molecules, encapsulation in microspheres are also able to protect their rapid degradation and clearance within the body. Most-widely used methods for the preparation of microspheres are phase separation-coacervation, emulsification-solidification and spray drying techniques.

2.2.1. Emulsification-Solidification Method Used for Encapsulating Biologically Active Agents

In emulsification-solidification method emulsification is made by oil-in-water or water-in-oil process. Oil-in-water emulsions are used for encapsulating hydrophobic proteins. While encapsulation of hydrophilic proteins can be achieved by water-in-oil emulsion process. In this method, polymer is dissolved in water and protein is added to the polymer solution. Next, this mixture is added into the oil phase with a volume larger than the volume of polymer solution and emulsification is induced with stirring, sonication or homogenization. Finally emulsion is solidified into microspheres with crosslinking reaction (Figure 2.5). In this technique pH value of water phase influences protein activity and has impact on microsphere formation, morphology and structure. The main disadvantages of this method is to exposure shear force in the processing steps (e.g., homogenization, and sonication). Some reports showed that the loss of protein activity or denaturation/ aggregation of protein during encapsulation could be minimized by using stabilizers such as poloxamer, bovine serum albumin (BSA) or hydroxypropyl- β -cyclodextrin (Sturesson and Carlfos 2000, Morlock et al. 1997, Sah 1999).

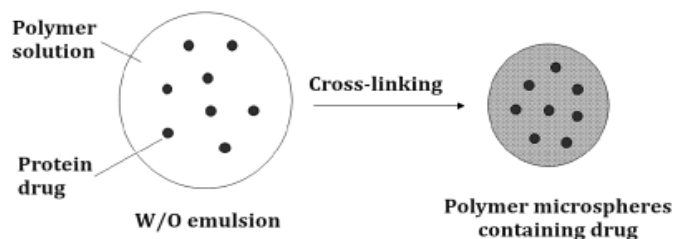


Figure 2.5. Water soluble polymer and protein in the form of microspheres after solidification in W/O emulsion process (Source: Wang et al. 2013).

For the encapsulation of hydrophilic proteins into hydrophobic polymers, double emulsion method is used. In this method, aqueous solution of hydrophilic protein is added to the polymer solution dissolved in a nonmiscible organic solvent and water-oil emulsion is formed by stirring or homogenization. After primary emulsion is achieved, emulsion is transferred into excess of aqueous medium with stabilizer such as poly (vinyl alcohol). After a second homogenization or stirring water-oil-water emulsion is formed. Finally, solvent is removed by heat or vacuum to obtain microspheres (Wang et al. 2013).

2.2.2. Other Methods Used for Encapsulating Biologically Active Agents

Encapsulation of proteins is also carried out with phase separation coacervation technique and spray drying methods. Microencapsulation with phase separation is performed in three steps: formation of polymer in coacervative droplets, adsorption of coacervative droplets on to drug surface and solidification of microcapsules. In order to induce phase separation of polymer solution; nonsolvent addition, temperature change, incompatible polymer or salt addition can be applied. Phase separation method has the enables efficient control of the particle size with a narrow size distribution by simply varying the concentration of added salts or the viscosity and amount of the nonsolvent and/or molecular weight of polymer used. On the other hand, aggregation of microspheres during preparation process is the drawback of this method (Yeo et al. 2001).

Spray drying is a mechanical process for the preparation of microspheres. In this method after dissolving hydrophilic or hydrophobic polymer in a suitable solvent,

protein is added and dispersed in polymer solution with high speed homogenization. Then the mixture is sprayed through a nozzle, dried and microspheres are precipitated into the collector (Wang et al. 2013). Spray drying is rapid, easy to scale up process and both hydrophilic and hydrophobic polymers can be used for encapsulation. However, the lost of materials due to sticking to the collector (drying chamber) and the effect of solvent on protein activity are the limit the usage of this method (Yeo et al. 2001).

2.3. Cells

Cells in tissue engineering are derived from donor tissue which is limited in supply. Stem cells are currently a major focus in regenerative medicine since they have remarkable potential to develop into many different cell types in the body during early life and growth. In addition, in many tissues they serve as a sort of internal repair system, dividing essentially without limit to replenish other cells as long as the person or animal is still alive. When a stem cell divides, each new cell has the potential either to remain a stem cell or become another type of cell with a more specialized function, such as a muscle cell, a red blood cell, or a brain cell.

Stem cells have the ability to do the following:

1. Proliferate and self-renew (making identical copies of them-selves) for a number of generations.
2. Differentiate into the major (if not all) lineages of the tissue they are derived from.
3. Regenerate the tissue and/or organ they were derived from (Ahmed 2009).

Scientists primarily worked with two kinds of stem cells from animals and humans: embryonic stem cells (ESC) and non-embryonic "somatic" or "adult" stem cells. ESCs have the ability to divide indefinitely and capacity to differentiate into most of the tissues of the body. ESCs can be directed to be maintained in culture in an undifferentiated state or differentiate into different cell types of three germ layer (mesoderm, ectoderm and endoderm). The differentiation also can be made with *in vitro* culture conditions. The simplest and most common strategies involved simply growing ESCs in a medium designed for the required cell type (Evans et al. 2006). Because of these type of potentials, ESCs are under very deep investigation in injury, regeneration and organ transplantation.

The usage of the adult stem cells is longer than ESCs. The first defined type of them is hematopoietic stem cell (HSC) which is isolated from bone marrow. Another cell type found in the bone marrow is the mesenchymal stem cells (MSCs). Investigations have shown that by changing the composition of the medium in which they are grown, MSCs can be selectively differentiated into bone cells (osteocytes), fat cells (adipocytes), and cartilage cells (chondrocytes). There are also numerous examples of evidence in the literature that these cells can differentiate into other lineages, including heart cells and neurons. But they do have limitations – they can only divide a finite number of times (depending on the age of the donor), which limits their supply, and they may accumulate genetic changes over time (Evans et al. 2006).

Besides the bone marrow, adult stem cells also exist around the body. For example, neural stem cells can be isolated from brain tissue, grown *in vitro*, and induced to differentiate into the three cell types of the brain – neurons, astrocytes, and oligodendrocytes. Similar stem cells are also thought to reside in other tissues as a repair mechanism against injury, for example in the skin. This important properties of the stem cells made them hot point to reconstruct the injured part of body but early investigations have shown that injection of stem cells to the removal part of the body has a minor potential to reform. Thus, the investigations turned search for finding suitable carriers which cells can attach, proliferate and differentiate, consequently scaffolds emerged as a potential solution. Scaffolds can be used to grow stem cells and regenerate damaged tissues and organs. Stem cells exist within a unique tissue-specific microenvironment commonly termed the stem cell niche. The extracellular matrix (ECM) comprises the structural component of the niche; in addition to providing the physical support matrix for cell attachment, migration and division, it also presents biochemical signals to cells that are modulated through molecular interactions with ECM proteins (Lim and Mao, 2009).

Scaffold used in the stem cell investigation must be physically stable in the implanted site, allow the homing, expansion and differentiation of stem cells, and be non-toxic and biodegradable (Hoffman 2014). In this concept nanomaterials especially functionalized nanofibers have been thought that will accelerate stem cells adherence and migration. Investigation the effect of nanofiber on stem cell behaviour in literature experiments concentrated on the electrospinning method. Materials used in electrospinning are natural or synthetic biopolymers or combination of both. They

include poly(l-lactic acid), alginates, silicon or chitosan, combination with collagen or gelatin (Premnath et al. 2013, Leung et al. 2013, Xin et al. 2007, Wang et al. 2008, Sarkar et al. 2013). The stem cells seeded electrospun nanofibers is widely used in bone and cartilage tissue engineering using MSCs. Induction of osteogenic pathway was also investigated with adipose-derived stem cells (ADSCs) in electrospun poly(l-lactic acid)/collagen nanofibers. Ravichandran et al. 2012 determined that ADSCs could proliferate and differentiate along the osteogenic pathway in absence of any induction medium when engineered with a cell adhesion peptide and functionalized to retain calcium phosphate (hydroxyapatite). In neural tissue engineering application neural stem cells were differentiated onto electrospun poly(l-lactic acid)/gelatin fibers (Binan et al. 2014). Poly-l-lactide (PLLA) and hybrid PLLA/collagen (PLLA/Coll) scaffolds fabricated by electrospinning were also used to differentiate MSCs into vascular endothelial cells (Jia et al. 2013).

Besides stem cells, countless model cell lines like cancer cell lines are recently used with the combination of scaffold. This combination aim to mimick tumor models in spesific cancer type like ovarian cancer (Yang and Zhao, 2011), lung cancer (Zhang et al. 2013), sarcoma (Fong et al. 2013), breast cancer (Horning et al. 2008), prostate cancer (Harma et al. 2010), stomach cancer (Sun et al. 2013), glioma (Kievit et al. 2013) to investigate the cell-scaffold interaction and chemotherapeutic resistance of anticancer drugs.

In some cases, cell lines can be used to investigate interactions of cells with the scaffold and response of cells to the spesific bioactive factors. In nerve tissue engineering PC12 cell line is widely-used which is derived from a transplantable rat pheochromocytoma. It was determined that PC12 cells respond reversibly to nerve growth factor (NGF) by induction of the neuronal phenotype. With the exposure of NGF for 7 days, PC12 cells cease to multiply and extend neurite structure which are branching varicose processes similar to those produced by sympathetic neurons in primary cell culture. If the treatment of NGF is continued up to 20 days the processes lenght can be reached to 500-1000 μm in length. In the case of removal of NGF from growth medium, degeneration processes of neurite is started within 24 hr and cell multiplication is strated within 72 hr (Greene and Tischler, 1976).

2.4. Nerve Tissue Engineering

In mammals, adult neurons lose their proliferative potential. The central nervous system, therefore, has limited regenerative capacity when inflicted with lesions resulting from trauma, stroke, or neuropathological conditions. Usage of stem cells in the regenerative medicine seems to be a big change especially for treatment of neurodegenerative disease such as Parkinson, Alzheimer and ALS (Amyotrophic Lateral Sclerosis). Tumor and blood clot removal result in volume loss, and also neurodegenerative diseases and hypoxic–ischemic injuries lead to necrotic and/or scar tissue formation. Restoration of these functions would necessitate replacing the necrotic or scar tissue with healthy cells, a concept known as reconstructive brain surgery (Chai and Leong 2007). Repair of neurological injuries in the central nervous system is complicated by the presence of natural inhibitors of nerve regeneration, notably neurite outgrowth inhibitor and myelin-associated glycoprotein. There are many scientific investigations to regenerate nerve using conventional autologous nerve grafts or from the newly developed therapeutic strategies for the reconstruction of damaged nerves with the usage of neural stem cells (NSCs) (Lim and Mao 2009). In the mammalian brain, NSCs originate from two specific regions, the subventricular zone and the dentate gyrus area of the hippocampus. Evidence suggests that NSCs are widely distributed in the adult brain (Chai and Leong 2007).

Typically, to induce differentiation of NSCs in 2D culture, cells are plated on laminin, epidermal growth factor (EGF)/fibroblast growth factor (FGF) are withdrawn, and serum added. Under laminin/serum induced differentiation the predominant cell type is astrocytes, followed by neurons and a low frequency of oligodendrocytes. If neurotrophic factors such as NGF, BDNF, and GDNF are added during differentiation the numbers of neurons increases significantly at the expense of astrocytes. If platelet derived growth factor is present the number of oligodendrocytes dramatically increases to make up the dominant cell type. Thus it is clear that cells are plastic in their differentiation potential and by changing the media composition, the proportion of the three neural cell types can be altered (Ahmet 2009).

Recent advancements in nerve regeneration have involved the application of tissue engineering principles and this has evolved a new perspective to neural therapy. The success of neural tissue engineering is mainly based on the regulation of cell

behavior and tissue progression through the development of a synthetic scaffold that is analogous to the natural extracellular matrix and can support three-dimensional cell cultures (Subramanian et al. 2009). Ideal properties of a scaffold for nerve regeneration is not different from general tissue engineering principles which are biocompatibility, minimum inflammatory, controlled biodegradability with non-toxic degradative products, porosity for vascularization and cell migration and three-dimensional matrices with appropriate mechanical properties to mimic the extracellular matrix (Subramanian et al. 2009).

Among different types of biomaterials, polymeric biomaterials are widely preferred as scaffolds for peripheral and central nerve regeneration both *in vitro* and *in vivo*. Mimicking ECM with polymers or polymers and cellular specific agent (collagen, collagen + specific amino acid sequences which are important for cellular attachment etc.) is a popular concept for the production of ideal scaffolds. Actually ECM has different composition of molecules which are not the same for each organ. Some ECM, for example in tendons contain a high proportion of fibrous protein where as cartilage contains a high proportion of polysaccharides that form a firm compression resistant gel, also bone ECM is hardened by deposition of Ca-phosphate crystals. ECM of the brain is composed lecticans which is proteoglycans that contain a lectin domain and hyaluronic acid binding domain are the major component of the brain ECM (Ruoslahti E. 1996). Matrix proteins common in other tissues are nearly absent in adult brain.

In tissue engineering studies hyaluronic acid (HA) has been chemically and physically incorporated into various tissue engineering scaffold matrices. For example chitosan–gelatin composite scaffolds modified with HA have been shown to increase the adhesion of fibroblasts. PLGA scaffolds modified with HA supported the growth of chondrocytes with maintenance of its original phenotype, showing great potential for cartilage tissue engineering (Chung and Park 2007).

For the advanced investigation on NSCs scaffolds, Wang and Spector (2009) developed HA collagen (Coll) scaffolds by a freeze drying technique and the crosslinking was carried out with water soluble carbodiimide. The results showed that HA–Coll scaffolds containing an open porous structure with a homogeneous pore size distribution could be fabricated. The mechanical properties of HA–Coll scaffolds prepared with a Coll: HA mixing ratio of 1: 2, and pure HA sponges, were comparable with brain tissue. Neural stem cells (NSCs) were seeded onto these scaffolds in order to

investigate their effects on neurogenic induction of the cells. When compared with Coll scaffold, in HA– Coll and HA scaffolds, cells appeared to assemble into clusters displaying the typical features of neurospheres. The intensity of expression and density of MAP2, which is used for labeling of dendritic trees of mature neurons, was much higher in the HA–Coll samples than in the HA scaffolds. In comparison, there was little expression of MAP2 by cells in the Coll scaffolds.

In another study, arginine–glycine–aspartic acid (RGD) immobilized hyaluronic acid hydrogels with open porous structure have been developed for brain tissue engineering (Cui et al. 2006). Both unmodified hydrogels and RGD immobilized hydrogels were implanted into the defects of cortex in rats and it was observed that the porous hydrogels functioned as a scaffold, supported the cell infiltration and angiogenesis, simultaneously inhibited the formation of glial scar. In addition, HA hydrogels modified with RGD were able to promote neurites extension.

In a recent study, Tang-Schomer et al. 2014, produced 3D brain-like tissue from silk and collagen for the real-time nondestructive assessments of brain homeostasis and injury. In literature *in vitro* 3D functional brain-like tissues have not been prepared. In their study complex functional 3D brain-like cortical tissue, maintained for months *in vitro*, with in modular 3D compartmentalized architectures and electrophysiological function was prepared. This brain-like tissue responds *in vitro* with biochemical and electrophysiological outcomes that mimic observations *in vivo*.

Valmikinathan et al. (2008) used poly (lactide-co-glycolide) (PLGA) microsphere-based spiral scaffold design with a nanofibrous surface that has enhanced surface area and possessed sufficient mechanical properties and porosities to support the nerve generation process. PLGA microparticles were synthesized using oil in water (O/W) emulsion method and nanofibers were prepared by electrospinning technique. They found that; the scaffolds have an open architecture that goes evenly through out the structure hence leaving enough volume for media influx and deeper cell penetration into the scaffolds. The *in vitro* tests conducted using Schwann cells showed that the nanofibrous spiral scaffolds promote higher cell attachment and proliferation when compared to contemporary tubular scaffolds or nanofiber-based tubular scaffolds. The nanofiber coating on the surface enhanced the surface area, mimicked the extracellular matrix and provided unidirectional alignment of cells along its direction.

In a recent investigation, Xu et al. (2010) studied the effects of poly(hydroxyalkanoate) (PHA) films and PHA nanofiber scaffolds on NSCs growth and differentiation. Polyhydroxyalkanoates (PHA) have been demonstrated to be a family of biopolymers with good biodegradability and noncytotoxicity. Their results showed that PHA nanofiber scaffolds, structurally similar to natural ECM, could support growth of NSCs. Compared with the PHA films, PHA nanofiber scaffolds showed stronger cellular adhesion, better connection and higher viability of NSCs which show the importance of 3-D scaffold systems. Ellis-Behnke et al. (2006) have found that a novel self-assembling peptide nanofiber scaffold implanted alone without cell cargo could support axonal regeneration through the site of an acute brain injury and could restore functional neuronal connectivity in the severed optic tract in animal models.

In peripheral nerve tissue regeneration various strategies for better recovery of nerve functions have developed. End-to-end suturing is one effective method for short nerve gaps but in the case of longer gaps tubular structures are necessary. Much of the research effort has focused on nerve guidance channels to enhance regeneration across nerve gaps. For this aim various bioengineered nerve grafts (nerve conduit) have been developed from polymeric materials ranging from naturally derived polymers to conventional nondegradable and biodegradable synthetic polymers. As a natural polymer chitosan (Wang et al. 2005, Wang et al. 2008), collagen (Bozkurt et al. 2007, Bozkurt et al. 2009, Kroehne et al. 2008), gelatin (Lu et al. 2007, Chen et al. 2005, Chang et al. 2007) and blend of alginate+chitosan (Pfister et al. 2007), collagen+chitosan (Hu et al. 2009) were used for the preparation of nerve conduit. As a synthetic polymer PCL (Chiono et al. 2008), PDLLA (Wang et al. 2003), PGA (Tanaka et al. 2006), PLGA (Widmer et al. 1998, Bini et al. 2004), PLLA (Evans et al. 1999) and blend of PLGA+gelatin (Li et al. 2007) were used.

As seen from Figure 2.6 different strategies were developed to repair peripheral nerve injury (Daly et al. 2012). One of these strategies is the use of intraluminal guidance structures and micro-grooved luminal designs to provide additional structure support and topographical guidance to regenerating axons and migrating of cells (Pabari et al. 2011). Electrospun fibrous conduits provide high flexibility and porosity, a high surface area-volume and allow guidance of cell migration and proliferation and axonal growth (Kim et al. 2008). Multichannel conduits were developed to control axonal dispersion, to optimize nutrient exchange or introduce external stimuli (Yao et al. 2010).

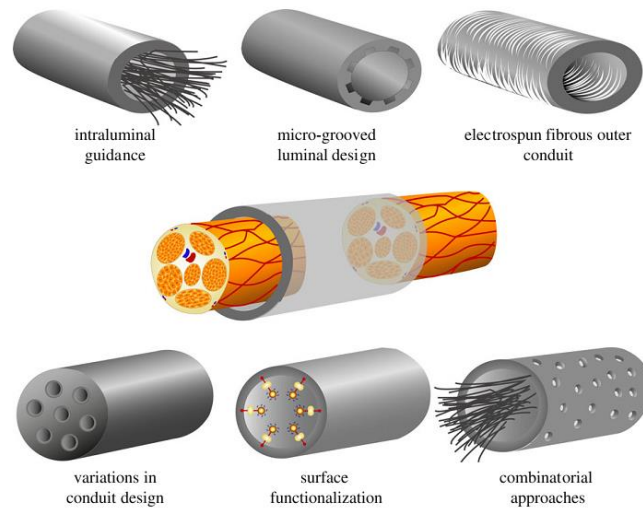


Figure 2.6. Structural repair strategies used for improving existing hollow nerve guidance conduits (Source: Daly et al. 2012).

The use of such strategies requires consideration of the size and distribution of these topographical features, as well as a suitable surface for cell–material interactions.

CHAPTER 3

EXPERIMENTAL

3.1. Materials

Paraffin with a melting point of 53-57°C, type B gelatin from bovine skin, 1-ethyl-3-(3-dimethyl-aminopropyl) carbodiimide HCl (EDC), N-hydroxysuccinimide (NHS), (2-(N-morpholino) ethanesulfonic acid) hydrate (MES), acetone, tetrazolium salt (3-[4,5-dimethylthiazolyl-2-yl]-2,5-diphenyltetrazolium bromide), sodium alginate from brown algae (medium viscosity), sodium chloride, sodium citrate, Poly-L-lysine hydrobromide (30,000-70,000), Thiazolyl Blue Tetrazolium Bromide, Phalloidin-TRICT were supplied by Sigma. 1,4-dioxane, n-Hexane, cyclohexane, acetone, ethanol, methanol, isooctane, tween 80, span 80, calcium chloride, 2.5S murine-NGF were all obtained from Merck. Poly (vinyl alcohol) (PVA) with a molecular weight of 25,000 was purchased from Polyscience. RPMI 1640, Horse Serum, Fetal Bovine Serum, L-glutamine and antibiotic (penicillin, streptomycin), 2,3-Bis(2-methoxy-4-nitro-5-sulfophenyl)-2H-tetrazolium-5-carboxanilide (XTT) were purchased from Biological Industries. Glutaraldehyde was from Alfa-easer, sieves were purchased from Reich, NGF ELISA kit from Boster Immunoleader and DAPI from Thermo Fisher Scientific.

3.2. Molding

To prepare scaffolds, a Teflon mold was designed and custom made. It has 24 wells, each with a diameter of 1.7 cm and depth of 1.5 cm (Figure 3.1). It is composed of two parts, lower part has 24 spurs which are suitable for upper part holes and these 2 parts are assembled to form an impermeable mold structure.



Figure 3.1. Custom made 20 well Teflon mold.

3.3. Preparation of Paraffin Spheres

Salt-leaching is a very popular technique to fabricate scaffolds from a variety of polymers. In this process after formation of polymer/salt composite the salt is leached out with water to form the pores of the polymer foam. But if the polymer is gelatin which is dissolved in water, porogen agents like sugar or salt cannot be used, thus, paraffin was chosen as a porogen agent.

To prepare paraffin spheres, the protocol suggested by Ma and Choi (2001) was used. First, 1% PVA solution was prepared in water bath at 80°C with magnetic stirring. 12 g paraffin in a glass vial was heated to melt on a hot plate at 72°C and added to the PVA solution. The mixture was vigorously stirred with a mechanical stirrer. Ice-cold water is poured into the stirred suspension to solidify the paraffin spheres. The suspension containing the paraffin spheres was then poured into a sieve with an opening of 100 μm to sift out the paraffin particles smaller than 100 μm . Next, paraffin spheres were washed with distilled water for three to five times to remove the residual PVA and dried in air for 1 week. Finally, the spheres were sieved with sieve series of 150 μm , 250 μm , 425 μm and 600 μm to separate them into different size ranges and stored in a desiccator until use.

3.4. Preparation of Gelatin Scaffolds

0.4 g of paraffin spheres were added to the teflon mold. A flat metal plate was used to help settlement and interconnection of spheres, on the top surface of the paraffin spheres. The mold was then preheated at 37 °C for 50, 100, 200 and 400 min to ensure that the paraffin spheres were interconnected.

3.4.1. Preparation of Nanofibrous Scaffolds

Scaffolds were fabricated by combining thermally induced phase separation (TIPS) and porogen leaching techniques (Liu and Ma, 2009). 1.0 g gelatin (type B, from bovine serum) was dissolved in 10 ml water and 10 ml ethanol solvent mixture at 45 °C on water bath. 0.35 ml of this solution was cast onto the paraffin sphere assemblies drop by drop. To remove air trapped inside the paraffin spheres assemblies vacuum was applied for 2-3 minutes at 37°C (Chen and Ma, 2004). The gelatin solution in the paraffin assembly is phase separated at -80 °C for 5h. Next, the composites were immersed in cold ethanol (-18 °C) for 24 h to remove from the mold and transferred into 1,4-dioxane for 24 h for solvent exchange. 1,4-dioxane was changed three times during 24 h. The composite was then kept in a freezer at -18°C for 12 h until completely frozen, freeze-dried for 4 days and vacuum dried at 52 mbar (according to 1,4-dioxane boiling point) at room temperature for another 3 days. To leach out paraffin spheres, gelatin/paraffin composites were soaked in hexane. Hexane was changed every day two times for 3 days to ensure paraffin removal from the scaffold. To accelerate the dissolution of paraffin spheres, this was done in an oven at 37 °C. Cyclohexane was then used to exchange hexane in the scaffold. Before freeze-drying, scaffolds were kept in the taken to the nitrogen injection evaporator for one hour to remove organic solvents, frozen at -18 °C for 12 h. As a final step, the scaffolds were freeze-dried at between -10°C and -5 °C for 4 days and then vacuum dried at 153 mbar (according to cyclohexane boiling point) at room temperature for another 3 days.

3.4.2. Preparation of Solid-Walled (SW) Scaffolds

A similar procedure was used to prepare the SW-gelatin scaffolds except that phase separation did not occur. After the gelatin solution was cast onto the paraffin spheres assembly, the gelatin/paraffin composite was air-dried for 1 week. Hexane was then used to leach out paraffin in the gelatin/paraffin composite and SW-gelatin scaffolds were obtained by direct air-drying.

3.5. Preparation of Channeled Nanofibrous Scaffolds

For the preparation of oriented scaffold, needles with different diameters were inserted into a capillary (Figure 3.2). Gelatin solution of varying concentrations injected into the mold. Mold was kept -20°C for phase separation for 5 h and transferred into ethanol to remove the needles and scaffolds from the mold and to exchange solvent with ethanol overnight. Samples were immersed into 1,4- dioxane for 2 days to stabilize the nanofibrous structure and freeze-dried for 3 days.

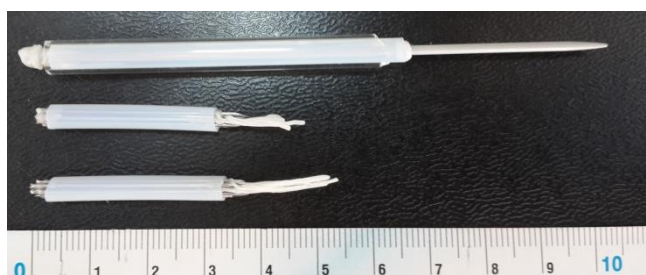


Figure 3.2. Appearance of the teflon molds with different number of needles.

3.6. Chemical Crosslinking of 3D NF and SW Gelatin Scaffolds

1-ethyl-3-(3-dimethyl-aminopropyl) carbodiimide HCl (EDC) with N-hydroxy-succinimide (NHS) were used as cross-linkers of gelatin scaffolds with NHS to EDC molar ratio of 0.2. (Figure 3.3). The reaction shown in Figure 3.3 was carried out in (2-(N-morpholino) ethanesulfonic acid) hydrate (MES) buffer (pH 5.3, 0.05 M) at 4°C for 24h. Acetone/water with a ratio of 90/10 (v/v) was used instead of pure water to protect

the nanofibrous structure (Liu and Ma 2009). After cross-linking reaction, the scaffolds were washed with distilled water at 37 °C for 3 times. Next, scaffolds were frozen at -18 °C for 12 h, freeze-dried for 2 days and stored in a desiccator for later use. Calculations for determining amount of EDC, NHS, free COOH, acetone and water used in the reaction were shown in Appendix A1.

Scaffolds were crosslinked with different molar ratios of EDC to free COOH groups in gelatin ($\text{EDC}/\text{COOH}_{\text{free}}$) and the degree of crosslinking density was determined by ninhydrin assay and swelling ratio of scaffolds.

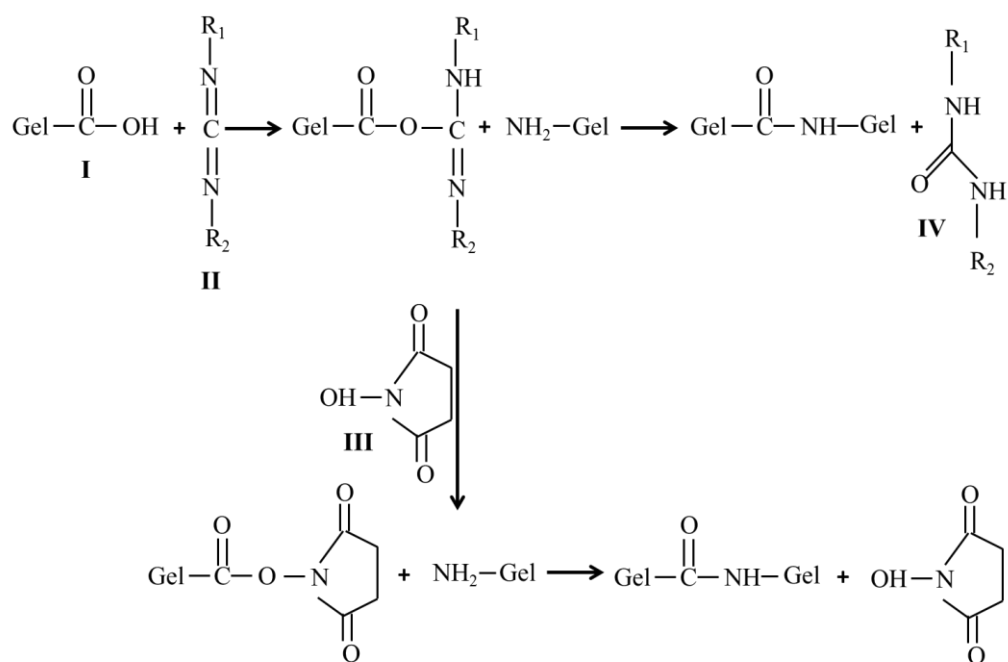


Figure 3.3. Crosslinking reaction of gelatin (I) with EDC (II) and NHS (III), (IV is iso-urea byproduct).

3.6.1. Ninhydrin Assay

Ninhydrin test is used for the determination of amino acids and proteins with a free $-\text{NH}_2$ group. When such an $-\text{NH}_2$ group reacts with ninhydrin, a purple-blue complex is formed. To determine the amount of free amino groups of gelatin after crosslinking reaction (Starcher B. 2001), ninhydrin reagent buffer was prepared by dissolving 200 mg of ninhydrin in a mixture of 7.5 ml of ethylene glycol and 2.5 ml of 4 N acetate buffer. Then, 250 ml of the stannous chloride was added to the suspension

with stirring. Preparation of 4 N sodium acetate buffer was prepared by dissolving 54.4 g of sodium acetate trihydrate in 10 ml of glacial acetic acid and water up to 50 ml total volume. The pH of solution was adjusted to 5.5. Stannous chloride solution was prepared with the addition of 5 mg of SnCl₂ to 50 ml of ethylene glycol. After preparing solutions scaffolds were taken to the glass tube and 1 ml of ninhydrin reagent was added onto crosslinked scaffolds in glass tube and tubes were floated in boiling water for 30 min. Then, tubes were removed from the bath and cooled to the room temperature. 100 µl of each sample was taken to the 96 well plates and absorbance was measured at 575 nm.

3.6.2. Determination of Swelling Ratio

In order to determine swelling ratio of scaffolds, crosslinked gelatin scaffolds were weighed (W_0) and they were immersed in phosphate buffer for 2 h at room temperature. The swollen scaffolds were blotted with a tissue, and weighed again (W). The swelling ratio was calculated according to the following formula:

$$S = \frac{(W - W_0)}{W_0} \quad (3.1)$$

3.7. Characterization

3.7.1. Surface Morphology Examination

The morphology of the paraffin spheres, solid-walled and nanofibrous scaffolds were examined by scanning electron microscopy (SEM) on a Philips XL-30SFG model. The samples were coated with gold using a Magnetron Sputter Coating Instrument.

3.7.2. Porosity

Porosity of the scaffolds, ε , was calculated as:

$$\varepsilon = 1 - D_p / D_o \quad (3.2)$$

where D_p is the skeletal density of gelatin foam, and D_o is the density of gelatin. D_p is determined by: $D_p = 4m/(\pi d^2 h)$, where m is the mass, d is the diameter, and h is the thickness of the foam. For gelatin type B (from calf skin, approx. 225 Bloom), $D_o = 1.35 \text{ g/cm}^3$. The fiber diameter and length of the NF scaffolds were evaluated from SEM images with the image analysis software.

3.7.3. Swelling Volume Ratio Measurement

The swelling volume ratio of scaffolds was measured after crosslinked scaffolds were immersed in water for 24 hours. The scaffold swelling volume ratio was quantified as V_1/V_0 , where V_0 and V_1 represent volume of the crosslinked scaffold before and after immersing in water.

3.7.4. Mechanical Test

Mechanical properties of scaffolds were determined according to the protocol suggested for open-cell foam type of materials similar to our scaffolds. Unidirectional compression test was performed on hydrated scaffold samples using a mechanical tester (Schimadsu AG-I 5 kN). All samples were circular discs 16 mm in diameter and 2 mm in thickness. Before mechanical test, scaffolds were kept in PBS (pH=7.4) for 24 h (Wang and Spector, 2009). Five specimens were tested for each sample. Values for the compressive modulus of elasticity was recorded at a strain of 0.5%. The averages values with standard deviations were reported.

Tensile test of channeled scaffolds was adapted in the shape of film (40.0mm long, 10.0 mm wide) and thickness of 0.45 mm, 0.60 mm and 0.70 mm for 4%, 5% and 6% gelatin films, respectively. Films were attached to the clamps (gauge length:10 mm) of the instrument and tested at a rate of 10 mm/min.

3.8. *In vitro* Degradation of Scaffolds with MMP-9 Enzyme

To determine *in vitro* degradation of nanofibrous and solid walled scaffold, their initial weights were recorded as W_0 . Then scaffolds were kept in PBS and PBS contained 15 ng/mL of Matrix Metalloproteinase-9 (MMP-9) (plasma level of MMP-9 in the body) at 37° C and medium was changed every 2 days. At the end of the 28 days, scaffolds were washed with water, lyophilized for 3 days and their weights were recorded (W_1). The degradation percent was calculated as:

$$\% \text{ Degradation} = \frac{(W_0 - W_1)}{W_0} \times 100 \quad (3.3)$$

3.9. Preparation of Alginate Microspheres

Alginate particles were prepared by homogenization and reticulation of alginate with calcium ions in a water-oil system (Ciofani et al. 2008). After mixing iso-octane, Tween 80 and Span 80, 1.0 % alginate solution was added to this mixture and homogenized at 15,000 rpm. During homogenization 100% CaCl_2 was added drop by drop to reticulate alginate polymer. After additional homogenization for 30 seconds, system was allowed to settle and upper phase was removed. Then particles were washed and fixed with acetone and water mixture 1:10 (v/v) at 10000 rpm. Protein loaded alginate microspheres were prepared during particle production step. 100 μl of 10 $\mu\text{g/ml}$ protein solution was added to the solution containing alginate solution and then this mixture was added to the isooctane, Tween 80 and Span 80. Poly(L-lysine) coating procedure of alginate microspheres was given at Appendix A.4.

3.10. Determination of NGF Loading and Release from Alginate Microspheres

For the determination of encapsulation efficiency of NGF, alginate microspheres were transferred to the siliconized tube and 1 ml of 3% (w/v) of Na-Citrate solution was added. The tube was rotated at 300 rpm in an orbital shaker. Ca^{2+} ions in the microspheres was replaced with Na^+ ions destroying the structure of the particles. Then tube was centrifuged at 10,000 rpm for 5 minutes and supernatant was kept at -20°C . NGF amount was determined with mouse NGF ELISA kit and encapsulation efficiency was calculated as:

$$\text{Encapsulation Efficiency (EE \%)} = \frac{\text{Loaded amount of NGF}}{\text{Initial amount of NGF}} \times 100 \quad (3.4)$$

For the release study, alginate microspheres were put into the 1 ml starvation medium (RPMI 1640 included 1% Horse Serum) and shaken at 180 rpm at 37°C . At the different time intervals, tubes were centrifuged at 10,000 rpm for 5 min and supernatant was analyzed to determine the concentration of released NGF. 1 ml fresh starvation medium was added on the precipitated particles to continue release studies.

3.11. Attachment of Alginate Microspheres onto Gelatin Scaffold and Release of NGF from the Scaffolds

Gelatin is a derivative of collagen and like collagen, gelatin also has the integrin binding domain RGD sequence. This property makes gelatin advantageous in the case of cell attachment. Moreover, in the presence of 1-ethyl-(dimethylaminopropyl) carbodiimide (EDC), amide linkages between Lysine residue of gelatin and the carboxylate moieties of alginate polysaccharide is formed on polymer backbone (Hermanson 1996). Thus, EDC was used not only for crosslinking the scaffold but also for attaching the alginate spheres to the scaffold (Figure 3.4).

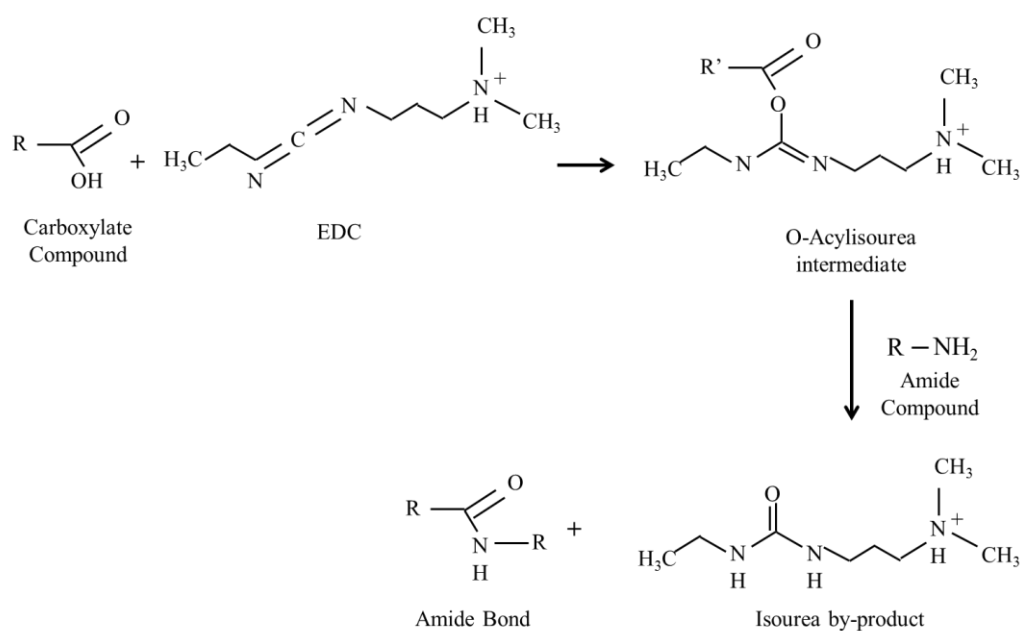


Figure 3.4. Crosslinking of alginate and gelatin in the presence of EDC (Source: Hermanson 1996).

For the attachment of microspheres, 1.8 mg of total alginate particles were separated and resuspended into 100 μ L of crosslinking solution in the same composition with crosslinking reaction and 50 μ L of this solution was added onto two sides of disc shaped scaffold with diameter of 16 mm and height of 2 mm. Scaffolds were kept in crosslinking solution for 24 h at +4°C. Crosslinked scaffolds were washed with deionized water 3 times and freeze-dried for 3 days.

Amount of alginate particles attached onto gelatin scaffold was determined with phenol sulfuric acid assay. The assay involves mixing sugar, water and phenol then adding sulfonic acid and allowing the heat of reaction to drive formation of the absorbing compound. In this method, 0.5 ml of alginate was mixed with 0.5 ml of distilled water followed by adding 1 ml of 5% (w/v) phenol and 5 ml of concentrated sulfuric acid. In the case of alginate attached scaffolds, scaffolds were taken into 1 mL water then 1 ml of 5% (w/v) phenol and 5 ml of concentrated sulfuric acid were added into the tube. The mixture was vortexed at room temperature for 15 min (Gu et al. 2004). The sample was then transferred to a 96-well plate, and absorbance was measured at 488 nm. As a negative control same size of plain scaffold and as a positive control alginate particles with the same amount attached to the gelatin scaffold were used. Percent of attachment of microspheres was calculated using Equation 3.5 where A_0 was absorbance value of microspheres attached onto gelatin scaffold (positive

control), A_1 was absorbance value of alginate microspheres attached gelatin scaffold after subtraction of only gelatin scaffold absorbance (negative control).

$$\% \text{ Attachment} = (A_1/A_0) \times 100 \quad (3.5)$$

3.12. *In vitro* Cell Culture

Rat adrenal pheochromocytoma (PC12) cell line was kindly donated by the group of Dr. Pınar AKAN (University of Dokuz Eylül, Department of Medical Biochemistry). Cells were cultured in 0.1 mg/ml poly-L-lysine coated 75 cm² flask in RPMI 1640 medium supplemented with 10% horse serum, 5% fetal bovine serum, 1% L-glutamine, 1% Penicilin/Streptomycin (100 U/ml penicillin and 100 µg/ml streptomycin) and incubated at 37 °C in a humidified with 5% CO₂ and 95% air.

3.12.1. Determination of Growth Curve for PC12 Cells

To determine growth curve of PC12 cells in a certain time, (3-(4,5-Dimethylthiazol-2-yl)-2,5-diphenyltetrazolium bromide (MTT) was used. PC12 cells were plated to the pre-coated 96 well plate at a concentration of 500 and 1000 cells/well and incubated with complete medium. At the end of certain time 15 µl of 5 mg/ml of MTT solution was added to the wells and kept at 37°C for 4 hours. Then solution was removed and 100 µl of DMSO was added to dissolve formazan salts. The absorbance of dissolved salt was measured at 540 nm. During the experiment, the culture medium was changed every three days with fresh media and experiments were performed quintet.

3.12.2. Determination of NFG Amount for the Differentiation of PC12 Cells

NGF amount required for the differentiation of PC12 cells was determined with microscopic observation. Cells were seeded to the PLL coated plate in complete medium for attachment, after 24 h cells were seeded with starvation medium including

diminished amount of horse serum following another 24 h NGF was added to the medium at 25ng/ml, 50 ng/ml and 100 ng/ml concentrations. The medium was changed every 2 days and experiments continued for 10 days. Cells grown only in starvation medium was used as controls.

3.12.3. Determination of Attachment and Proliferation of PC12 Cell onto Gelatin Scaffold

PC12 cells were seeded onto cross-linked SW and NF gelatin scaffolds. After overnight penetration, samples were harvested, washed in PBS, fixed in 2.5% glutaraldehyde for 20 min, dehydrated in a series of graded concentrations of ethanol (30%, 50%, 70%, 80%, 90%, 100%) each for 5 min and vacuum-dried. Dehydrated constructs were cut, coated with gold and examined in SEM (Li et. 2005).

The fixed cells were permeabilized with 0.5% Triton-X for 10 minutes. Then cells were dyed with Phalloidin (0.5 µg/ml) for 45 minutes and DAPI (1 µg/ml) for 10 minutes. Next, scaffolds were embedded to the Tissue-Tek® O.C.T.™ and sectioned with cryotome. Sections were coated with mounting media and observed with fluorescent microscope.

In order to determine proliferation of PC12 in the gelatin scaffold, 2,3-bis-(2-methoxy-4-nitro-5-sulphophenyl)-2H-tetrazolium-5-carboxanilide (XTT) has been used to replace MTT, since formed formazan dye is water soluble. Only in living cells mitochondria is capable to reduce XTT to form an orange colored water soluble dye. Therefore, the concentration of the dye is proportional to the number of metabolically active cells (WEB 1). To determine proliferation, cell culture plates were coated with Poly (2-hydroxyethyl methacrylate) to inhibit adhesion of cells to the plates. Scaffolds were pre-wetted in pre-coated 96 well plate for overnight. Cells were seeded onto pre-wetted scaffolds and at the end of predetermined times, 50 µL of XTT working solution was added to the wells and kept at 37°C for 4 hours. Then scaffolds were removed from wells and photometric measurement was carried out at 450 nm.

3.13. Determination Bioactivity of Released NGF from Alginate Microspheres

Activity of NGF released from microspheres was determined with PC12 cell assay. Microspheres were first kept in PBS solution for 24 h in order to destroy the structure. After centrifugation at 10,000 rpm for 5 minutes, supernatant was separated and kept -20°C until needed. These solutions were added every 2 days to the cell culture medium of PC12.

3.14. Determination of PC12 Cell Differentiation on the NGF Loaded Alginate Microspheres Attached Nanofibrous Gelatin Scaffold

Scaffolds incorporated with NGF loaded microspheres were put into 24 well plate and 30,000 cells/scaffold were added on each scaffold and 300 μ L of starvation medium was added to the wells. Medium was changed every 2 days and at the end of the 4th and 10th days scaffolds were removed from wells and washed in PBS, fixed with 2.5% glutaraldehyde for 20 min, dehydrated in a series of graded concentrations of ethanol (30%, 50%, 70%, 80%, 90%, 100%) each for 5 min and vacuum-dried. Dehydrated constructs were cut, coated with gold and examined in SEM.

3.15. Statistical Analysis

The significant differences between the groups were evaluated by ANOVA analysis by Tukey's method with 95% confidence interval. The results were presented as mean \pm standart deviations which were calculated from at least three independent experiments.

CHAPTER 4

RESULTS AND DISCUSSIONS

This thesis aims to fabricate macroporous nanofibrous scaffolds incorporated with protein loaded microspheres for neural tissue engineering applications. The results obtained are grouped under four sections. In the first section nanofibrous and solid-walled scaffolds were characterized in terms of their structural and mechanical properties. In the second part preparation of nerve growth factor (NGF) loaded alginate microspheres were discussed, release of NGF from alginate particles was investigated and attachment of microspheres to the scaffold was characterized. In the third section, the growth behavior of PC12 cells chosen as a model neural cell line, response of the cells to the different NGF concentration in 2D culture and their attachment and proliferation behavior in the nanofibrous (NF) and solid walled (SW) gelatin scaffolds were investigated. In the fourth section, the differentiation of PC12 cells in the nanofibrous scaffolds integrated with NGF loaded microspheres was investigated.

4.1. Preparation and Characterization of Macroporous Nanofibrous and Solid-Walled Scaffolds

4.1.1. Preparation of Porogen Agent

Macroporous structure in the scaffolds was created with the help of a porogen agent, paraffin which was emulsified in a heated Poly (vinyl alcohol) (PVA) solution. Ma et al. (2001) used emulsification and dispersion method to produce paraffin spheres with a uniform size distribution. They reported that the stirring rate and the concentration of the PVA solution were important in controlling the size distribution and the shape of the spheres. High stirring rates and high PVA concentration resulted in smaller particles with a uniform spherical shape, whereas slow stirring rates and low PVA concentration resulted in larger nonspherical particles. Based on these findings, in this study, three different concentrations of PVA (0.5%, 0.75% and 1.0%) were tried to

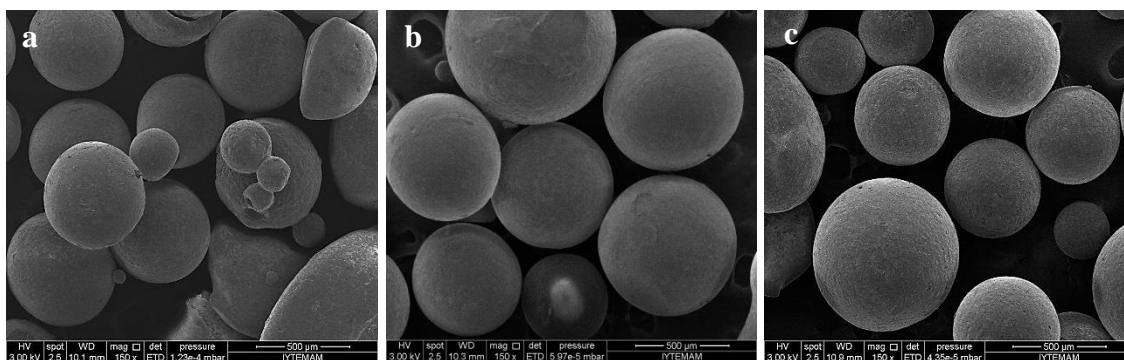


Figure 4.1. SEM micrographs of paraffin particles prepared with different PVA concentrations. a- 0.5 %, b- 0.75 %, c- 1.0 %. Stirring rate: 578 rpm.

obtain uniform spherical particles. It was observed that the concentration of PVA did not influence the particle shape, they were all spherical, however in 1.0% PVA concentration paraffin spheres were smallest and their shapes were uniform (Figure 4.1).

For a fixed amount of paraffin and PVA concentration (1%), volume of PVA solution and stirring rates were changed to observe their effects on the shape of the particles (Table 4.1). It was observed that to achieve appropriate dispersion and spherical particles, volume of the PVA solution should be above 400 ml. Spherical paraffin particles with desired size ranges were obtained with 600 ml of PVA solution at a stirring rate of 578 rpm (Figure 4.2).

Table 4.1. The influences of volume of PVA solution, amount of paraffin and stirring rate on the shape of paraffin particles.

Volume of 1 % PVA solution (ml)	Amount of paraffin (g)	Stirring rate (rpm)	Shape of the particles
100	5	320	Sheet and rope like structure around rotor screw
200	5	400	Sheet and rope like structure around rotor screw, non spherical paraffin particles
400	5	400	Sheet and rope like structure around rotor screw, spherical particles
600	12	500	No sheet like structure and spheres were produced with different sizes
600	12	578	Smaller spheres were produced

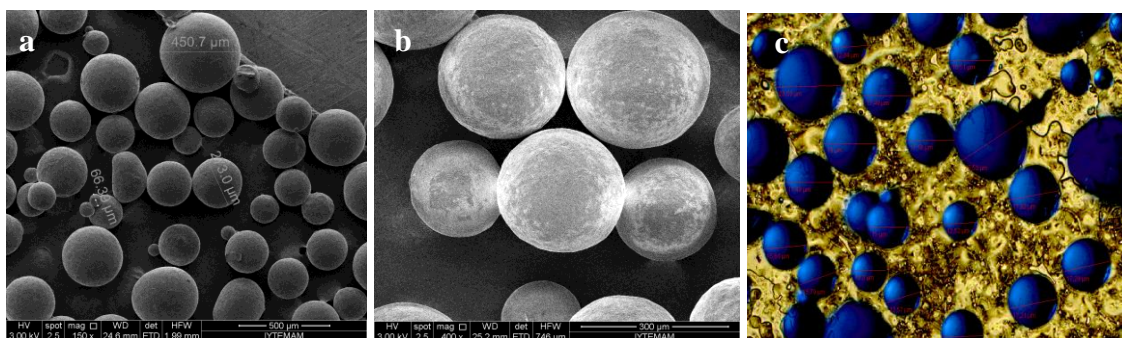


Figure 4.2. SEM pictures of paraffin spheres with a magnification of A-150X, B- 400X and C- Phase contrast microscope images of paraffin spheres produced in 600 ml solution containing 1% PVA and stirred at a rate of 578 rpm.

Paraffin spheres were dried in air, and then sieved into 2 different size ranges; 250-425 μm and 425-600 μm . The reproducibility of microspheres production was checked in terms of average particle size and size distribution determined with the phase contrast microscope measurements (Figure 4.3). For this purpose, particles obtained from three different batches were stucked onto the coverslips and for each batch, at least 300 measurements were taken. The results summarized in Table 4.2 showed that the size of the spheres was ranged between 100-800 μm with maximum yield at around 400 μm (Figure 4.3).

Table 4.2. Maximum and minimum sizes of paraffin spheres

	Max (μm)	Min (μm)	Mean (μm)	Std. Dev.
1	836	119	406	134
2	829	128	402	121
3	865	101	359	175

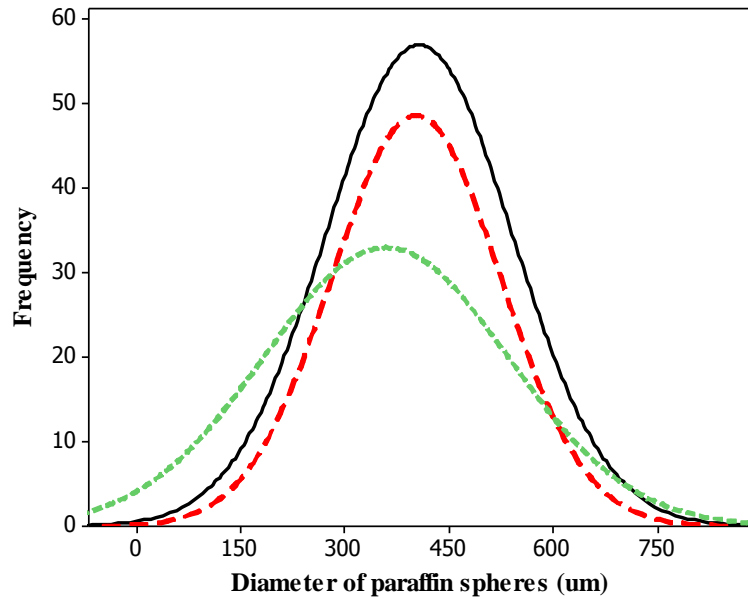


Figure 4.3. Particle size distribution of paraffin spheres obtained from the three different batches.

4.1.2. Preparation of Nanofibrous and Solid Walled Scaffolds

An ideal scaffold should have well-connected macroporous structure. In order to provide interconnectivity of macropores, paraffin spheres were preheated at 37 °C for 20 min, 50 min, 200 min and 400 min in a Teflon mold. For the preparation of solid walled scaffold, gelatin solution was added onto paraffin spheres, air dried for 1 week and paraffin spheres were removed with hexane. The SEM pictures in Figure 4.4 showed that all the preheating times allowed interconnection of pores; however more interconnected structures were observed with the 200 and 400 min heating times. Thus, 200 and 400 min preheating times were chosen for the preparation of the scaffolds. Nanofibrous structure in a scaffold plays a significant role in mimicking natural extracellular matrix environment. Nanofibrous scaffolds were prepared with temperature induced phase separation (TIPS) technique. In TIPS technique, under certain temperature, a homogeneous polymer solution becomes thermodynamically unstable and separates into a polymer-rich phase and a polymer-lean phase. After removal of the solvent, the polymer-lean domains become pores, while the solidified polymer-rich phase forms a 3D structure (Khang et al. 2007). The choice of solvent/nonsolvent system is critical for generating nanofibrous structure in TIPS

technique. In this study we have chosen ethanol as a nonsolvent of the gelatin to adjust the interactions between gelatin and solvent molecules, hence, altering phase separation condition when gelatin solution underwent gelation.

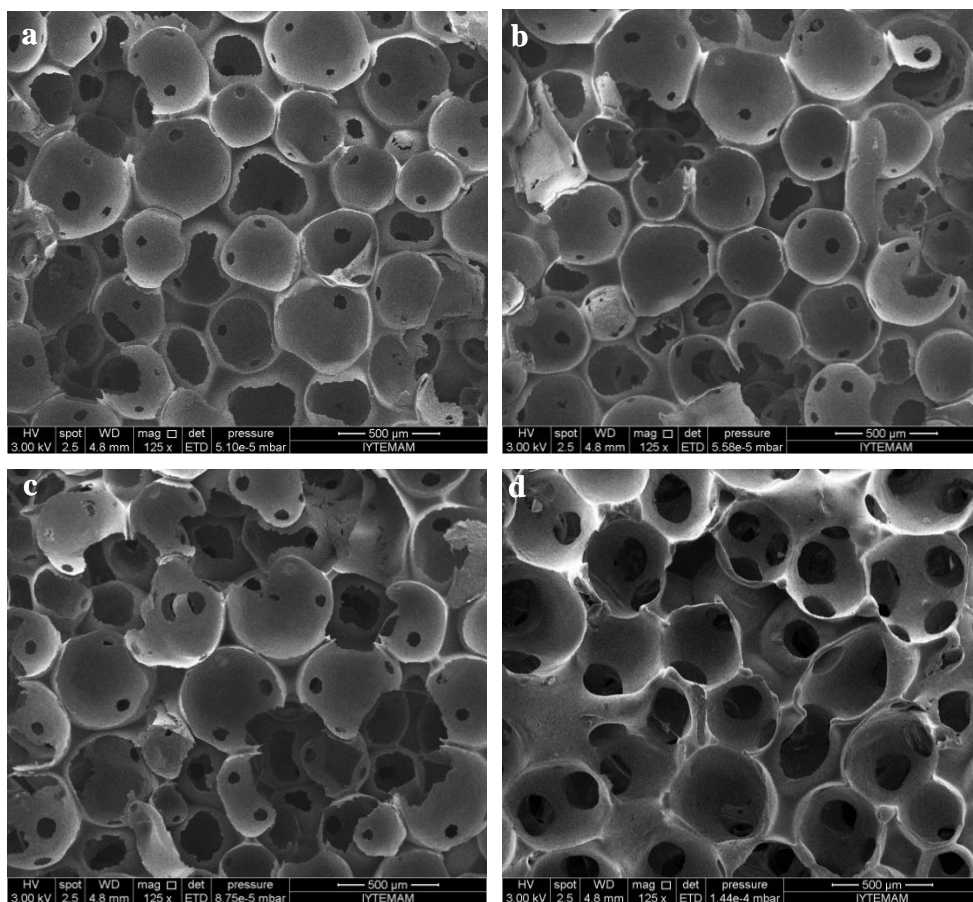


Figure 4.4. SEM images of the solid walled scaffolds obtained with different pre-heat treatment times; a- 20 min, b-50 min, c-200 min, d-400 min at 37°C.

The appearance of NF scaffolds prepared with TIPS was white and opaque; whereas air dried SW scaffold was yellowish (Figure 4.5). The pore wall surface of the gelatin scaffold which was air dried was smooth and nanofibrous architecture was not observed (Figure 4.6a and 4.6b). On the other hand, the scaffold prepared with TIPS method had a nano-fibrous network (Figure 4.6c and 4.6d). Liu and Ma (2009) reported that the solvent exchange after gelatin solution was phase separated and became a gelatin gel, was an important step in maintaining the nanofibrous structure. They obtained gelatin foam when the gelatin gel was directly freeze-dried without solvent exchange after phase separation. The structure of the foam was found similar to the solid walled scaffolds.

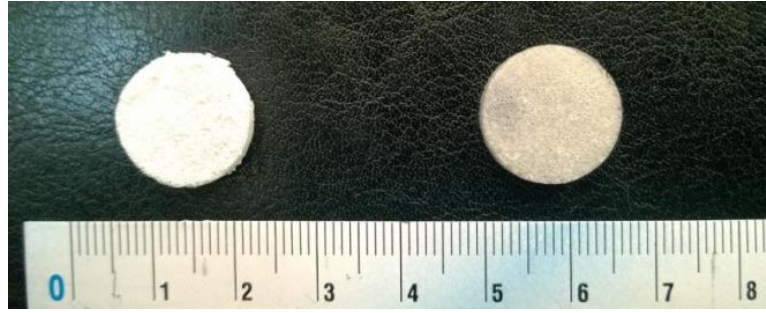


Figure 4.5. General appearance of NF(left) and SW(right) scaffolds.

In the literature, different parameters such as type of nonsolvent (ethanol, methanol, acetone, dioxane), amount of solvent and concentration of gelatin were changed to produce macroporous nanofibrous structure (Liu and Ma, 2009). In our experiments, we prepared scaffolds with 5% and 10% gelatin concentrations, 250–425 μm and 425–600 μm sized paraffin spheres as pore forming agents and 200 and 400 min interconnection times. In all experiments, gelatin was dissolved in 50/50(v/v) ethanol/water solvent mixture. Interconnected, macroporous nanofibrous scaffolds were obtained when the gelatin concentration was 10% (Figure 4.7) using both 250-425 μm and 425-600 μm sized paraffin spheres.

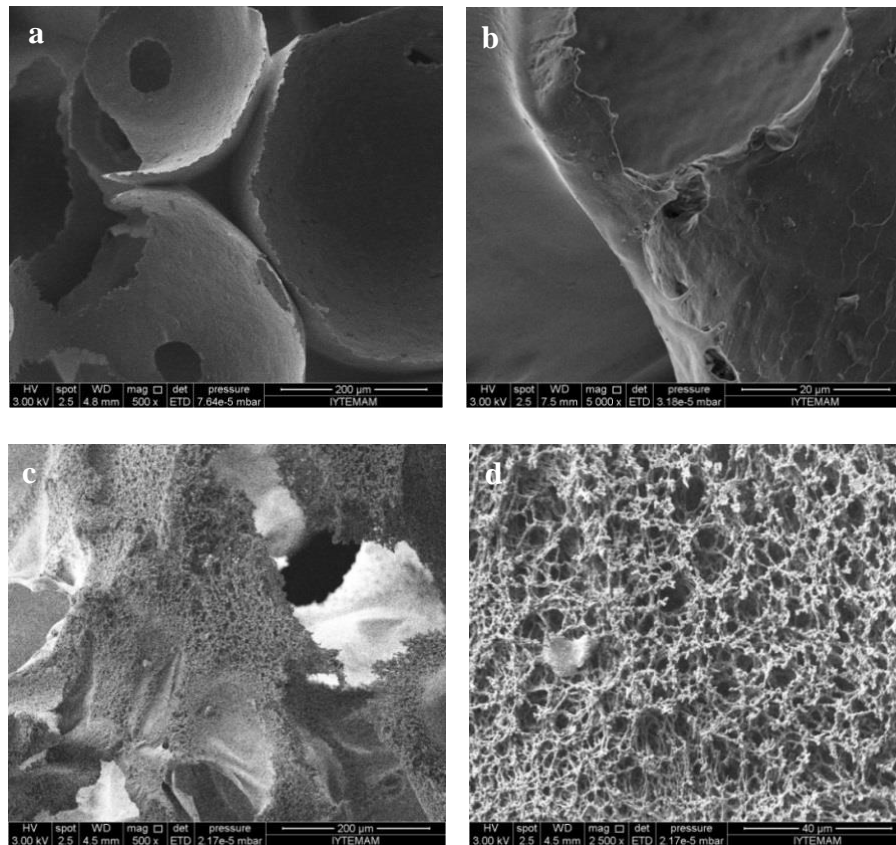


Figure 4.6. SEM micrographs of a-Solid-walled gelatin scaffold, x500; b- pore wall morphology of a, x 5,000; c- NF-gelatin scaffold, x500; d- NF-gelatin scaffold, x 2500.

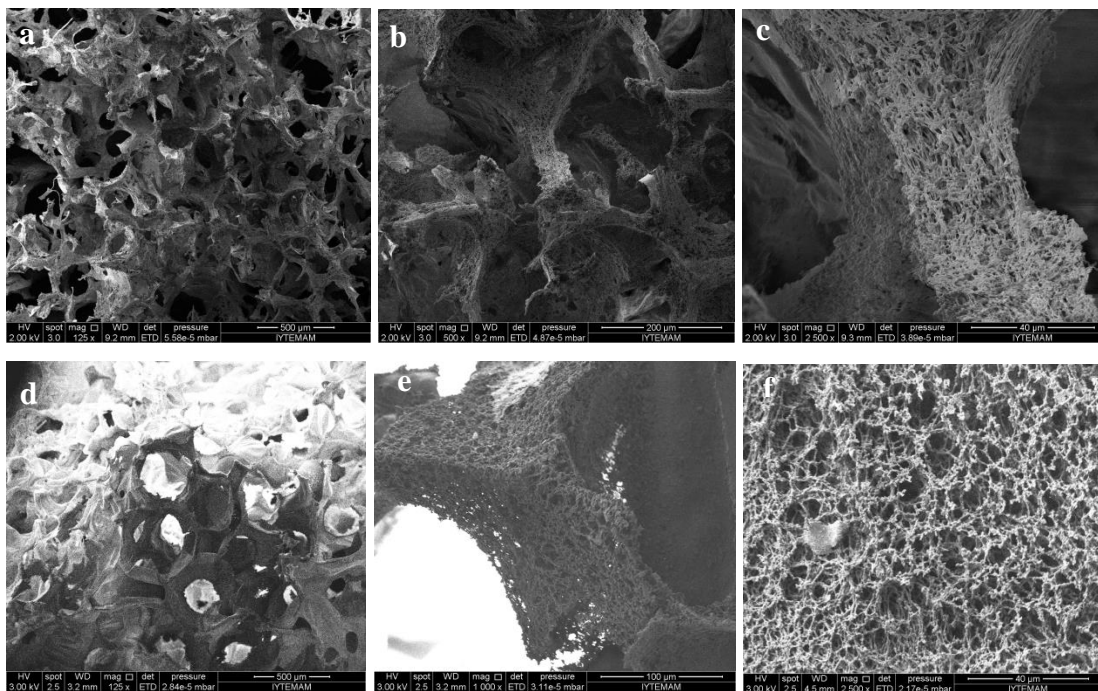


Figure 4.7. NF scaffolds prepared with 10% gelatin concentration and a-c; 250-425 μm, d-f; 425-600 μm paraffin spheres. Preheating time; 400 min.

4.1.3. Chemical Crosslinking of Nanofibrous and Solid Walled Scaffolds

The thermal and mechanical stability of gelatin should be improved by crosslinking. For the crosslinking of gelatin, several physical and chemical crosslinking methods have been described. Among them the combination of carbodiimide with NHS is generally considered to result in an efficient crosslinking reaction (Kuijpers et al. 2000). In crosslinking reaction, Liu and Ma (2009) used acetone/water or dioxane/water instead of pure water along with carbodiimide/NHS. In their experiment the EDC:gelatin ratio was 5:1 (w/w) and they observed that nanofibrous structure of gelatin scaffolds can be preserved when acetone/water or dioxane/water mixture was used. Another approach for the crosslinking of gelatin matrix is to use mole ratio of EDC to free carboxylic acid in gelatin. In our study, these two approaches were tried for crosslinking of scaffolds and as seen from the SEM images in Figure 4.8 that nanofibrous structure was protected in both cases. Amount of acetone required crosslinking reaction was calculated as 156.5 ml and 21.6 ml, when EDC:gelatin (w/w)

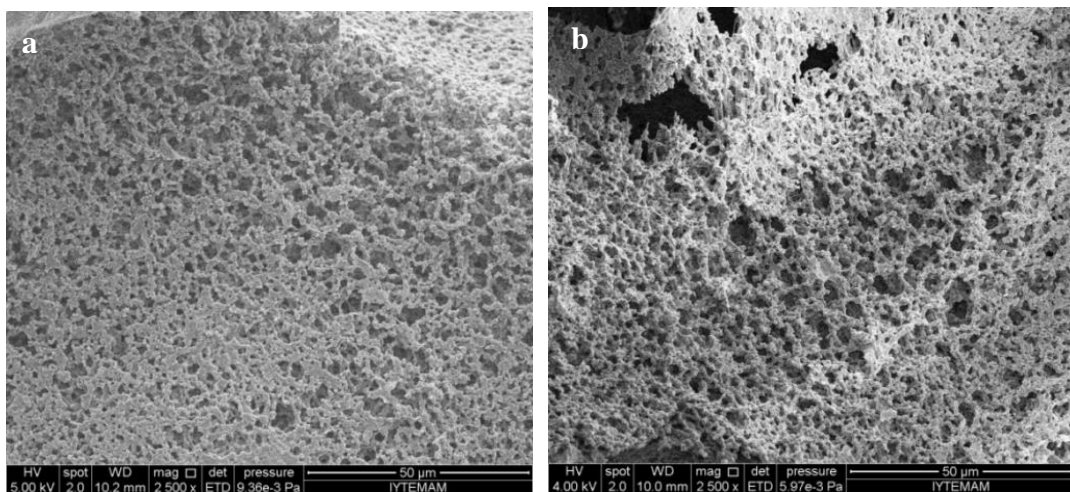


Figure 4.8. a- Cross-linked nanofibrous scaffold according to EDC: gelatin (5: 1) (w/w), b- Cross-linked NF-scaffold according to EDC: COOH_{free} (2: 1) (mole/mole).

and EDC: COOH_{free} (mole/mole) were 5:1 and as 2:1, respectively. Based on this results, it was decided to continue crosslinking reaction with acetone: water ratio of 90/10 (v/v) and EDC: COOH_{free} of 2:1 since much lower amount of acetone is required when EDC:COOH_{free} ratio is used as a basis.

In order to determine optimum EDC:COOH_{free} (mole/mole) ratio for the crosslinking reaction, free amino groups in gelatin was determined based on ninhydrin assay. Ninhydrin is originally yellow and when it reacts with with amino acid, it turns into deep purple and absorbance of this complex measured at 575 nm is directly correlated with free amino groups. Figure 4.9 shows that when EDC:COOH_{free} ratio was increased from 0 to 2, the absorbance decreased significantly which was an indication of the increase in degree of crosslinking of the scaffolds.

The swelling ratio of crosslinked scaffolds after storage in PBS solution for two hours has also been determined to choose optimum EDC/COOH_{free} ratio. By increasing EDC/COOH_{free} ratio from 0.2 to 2, the swelling capacity of the scaffolds decreased significantly as a consequence of reduced amine groups in gelatin, hence, less interaction between water and gelatin (Figure 4.10). The data shown in Figure 4.10 is in complete agreement with ninhydrin test results. According to both data, the highest crosslinking density was obtained at EDC/COOH_{free} ratio of 2, therefore this value has been chosen to prepare scaffolds for long-term biomedical applications with sufficient mechanical stability. Kuijpers et al. (2000) determined that minimum EDC:COOH_{free} ratio should be 0.8 to obtain thermally stable gelatin gels.

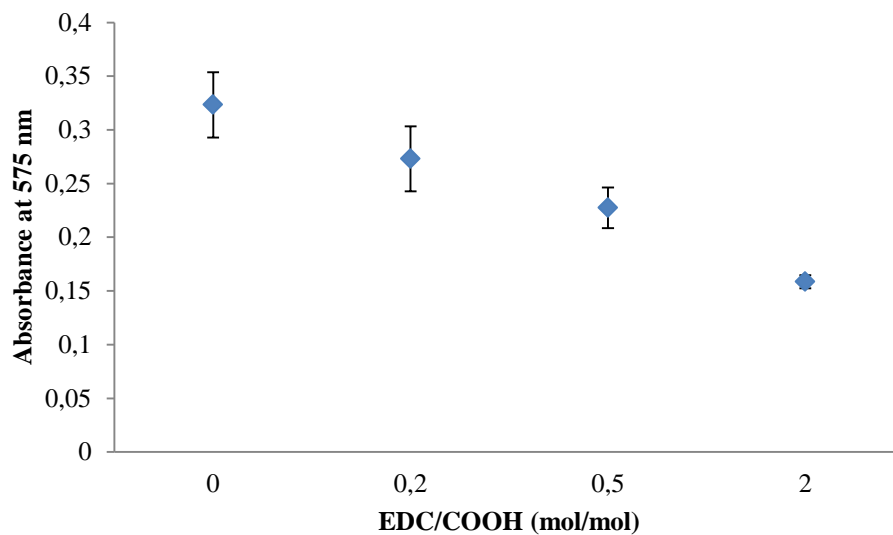


Figure 4.9. Effect of increasing ratio of EDC/COOH_{free} (mol/mol) on absorbance value.

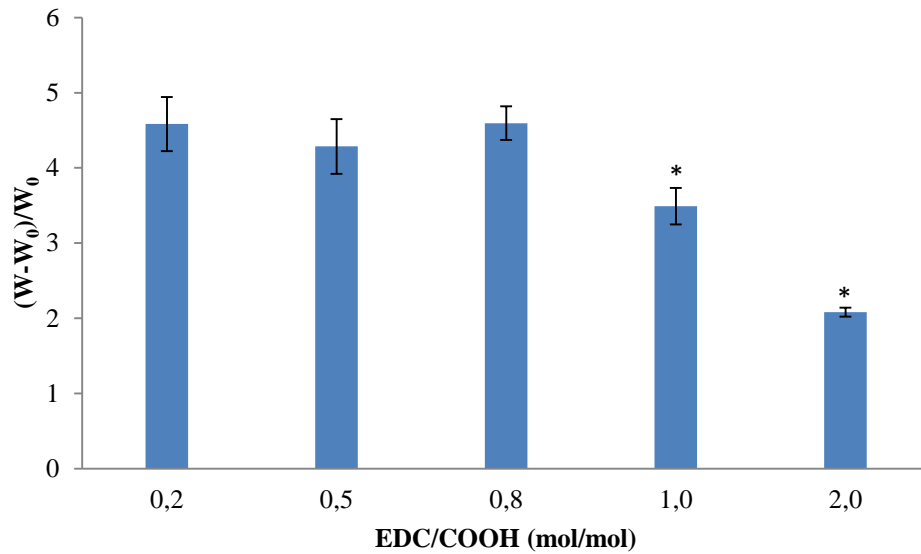


Figure 4.10. Swelling ratio of crosslinked gelatin scaffolds in phosphate buffer at room temperature. The molar ratio of NHS to EDC was 0.2.

4.1.4. Characterization of Macroporous Solid Walled and Nanofibrous Scaffolds

4.1.4.1. Porosity

The porosities of the scaffolds calculated from Equation (3.2) are listed in Table 4.3. It is seen that increasing preheating time from 200 min to 400 min did not cause significant difference in the porosity of the NF and SW scaffolds. In addition, the porosities of nanofibrous and solid walled scaffolds were found similar. Yang et al. (2004) developed porous polymeric nanofibrous scaffold using a synthetic biodegradable poly(L-lactic acid) for the *in vitro* culture of nerve stem cells. They determined the porosity of scaffolds around 85%. In another study of the same group, the porosities of the scaffolds developed for the neural tissue engineering application changed between 85-94% to depending on the concentration of polymer solution (Yang et al. 2005). The porosities of the scaffolds prepared in this study varied between 92% and 97% and these values are in agreement with those reported by Liu and Ma (2009).

Table 4.3. The influence of preheating time on the porosity of the scaffolds. Gelatin concentration: 5% and the size of the paraffin: 425-600 μm .

Type of scaffold	Preheating time (min)	Porosity
Nanofibrous	200	0.95 \pm 0.04
	400	0.97 \pm 0.07
Solid Walled	200	0.91 \pm 0.15
	400	0.94 \pm 0.08

4.1.4.2. Fiber Length and Diameter

As shown in Figure 4.11, the regions between binodal and spinodal is thermodynamically metastable. In the metastable region at low polymer concentration powder like polymer solid is obtained as a result of droplets of polymer-rich phase dispersed in the polymer-lean phase (Nam and Park, 1999). With 5% gelatin concentration, bead-like structure was observed as shown in Figure 4.12a which indicated that phase separation occurred in the metastable region. In the spinodal region, phase separation occurs through spinodal decomposition and the structure in which both the polymer-rich and polymer-lean phases are interconnected is obtained (Ma and Zhang, 1999). By increasing concentration to 10%, it was possible to move into spinodal region, hence, nanofiber structure was observed (Figure 4.12c-d). The average fiber diameter and length were determined as 528 nm and 4390 nm, respectively. It is known that in natural extracellular matrix, collagen fibers vary in diameter from 50 to 500 nm. With this fact it can be said that the fiber sizes of NF scaffold mimic size of natural collagen fiber bundles.

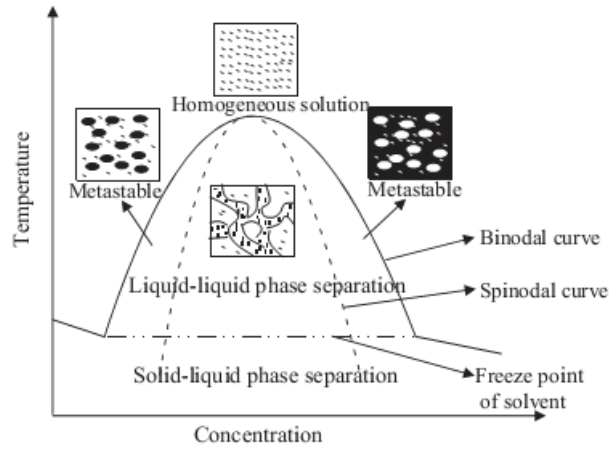


Figure 4.11. Schematic phase diagram for temperature induced phase separation (Source: Yang et al. 2004).

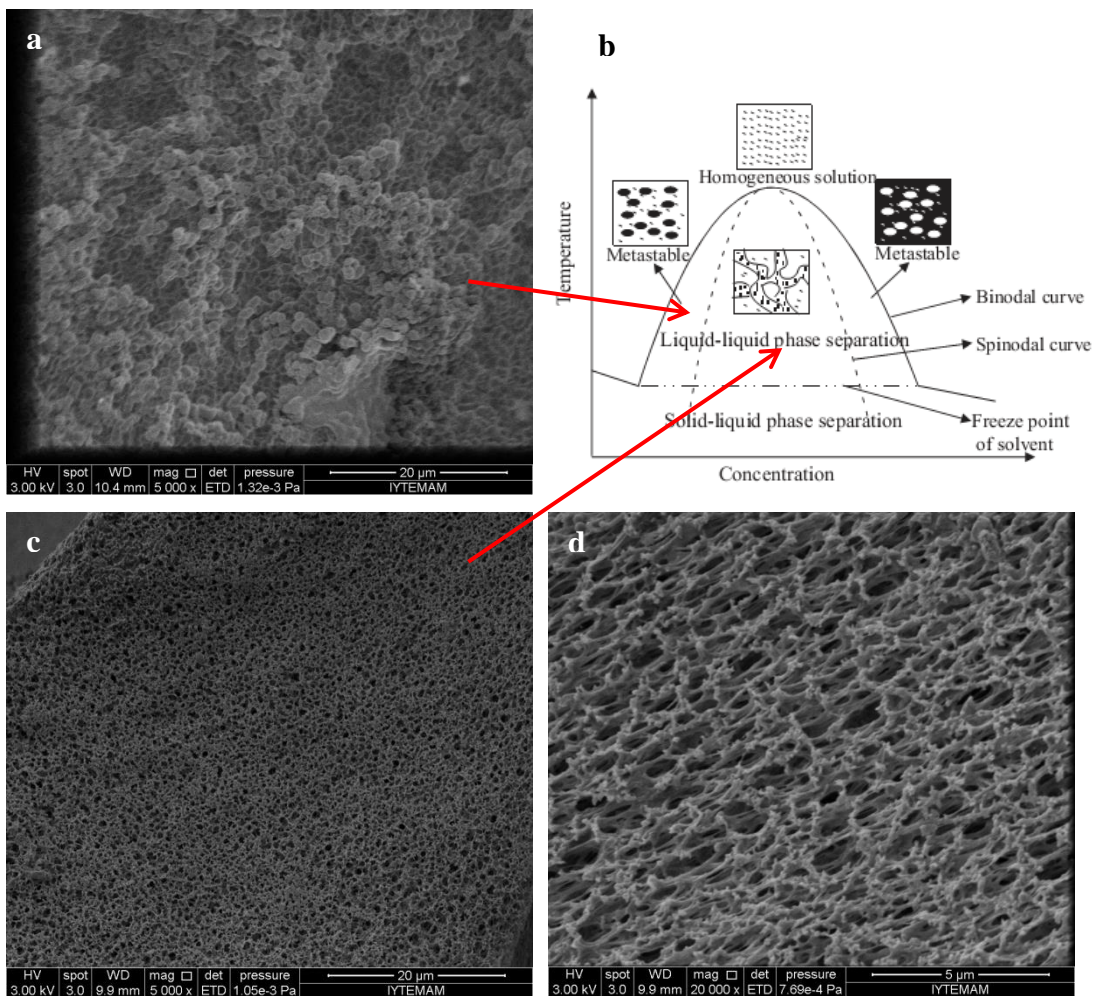


Figure 4.12. Scaffold prepared with TIPS a- 5% gelatin solution X5000, b- Schematic phase diagram of polymer solution (Source: Yang et al. 2004), c- 10% gelatin solution X5000, d- 10% gelatin solution X20000 preheating times 200 min.

4.1.4.3. Swelling Volume Ratio

To improve thermal and mechanical stabilities of gelatin scaffold before seeding the cells, the degree of crosslinking should be high. The efficiency of crosslinking reaction was determined by measuring the swelling volume ratio (V_1/V_0) of the scaffolds. It was seen that the volumes of crosslinked NF and SW scaffolds did not change significantly after immersion in water for 24 hours (Figure 4.13). This simply indicated that water soluble gelatin was completely crosslinked, hence, its swelling in water was prevented. Dimensional stability of the NF scaffolds was found better than that of SW ones as seen from standart deviation values. This can be explained by higher surface area to volume ratio in nanofibrous structure allowing more effective crosslinking rection compared to SW structures.

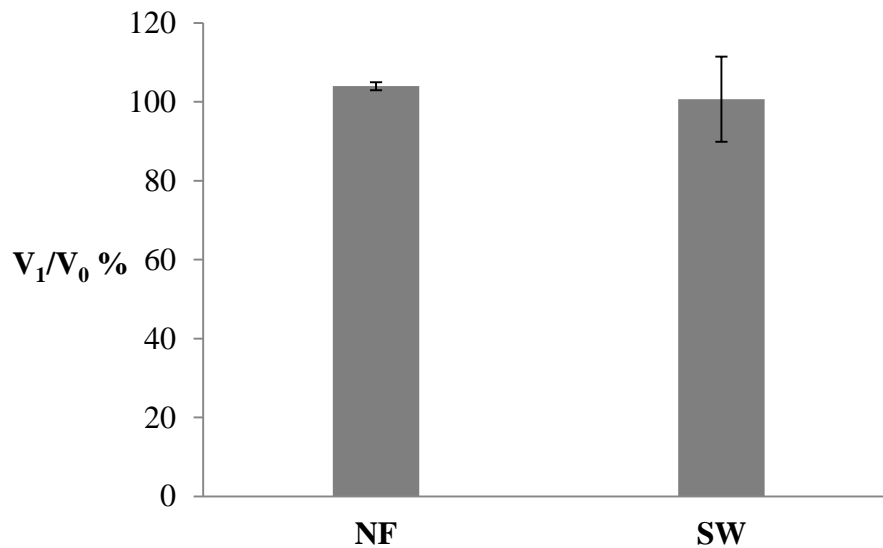


Figure 4.13. Swelling volume ratio of NF and SW scaffolds after crosslinking in acetone: water ratio of 90/10 (v/v) solution and EDC: $\text{COOH}_{\text{free}}$ (mole/mole) ratio of 2:1.

4.1.4.4. Mechanical Properties

Mechanical properties of the scaffolds should be similar to the native environment (e.g. elastic modulus). Neural cells like other cells sense mechanical properties such as matrix stiffness and respond through cell colonization, migration and biased differentiation, and alter neurite formation and trajectory. This brings a major scaffold design challenge because native brain tissue typically has an elastic modulus of 0.5-5 kPa (Pettikiriachchi et al, 2010).

After crosslinking reaction, the mechanical properties of SW and NF scaffolds were examined. The results showed that both scaffolds have a typical compressive stress-strain curve for the hydrated scaffolds and displayed characteristic of open-cell foams (Figure 4.14). In the open-cell foam the linear elastic, collapse plateaus and densification regimes are generally observed (Wang and Spector 2009). In our experiments, the linear elastic-collapse plateau transition was observed at approximately 0.5% strain.

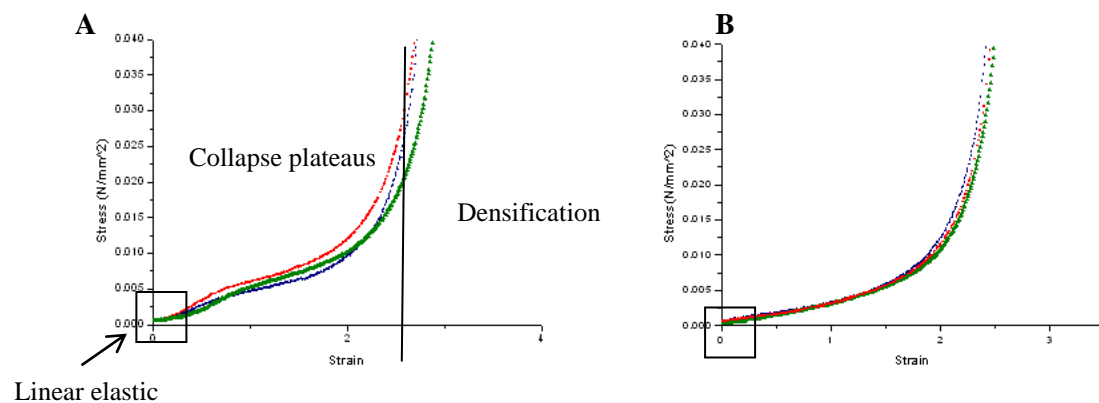


Figure 4.14. Stress-strain curves from the mechanical test A; Solid-walled, B; Nanofibrous scaffolds.

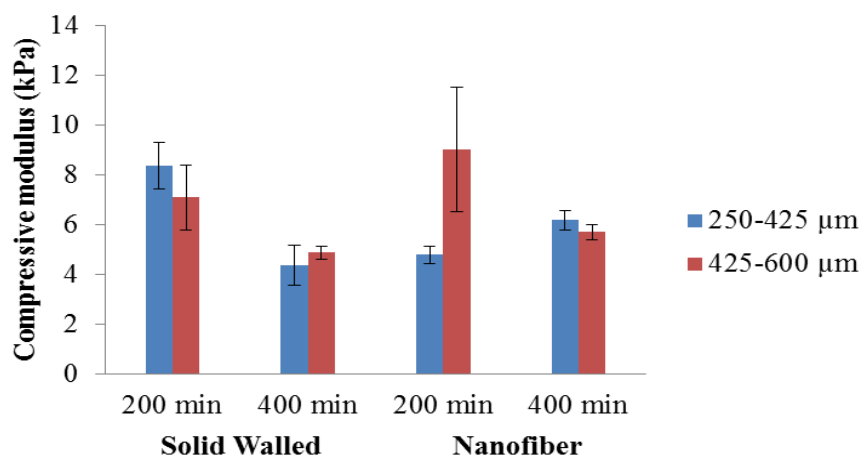


Figure 4.15. The effects of interconnection time on compressive modulus of solid walled and nanofiber scaffolds prepared with 10% gelatin solution.

The compressive modulus of solid walled scaffolds decreased when the heat treatment time was increased from 200 min to 400 min (Figure 4.15). The same effect was not significantly observed in the nanofibrous scaffolds. In fact, the modulus of the nanofibrous scaffold with macropore size of 250-425 μm increased by increasing the heat treatment time from 200 to 400 min. The macropore size did not have a significant influence on the modulus of both types of scaffolds. With 400 min heating time, the compressive modulus of nanofibrous scaffolds were found significantly higher ($p < 0.05$) than the solid walled ones for both macropore sizes. Based on the results shown in Table 4.4, we have decided to prepare scaffolds with 250-425 μm sized paraffin spheres and 200 min heating time, since the NF scaffolds prepared with these conditions had modulus (4.78 ± 0.33 kPa) in the range of brain tissue elastic modulus (0.5-5 kPa).

Table 4.4. Compressive modulus (kPa) of scaffolds prepared with 10% gelatin concentration.

Diameter of paraffin spheres	Solid walled preheating time		Nanofibrous preheating time	
	200 min	400 min	200 min	400 min
250-425 μm	8.4	4.4	4.8	6.2
425-600 μm	7.1	4.9	9.0	5.7

4.1.4.5. *In vitro* Degradation of Scaffolds

Tissue engineered construct should have degradation rate tunable in repair or regeneration process of tissue. We have determined degradation behaviour of scaffolds, in PBS and Matrix Metalloprotease-9 (MMP-9) included PBS medium to mimic enzymatic level in the body. We have observed that at the end of 28 days, there was no significant difference between *in vitro* degradation rates of solid walled and nanofibrous scaffolds in PBS solution (Figure 4.16). However in the presence of MMP-9 enzyme, degradation percent of solid walled scaffold was significantly higher than nanofibrous scaffold. About 50% of the solid walled scaffold was degraded in 28 days while degradation of the nanofibrous scaffold was only 14%. In the case of brain tissue engineering targeted regeneration time is not known because of unsatisfactory investigations or applications. *In vivo* studies have shown that human peripheral nerves regenerate at a rate of approximately 1 inch per month, full recovery of function changes from 9 to 12 months to 2-3 years depending on location of defect (Höke A. 2011). As seen from Figure 4.16, nanofibrous structure has lower degradation rates especially in enzymatic environment than the solid walled structure. This can be attributed to more efficient crosslinking of the NF scaffold due to their surface area to volume ratio.

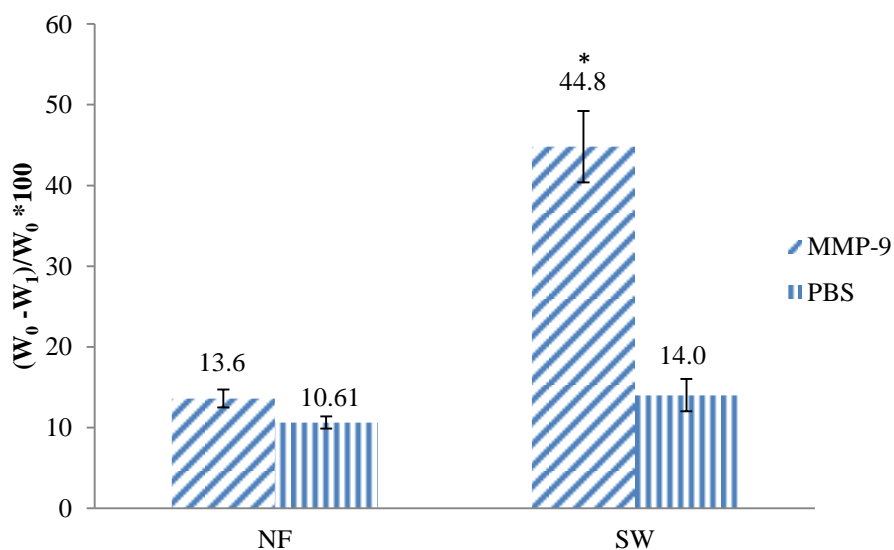


Figure 4.16. Degradation percent of solid walled and nanofibrous scaffold in PBS and in MMP-9 included PBS.

4.2. Preparation and Characterization of Channeled Nanofibrous Gelatin Scaffolds

Nerve tissue engineering is a broad area including both central nervous system and peripheral nervous system. To facilitate tissue regeneration, an ideal scaffold should resemble the characteristic structure of the natural extracellular matrix. Disc shape macroporous nanofibrous scaffolds characterized in the previous section were proposed for treating the injuries in brain. Peripheral nerves form an aligned multi-leveled tubular bundle structure. To prepare oriented nanofibrous scaffolds for peripheral nerve tissue engineering applications, we combined injection molding and thermally induced phase separation techniques. To create open channeled scaffolds, the molds were first assembled by inserting long needles into a teflon tube (Figure 4.17).



Figure 4.17. General appearance of mold and prepared scaffold.

For the preparation of disc shaped NF gelatin scaffold, 5-10 % (w/v) of gelatin was dissolved in 50/50 (v/v) ethanol/water solution and phase separation was achieved at -80°C for 5 hours. The same conditions were first tried to prepare nanofibrous channeled structure. However at the end of 5 hours, gelatin solution did not pass to the gel phase and phase separation was not observed. In temperature induced phase separation technique, demixing is usually stimulated by either loading the solution below a binodal solubility curve or exposure of the solution to an immiscible solvent (Shao et al. 2012). Temperature and solvent/nonsolvent ratio are important parameters to achieve separation. Figure 4.18-a through 4.18-c show that at -80°C when gelatin dissolved in 100% water, the solid walled, microchanneled structure was obtained. This type of structure is characteristic for solid-liquid phase separation. When the temperature of the polymer solution is lower than the freezing point (crystallization temperature) of the solvent, solvent crystallized, and after removing solvent crystals, channel like structure is formed (Figure 4.18-c). These channeles are parallel to the

direction of solidification (heat transfer direction) (Zhang and Ma, 1999). To obtain solid-liquid phase separation, temperature was increased to +4°C, then, nanofibrous structure was obtained (Figure 4.19) for all the scaffolds prepared from 2.5%, 3% and 3.5% gelatin concentration. With the increased polymer concentration, fiber length was decreased but fiber diameter was increased (Table 4.5). All the channeled nanofibrous scaffolds also had the porosities higher than 90%.

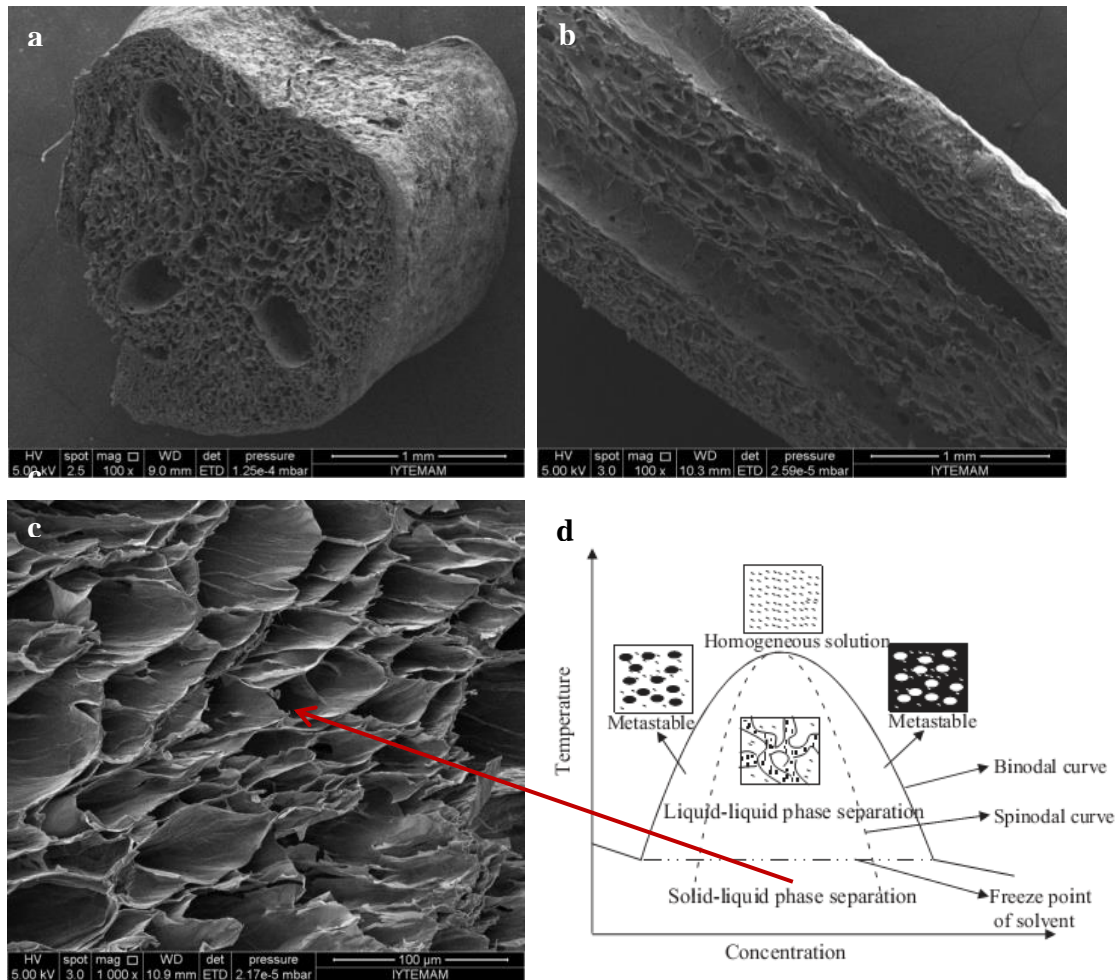


Figure 4.18. SEM micrograph of four channel solid walled gelatin scaffold prepared from 5% (w/v) gelatin solution at -80°C a; vertical cross-section, b; horizontal cross-section with channel structure, c; tubular micro-channels structures, d; Schematic phase diagram of polymer solution (Source: Yang et al. 2004).

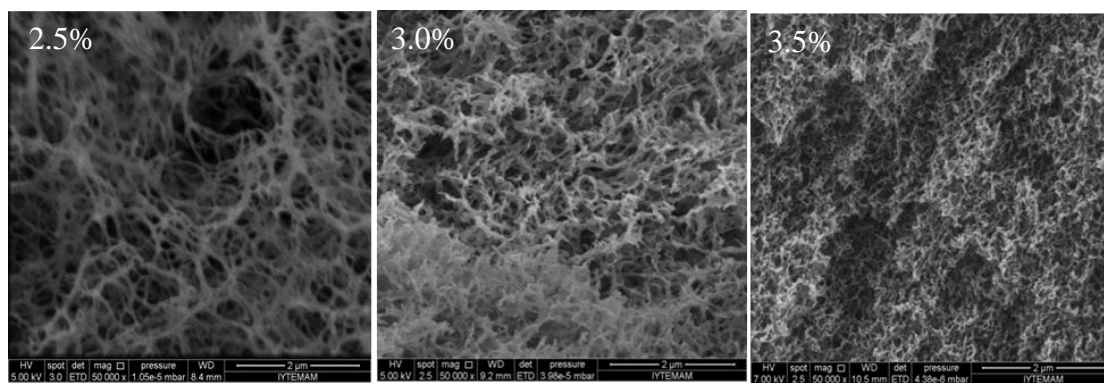


Figure 4.19. Nano-fibrous scaffold prepared from different concentration of gelatin solution at +4 °C.

Table 4.5. Fiber length and diameter of gelatin scaffolds prepared at +4 °C.

% gelatin concentration (w/v)	Fiber length (nm)	Fiber diameter (nm)	Porosity (%)
2.5	218.5	39.2	92.8
3.0	204.7	44.7	92.3
3.5	190.8	50.6	91.4

Although nanofibrous structure was obtained at +4°C, it was difficult to remove scaffolds from the mold without damaging the structure. Consequently, in the third set of experiments, the phase separation temperature was decreased to -20°C and ethanol content mixed in water was changed from 10% (v/v) to 40% (Table 4.6). Except the lowest ethanol/water ratio of 10/90, the nanofibrous scaffolds could be produced from the ethanol/water ratio of 20/80, 30/70 and 40/60 as shown in Figure 4.20. With the highest ethanol/water ratio (40/60), bead like structure was also observed (Figure 4.20-a) while nanofiber structures formed on the fibers when the ethanol proportion was decreased to 30/70 (Figure 4.20-b). Further decrease in the ethanol content to 20/80 caused big holes in the nanofibrous structure (Figure 4.20-c). Thus, ethanol/water ratio of 30/70 was chosen optimal to keep nanofiber structure while preventing hole like structure formation. To investigate the influence of gelatin concentration on the nanofibrous structure, scaffolds were prepared from 4%, 5% and 6% (w/v) gelatin dissolved in 30/70 (v/v) ethanol/water mixture. As seen from Table 4.7, with the

increased gelatin concentration, the fiber length and porosity of the scaffolds decreased while diameter of the fibers increased.

Table 4.6. Freezing point of ethanol based water solutions.

Ethanol concentration (% by volume)	10	20	30	40	50
Temperature (°C)	-4	-9	-15	-23	-32

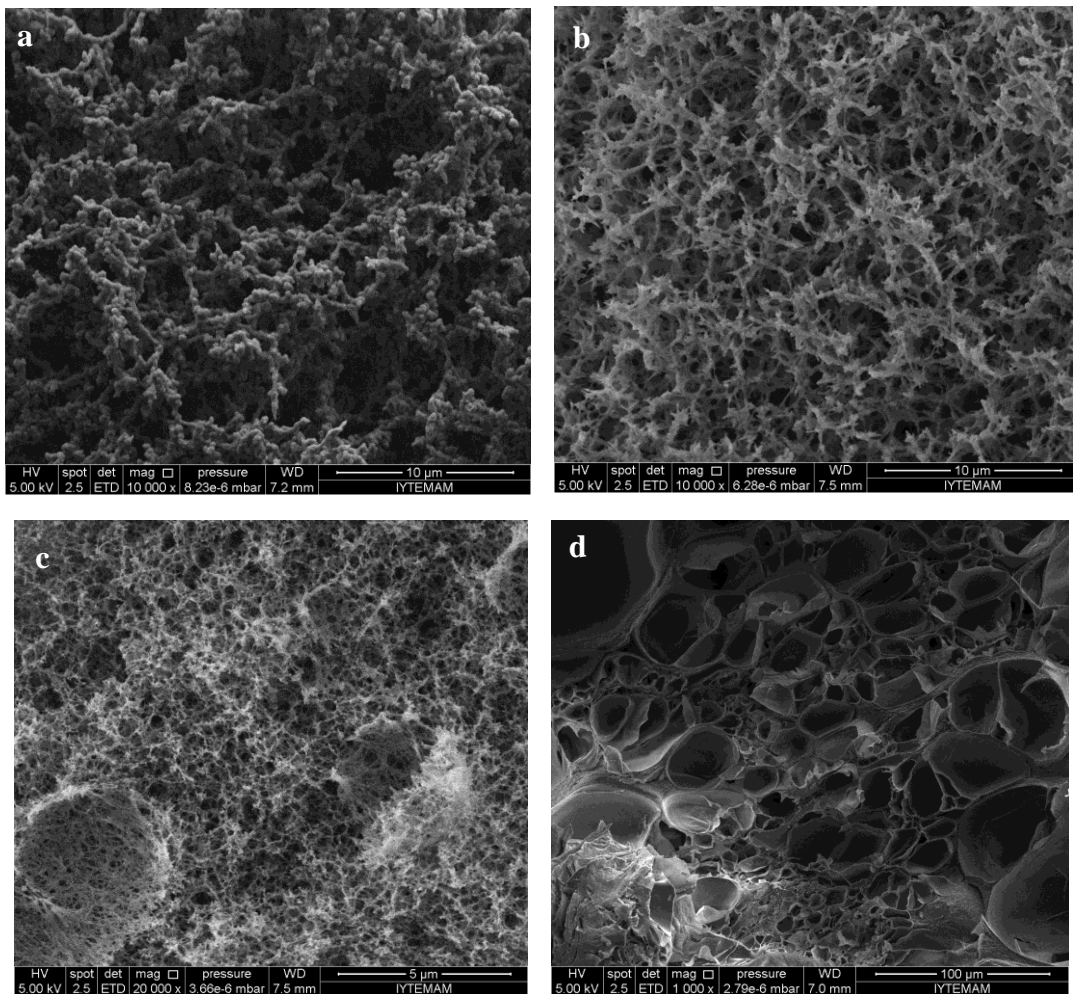


Figure 4.20. Gelatin scaffolds prepared with a; 40/60 (v/v), b; 30/70, c; 20/80, d; 10/90 ethanol/water solution. All examples gelatin concentration was 5% (w/v) and phase separation was -20°C .

Table 4.7. Fiber length, fiber diameter and porosity of gelatin scaffolds prepared at -20°C.

% gelatin concentration (w/v)	Fiber length (nm)	Fiber diameter (nm)	Porosity (%)
4	826.2	147.5	93
5	774.8	187.7	92
6	720.6	212.5	90

Mechanical properties of conduits could not be measured due to absence of appropriate experimental set up. Therefore, we prepared this films instead of nerve conduits and measured the mechanical properties of three films in terms of ultimate tensile strength (UTS) and Young's modulus. The results plotted in Figure 4.21 showed that both the tensile stress and modulus of the films increased by increasing gelatin concentration from 4% to 6%. In the literature the UTS and elastic modulus for acellular nerve were reported as 1.4 MPa and 0.576 MPa, respectively (Borschel et al. 2003). The values shown in Figure 4.21 are lower than the literature values since the films used for the test were very thin. The wall thickness of nerve conduits prepared is larger than that of the films. Thus, it is expected that the mechanical properties of the conduits should be higher than the films and similar to desired values for peripheral nerve tissue engineering applications.

Our aim for the preparation of this new system was to fabricate a nerve guidance conduit which has a nanofiber structure. As an alternative to autografts, nerve conduits have a number of advantages for nerve repair, including limited myofibroblast infiltration, reduced neuroma and scar formation, reduction in collateral sprouting and no associated donor site morbidity. In addition conduits facilitate the accumulation of a high concentration of neurotrophic factors; ultimately guiding regenerating nerves to their distal targets (Daly et al. 2012). Fibrous conduits were usually fabricated with the electrospinning method (Clements et al. 2009). Preparation of nanofiber conduit with TIPS method was first performed by Sun et al. (2012) from PLLA. In literature, preparation of multichannelled nerve conduit from natural polymer collagen was also reported (Yao et al, 2010). In this study we used gelatin for the first time and achieved to fabricate one and multichanneled nanofibrous nerve conduit from a natural polymer (Figure 4.22).

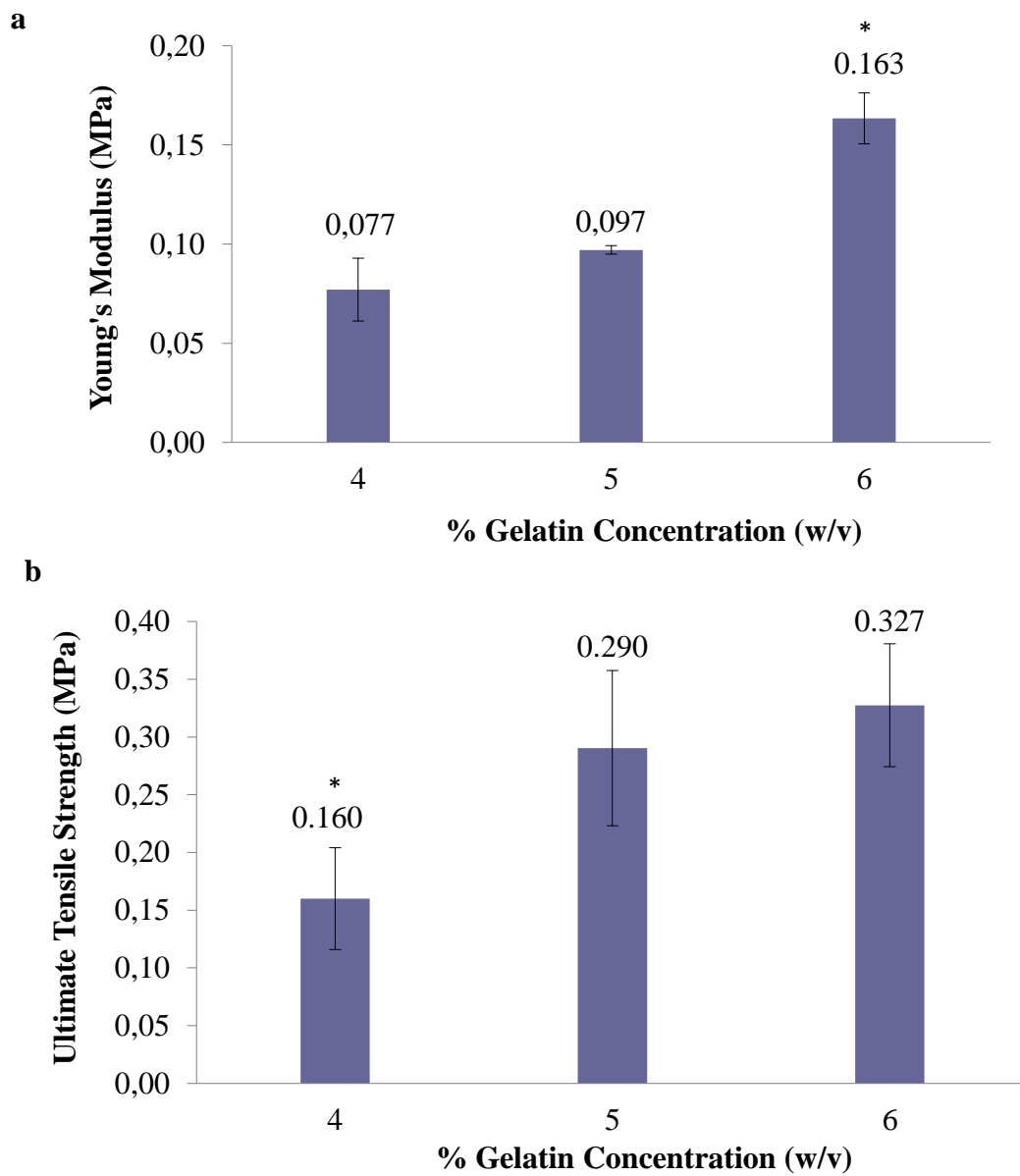


Figure 4.21. Mechanical properties of nanofiber gelatin matrix in terms of a; Young's Modulus, b; Ultimate tensile strength.

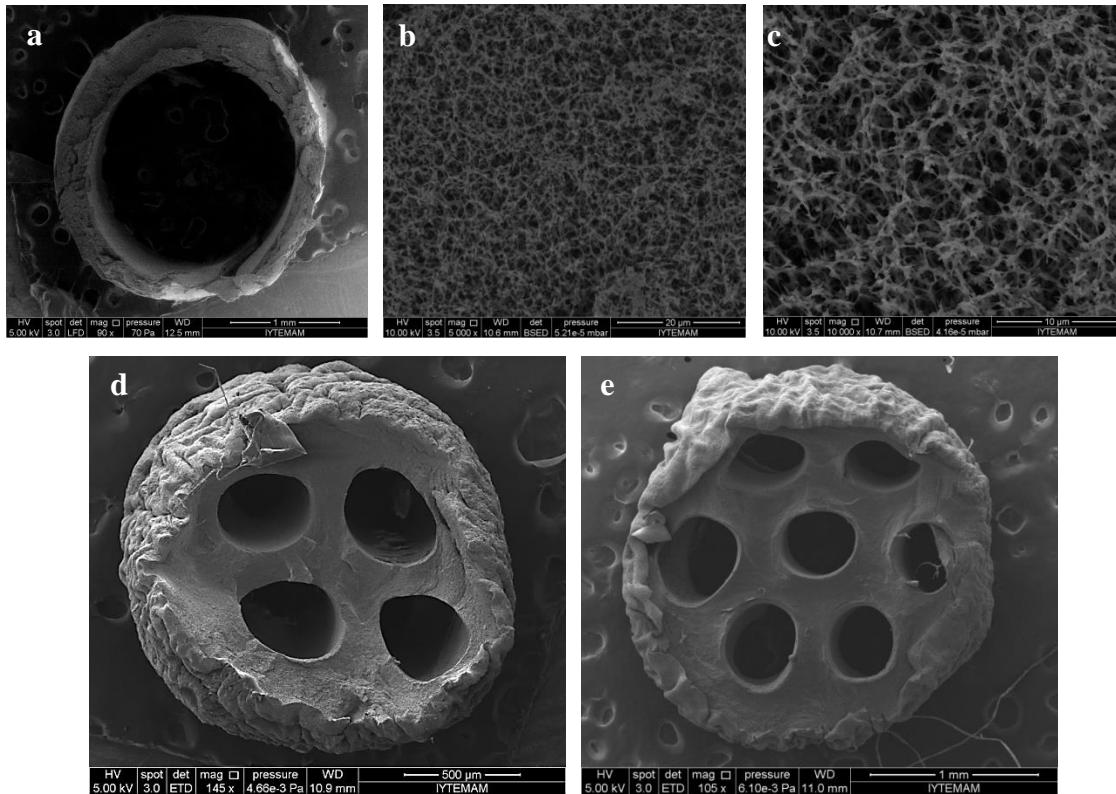


Figure 4.22. Nanofibrous gelatin conduit with a-c; one channeled, d; 4 channeled and e; 7 channeled prepared from 5% gelatin solution in 70/30 water/ethanol and phase separated at -20°C .

4.3. Preparation of NGF Loaded Alginate Microspheres

It has been reported that nerve growth factor (NGF) promotes both growth and survival of axons of the peripheral and central nervous system (Sofroniew et al. 2001). To increase limited stability of NGF at physiological conditions and to achieve its controlled release, we encapsulate NGF in alginate. Alginate was chosen since it has strong interaction with high isoelectric point proteins (Wells et al. 2007). Alginate microspheres were prepared by homogenization and reticulation of alginate with calcium ions in a water-oil system. In this system homogenization was carried out with rotor stator type high speed homogenizer in which the drops in the disperse phase are broken up to a large extent by forces of inertia and shearing in turbulent flow (Schultz et al. 2004). The reticulation process consists of the simple substitution of sodium ions with calcium ions (Ciofani et al. 2007). Water-oil emulsion system was used is composed of three components; oil phase (iso-octane) as continuous phase, surfactant (combination of Span 80 and Tween 80) and water phase (alginate solution) as

dispersed phase. Span 80 is a typical oil-soluble surfactant and is effective at reducing interfacial tension in water-oil emulsion system. When we used only Span 80 as a surfactant, the emulsion and particle preparation could not be achieved. The interaction between alginate and CaCl_2 is very strong and fast. Span 80 only was not enough in reducing interfacial tension between oil phase and water phase and particle formation did not occur. With the addition of CaCl_2 it was observed that Ca-alginate precipitated at the bottom of tube. With a hydrophilic surfactant, Tween 80 spherical particles were prepared but the particles were not stable and they were all on the surface of water. It was reported that combination of Tween 80 (hydrophilic surfactant) and Span 80 (lipophilic surfactant) in oil-in-water or water-in-oil system resulted in efficient emulsification (Porras et al. 2008). Based on this knowledge, mixture of two surfactants with a ratio of 1:1 (v/v) was used which lead to a heterogeneous system with particles both at the bottom and at the top. Porras et al. (2004) reported that when the surfactant concentrations were lower than 5 wt%, water was not solubilized or dispersed in appreciable quantity in water-oil system. To obtain a homogeneous system with all particles precipitated at the bottom, we changed the ratio of Span 80:Tween 80 (v/v) and the results were summarized in Table 4.8. It was possible to collect all the particles at the bottom of the flask when the amount of Span 80 was decreased while the amount of Tween 80 was increased.

In order to observe the effect of alginate concentration on size of microspheres, three alginate concentrations (0.1%, 0.5% and 1.0%) were used. The diameter of the microspheres was measured with inverted phase contrast microscope. Changing alginate concentration from 0.1% to 0.5% increased the diameter of the spheres from 1.7 μm to 5.2 μm (Figure 4.23). To observe effect of microsphere size on protein loading and release in our further experiments, it was decided to use 0.1% and 1.0% (w/v) alginate particles (Figure 4.24).

Table 4.8. Volume of surfactants in water-oil emulsion system composed of 20 mL of iso-octane and 4 ml alginate solution.

Span 80 (μL)	Tween 80 (μL)	Ratio (v/v)	Particle type
250	-	-	Particles could not be obtained
125	125	1: 1	Heterogenous porous particles
1000	1000	1: 1	Heterogenous particles with smooth surfaces
778	222	3.5: 1	Heterogenous particles and swollen alginate
650	350	1.85: 1	Homogenous particles collected at the bottom
600	400	1.5: 1	Homogenous particles collected at the bottom
550	450	1.22: 1	Homogenous particles collected at the bottom

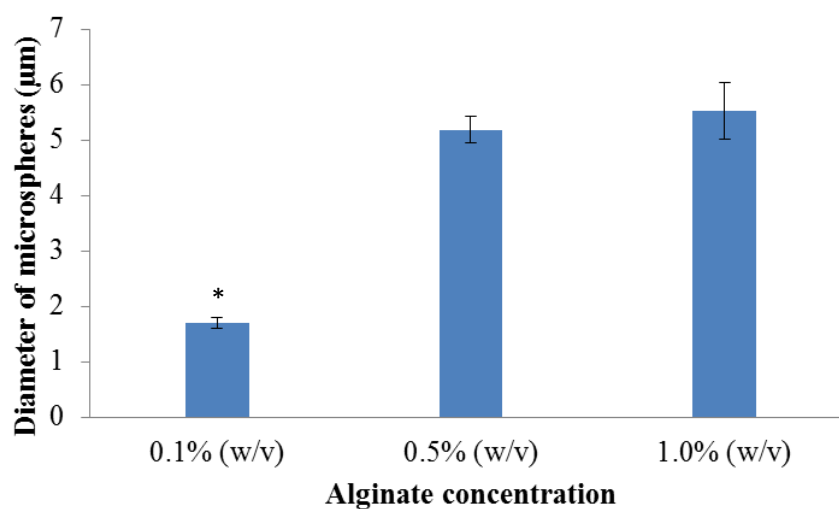


Figure 4.23. Diameter of alginate microspheres.

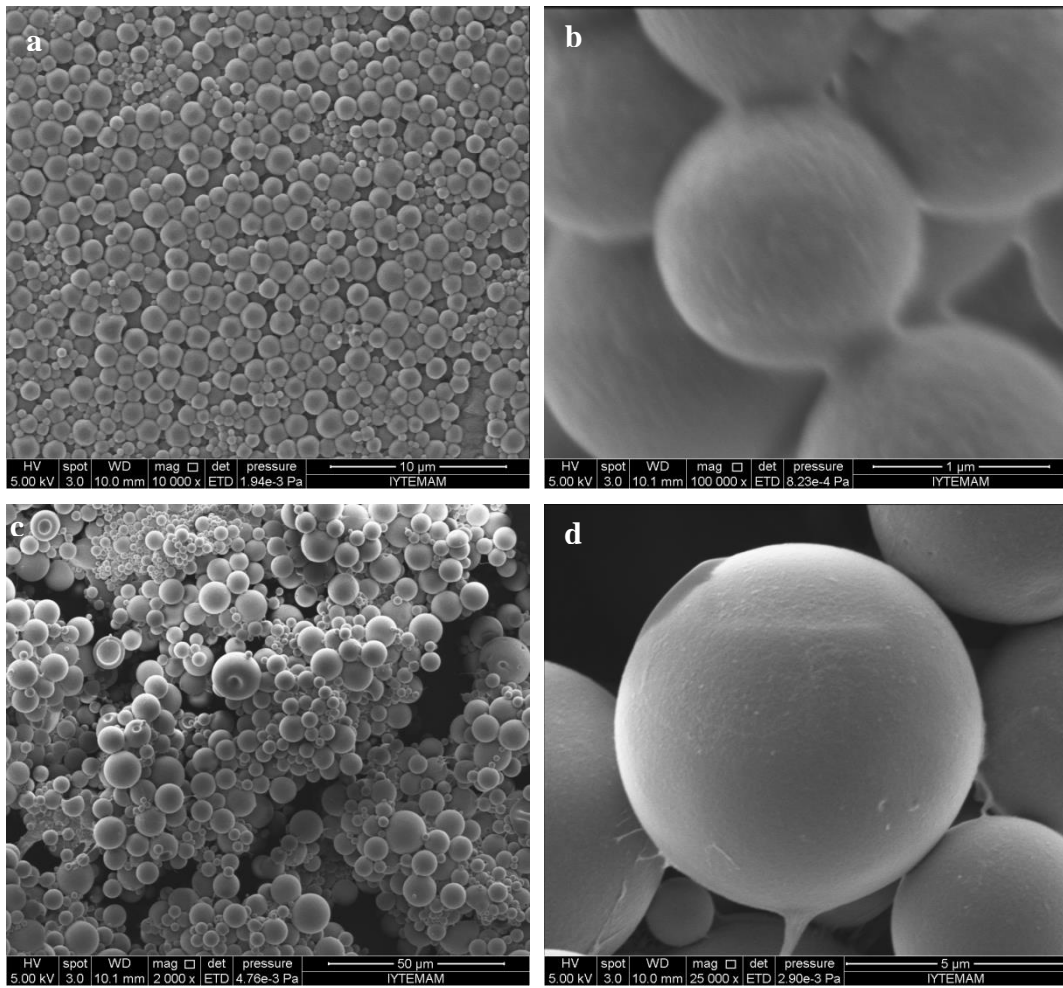


Figure 4.24. Microspheres prepared with a-b; 0.1 % (w/v) alginate and c-d; 1 % (w/v) alginate.

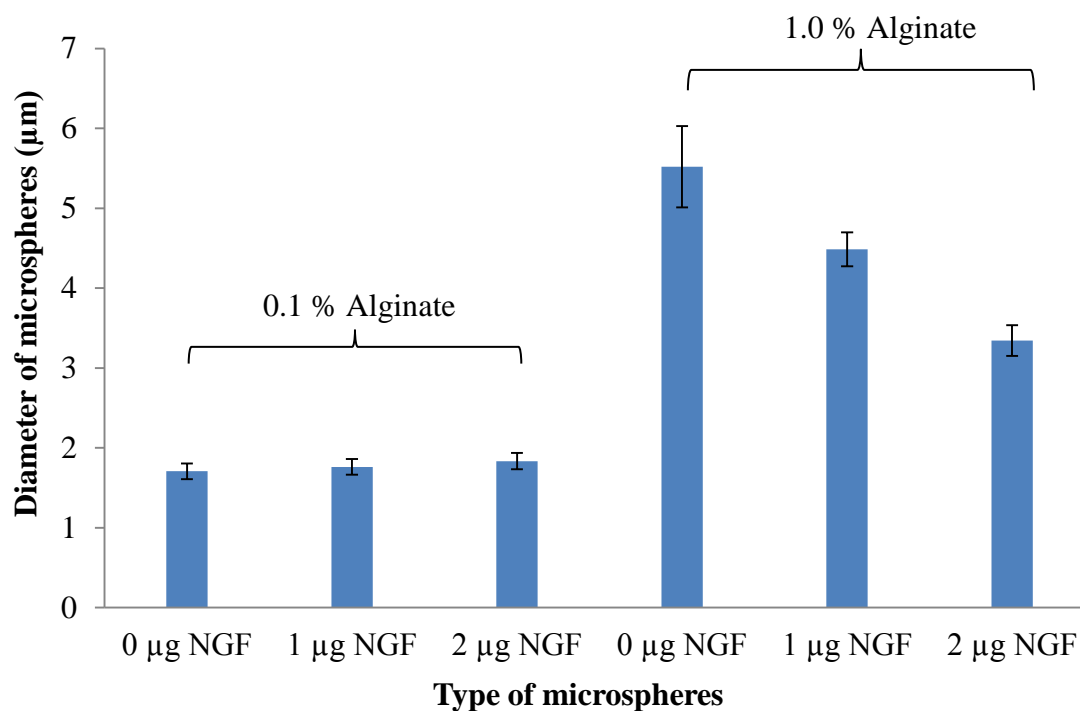


Figure 4.25. Diameters of NGF loaded and nonloaded microspheres.

4.3.1. NGF Loading to the Ca-alginate Microspheres

1 µg and 2 µg NGF was added into two different concentration of alginate solutions. The diameter of the NGF loaded spheres prepared from 0.1% alginate did not change significantly as seen in Figure 4.25. On the other hand, 1% alginate microspheres became smaller as the loading level of NGF increased. For crosslinking both 0.1% and 1% alginate particles, same volume of CaCl₂ was used. More free carboxylate groups are present in the structure of 1% alginate particles at the end of the crosslinking and these free groups strongly interact with positively charged groups in NGF. Consequently, the size of 1% alginate particles decreased as the NGF loading level increased.

In literature, proteins were loaded into alginate particles in different concentrations. The concentration of BSA and lysozyme in loading solutions were in the range of 1-20 mg/ml (Wells and Sheardown, 2007) while for VEGF and NGF corresponding values were 20 µg/ml (Jay and Saltzman 2009) and 1 µg/ml (Ciofani et al. 2008), respectively. In our study 1µg/mL of NGF was added into alginate solution and its encapsulation efficiency was determined as 100% and 85% when loaded into

microspheres prepared from 1% and 0.1% alginate, respectively. Encapsulation efficiency with 1% alginate particles was found higher due to their stronger interaction with NGF as a result of more free COOH groups in these particles.

4.3.2. Attachment of NGF Loaded Alginate Microspheres into Macroporous Gelatin Scaffold

In this experiment the attachment of microspheres to the nanofibrous scaffold was performed with post-seeding method. Alginate microspheres were attached onto nanofibrous scaffold with carbodiimide reaction (Figure 4.26). 1.8 mg of NGF loaded alginate microspheres were attached onto the disc shaped scaffold has the diameter of 16 mm and height of 2 mm (Figure 4.27). As seen from Figure 4.27 that the attachment of alginate microspheres into gelatin scaffold was not caused the morphological or structure change in the both types of scaffolds. The attachment percent of alginate microspheres in this system was quantified with phenol-sulfuric acid assay. Attachment percent of alginate particles to the gelatin scaffold was determined as 94%.

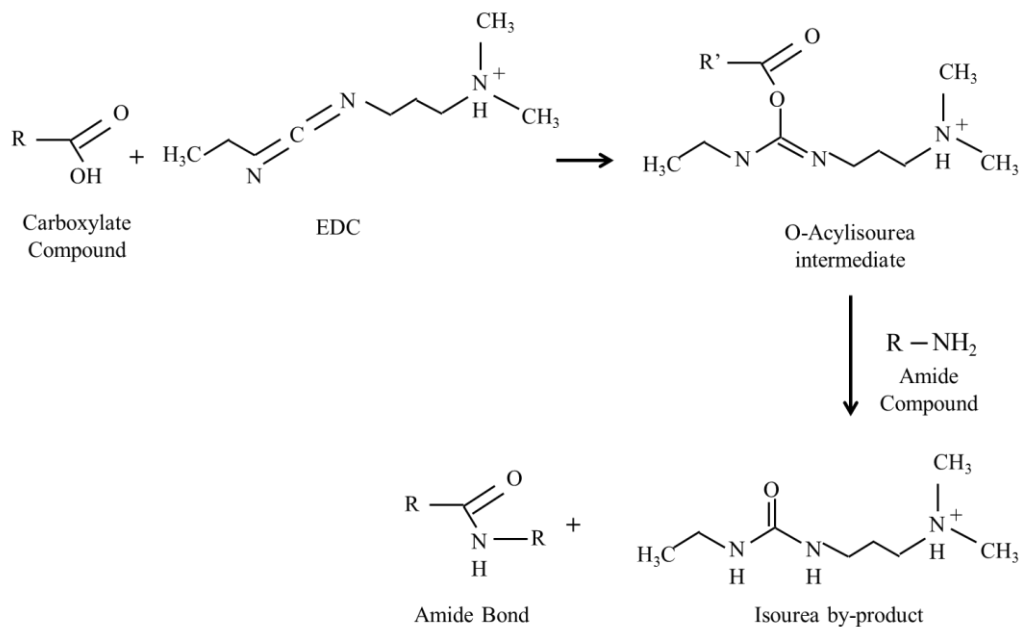


Figure 4.26. Chemical crosslinking of alginate and gelatin in the presence of EDC (Source: Hermanson 1996).

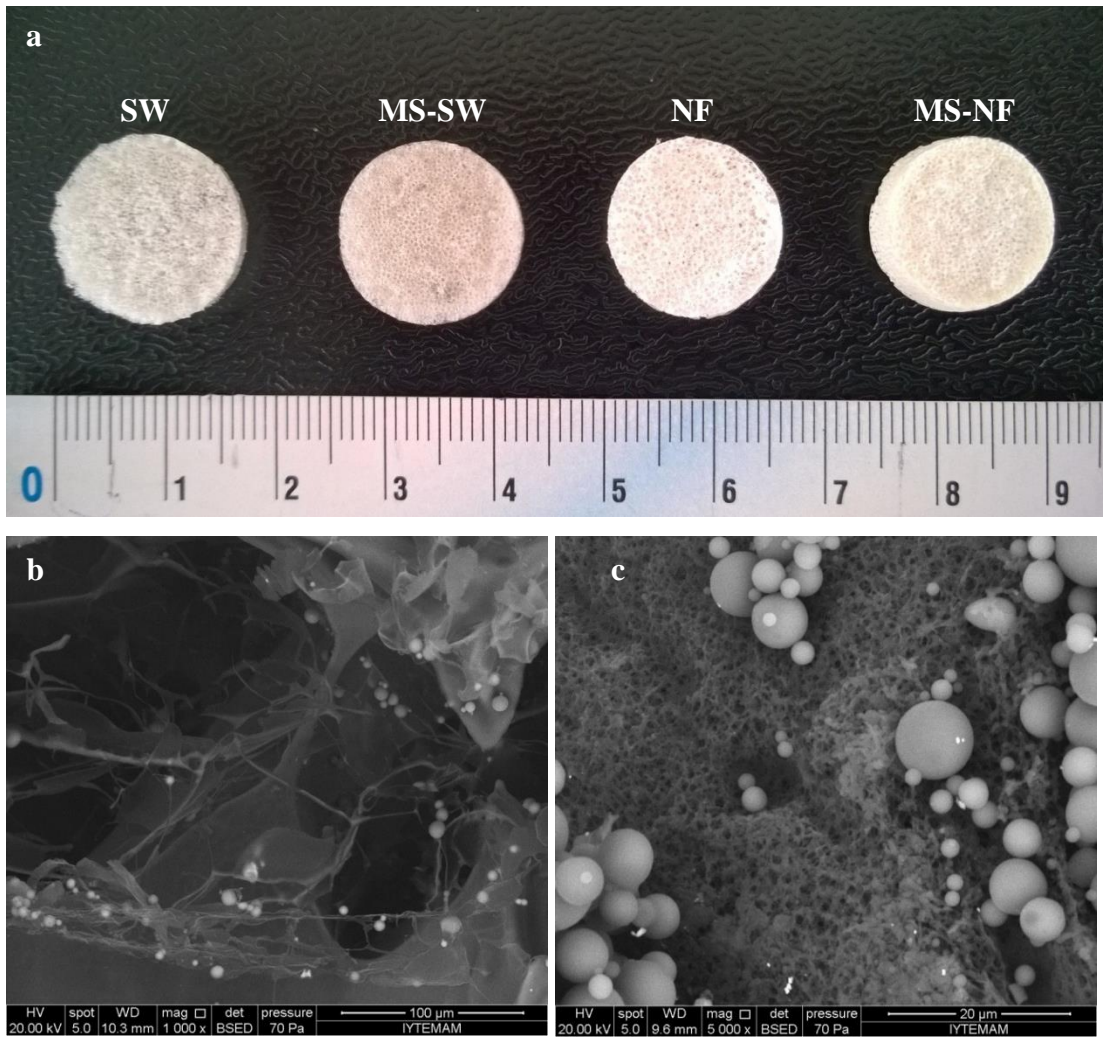


Figure 4.27. a; General appearance of scaffolds (SW and NF) and scaffolds integrated with NGF loaded microspheres (MS-SW and MS-NF), SEM images of microsphere attached scaffolds b; MS-SW and c; MS-NF.

4.3.3. NGF Release from Alginate Microspheres

The *in vitro* release of NGF from uncoated alginate spheres (F), poly-L-lysine coated alginate spheres (C) and the uncoated alginate spheres attached onto NF scaffold (A) was measured. The microspheres attached to the scaffolds in this experiment have the total 235 ng of NGF for 1% alginate system and 200 ng of NGF for 0.1% system. The differentiation medium for the cells including RPMI 1640 and 1% horse serum was used as a release medium. As seen from Figure 4.28-a and 4.28-b, burst release profiles have been observed in the first 5 hours with NGF loaded into free or attached alginate microspheres. The burst release can be explained with diffusion of water into alginate gels and release of NGF loosely attached on the surface of the particles. At later times,

the release is controlled by diffusion of NGF through alginate matrix and dissolution of alginate spheres caused by bulk erosion and decrosslinking. As expected, the fastest release occurred from free, uncoated alginate spheres. Coating of alginate spheres with poly-L-lysine (PLL) decreased the release rate of NGF. The PLL coating on 0.1% alginate particles influenced the release rate more significantly than the coating on 1% alginate particles. The release rate of NGF from coated 0.1% alginate particles (C) was found lower than the release from the uncoated, immobilized 0.1% alginate particles (A).

Figure 4.29 compares the release profiles of NGF from the scaffolds on which coated and uncoated 0.1% alginate spheres were immobilized. According to the results, the release rate of NGF from the scaffold incorporated with uncoated alginate spheres was 860 pg/h for 10 days and 370 pg/h in the case of coated and attached microspheres. Coating of alginate particles with PLL decreased the release rate of NGF 2.3 fold and increased release time from 10 days to 30 days.

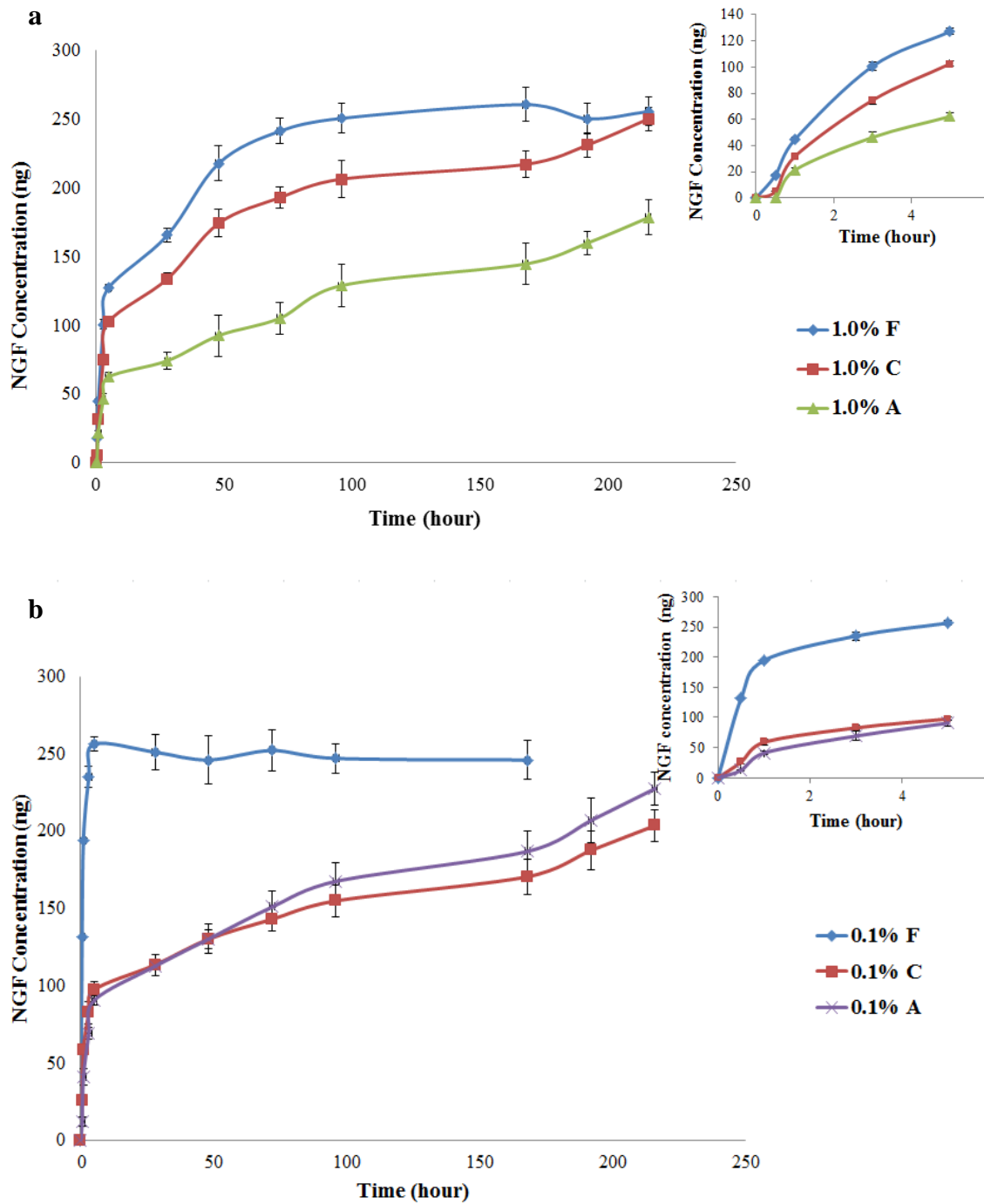


Figure 4.28. Release profiles of NGF from a- 1.0% and b-0.1% alginate microspheres.

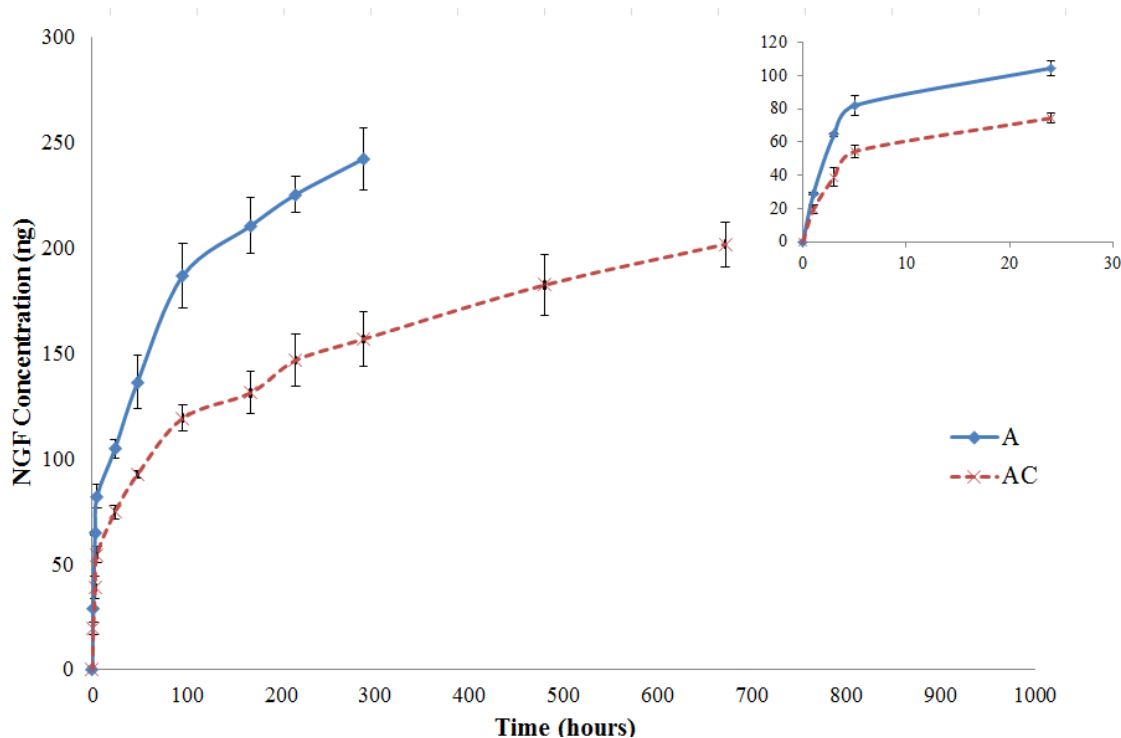


Figure 4.29. Release profile of NGF from 0.1% alginate particles incorporated nanofibrous gelatin scaffold.

4.4. PC12 Cell Culture

In the nerve tissue engineering studies, one of the commonly used culture systems is PC12 cell line derived from a transplantable rat pheochromocytoma. PC12 cells are small, irregularly shaped cells and when they are cultured on PLL coated cell culture plate, they adhere to the plate surface. A notable feature of PC12 cells is that they respond to nerve growth factor (NGF). In response to NGF, PC12 cells are converted from proliferating chromaffin-like cells to nondividing sympathetic-neuron-like cells that extend axons and become electrically excitable (Aletta J.M. et al. 1996). Before investigating cell attachment, proliferation and differentiation of PC12 cells on the scaffold, the growth curve of PC12 cell was determined in order to analyze the growth characteristics of cell line.

4.4.1. Growth Curve of PC12 Cells

To determine growth curve of PC12 cells, 500 and 1000 cell/well were seeded to the 96 well plate in three different cell culture medium. Cells were grown in complete medium (CM), starvation medium (SM) and starvation medium containing 50 ng/mL NGF (SM+NGF). Results have shown that at the 500 cell/well concentration, 13 days was not enough to reach complement stage of growth curve. In CM, cells were in lag phase until the 6th day then log phase started and at the end of 13th day, it was seen that PC12 cells were at the beginning of stationary phase (Figure 4.30-a). At the concentration of 1000 cell/well, cells were in the lag phase until the 4th day and in the log phase between 4th-8th days. Stationary phase was observed between 8-13th days (Figure 4.31-a). PC12 cells which were grown in SM and SM+NGF media had similar behaviour until the 8th day in both concentrations of cells (Figure 4.30-b and 4.31-b). After the end of 8th day, number of cells in SM medium increased whereas number of cells in the SM+NGF medium did not change significantly. These results are compatible with the growth characteristic of PC12 cells (Greene and Tischler, 1976). In literature it was shown that with the exposure of NGF for 7 days in low serum concentration (SM), PC12 cells cease to multiply. When the PC12 cells growth in the complete medium which has 10% horse serum and 5% fetal bovine serum, the general population is proliferating while only some cells extend neurites exposure to NGF (Greene and Tischler, 1976; Greene, 1978). To obtain apparently more homogeneous response to NGF, PC12 cells are growth in serum starvation medium (1% Horse serum). In this medium cells are synchronized and yield a more homogeneous population of cells available to differentiate (Rudkin et al. 1989).

In the most of NGF release studies address to use PC12 cells. Therefore, in our study we used PC12 cells as an indicator of active form of NGF released from alginate microspheres.

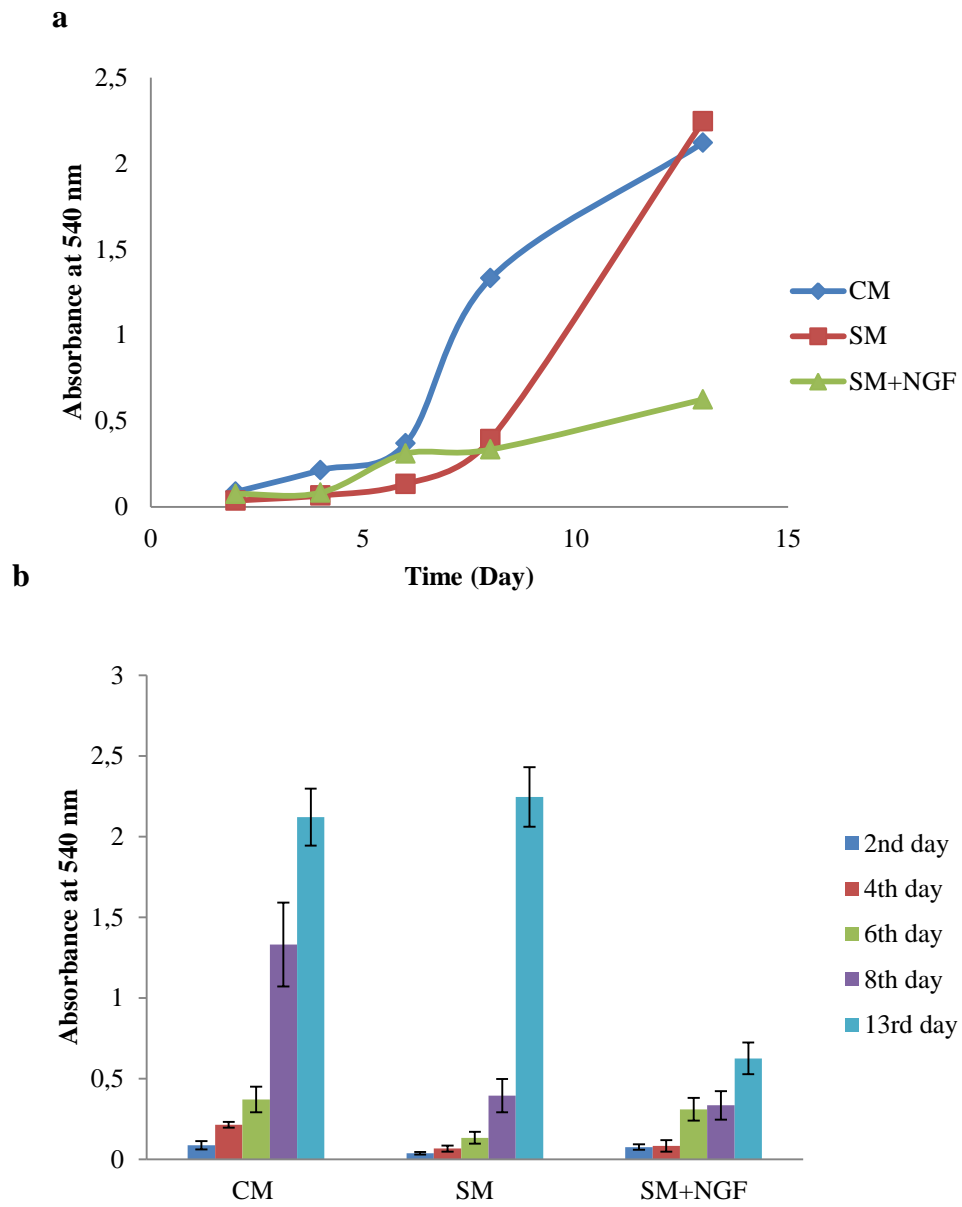


Figure 4.30. Behaviour of PC12 cells in the concentration of 500 cell/well in different cell culture media during 13 days in CM; complete medium, SM; starvation medium, SM+NGF; NGF added starvation medium.

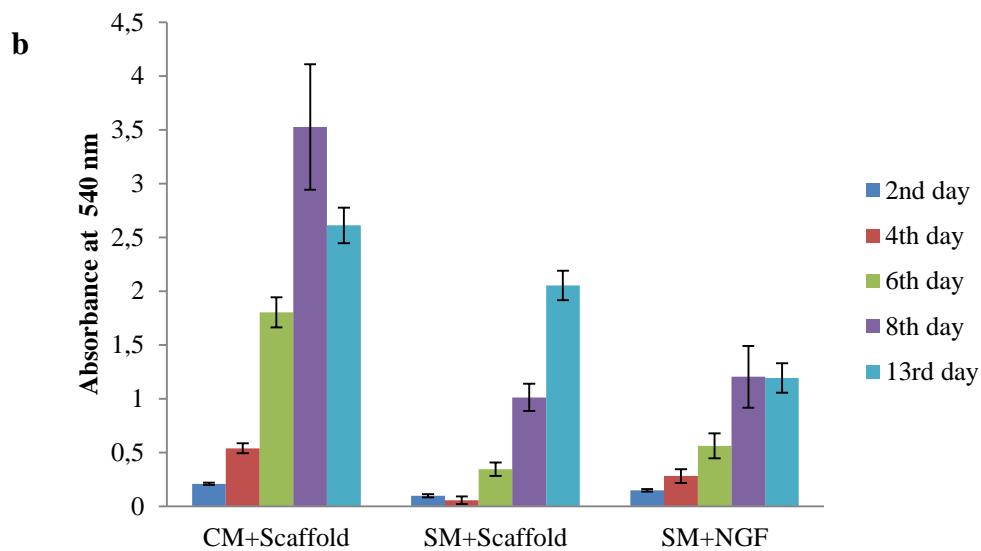
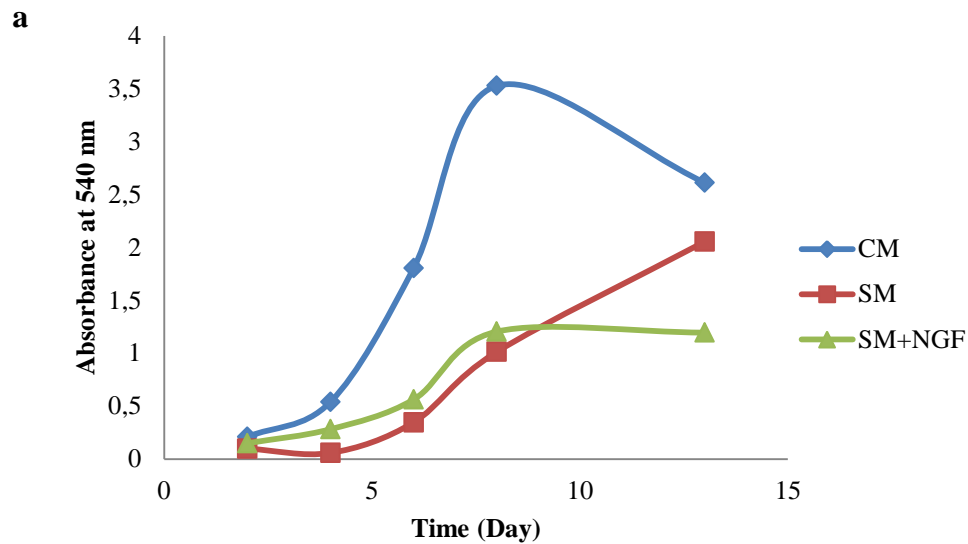


Figure 4.31. Behaviour of PC12 cells in the concentration of 1000 cell/well in different cell culture media during 13 days in CM; complete medium, SM; starvation medium, SM+NGF; NGF added starvation medium.

4.4.2. Amount of Free NGF Required for Differentiation of PC12 Cells

In literature two different NGF concentrations (50 ng/ml and 100 ng/ml) were used for NGF-induced differentiation (cells with at least one neurite with a length equal to the cell body diameter) and neurite growth (length of longest neurite) (Das et al. 2004). In this study we tried 25, 50 and 100 ng/ml of NGF concentrations. 1250 cells were seeded into 24 well plate and NGF was added to the plate every 2 days. It was

seen from Figure 4.32 and 4.33 that in all concentrations of NGF (25 ng/ml, 50 ng/ml and 100 ng/ml), neurites were observed at the end of 7 and 10 days and neurite lengths were measured with ImageJ. As seen from Figure 4.34, no significant differences were observed between neurite lengths on the 7th and 10th days when 25 ng/ml NGF was added. On the other hand, neurite lengths increased significantly as the incubation time changed from 7 to 10 days. Microscopic images indicated that on the 7th day, some of the cells incubated with 25 ng/ml of NGF did not extend into neurites (Figure 4.32-a), however at the end of the 10 days, all of the cells had neurites regardless of the NGF concentration (Figure 4.33). Based on this data, free NGF concentration for future experiments was chosen as 50 ng/ml.

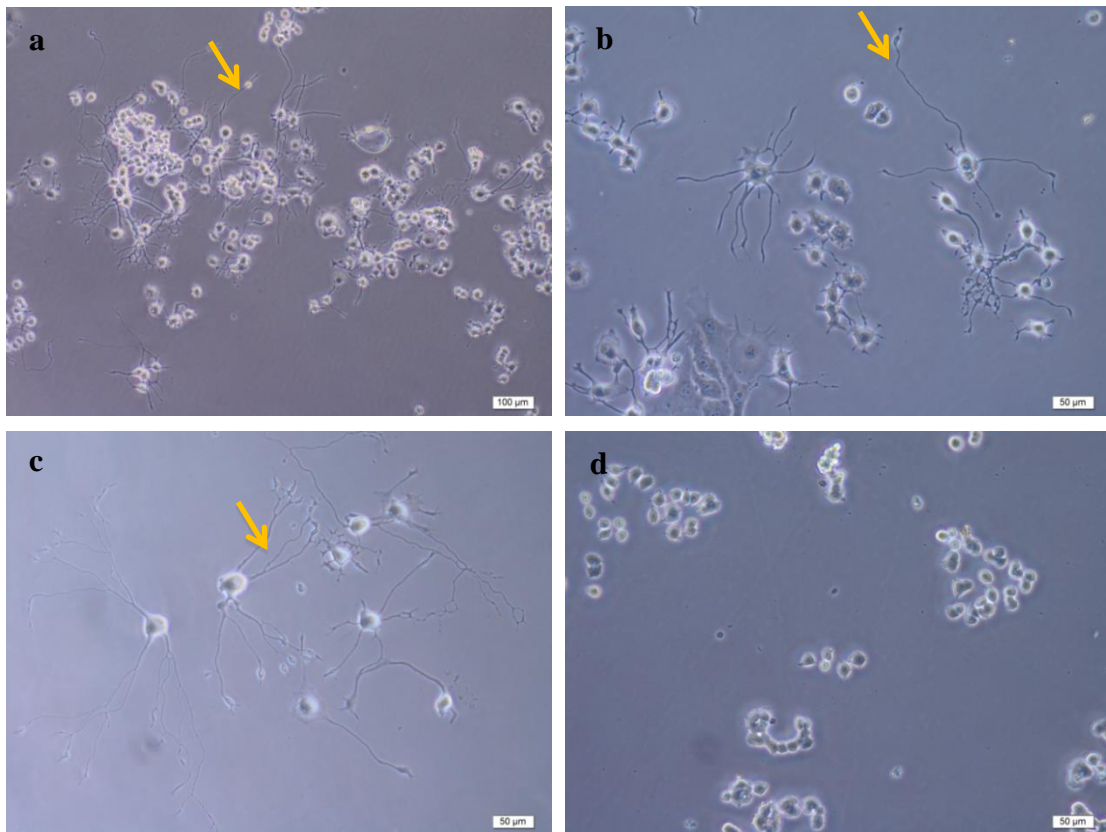


Figure 4.32. 7th day images of PC12 cells in SM with a; 25 ng/ml, b; 50 ng/ml, c;100 ng/ml, d; no NGF.

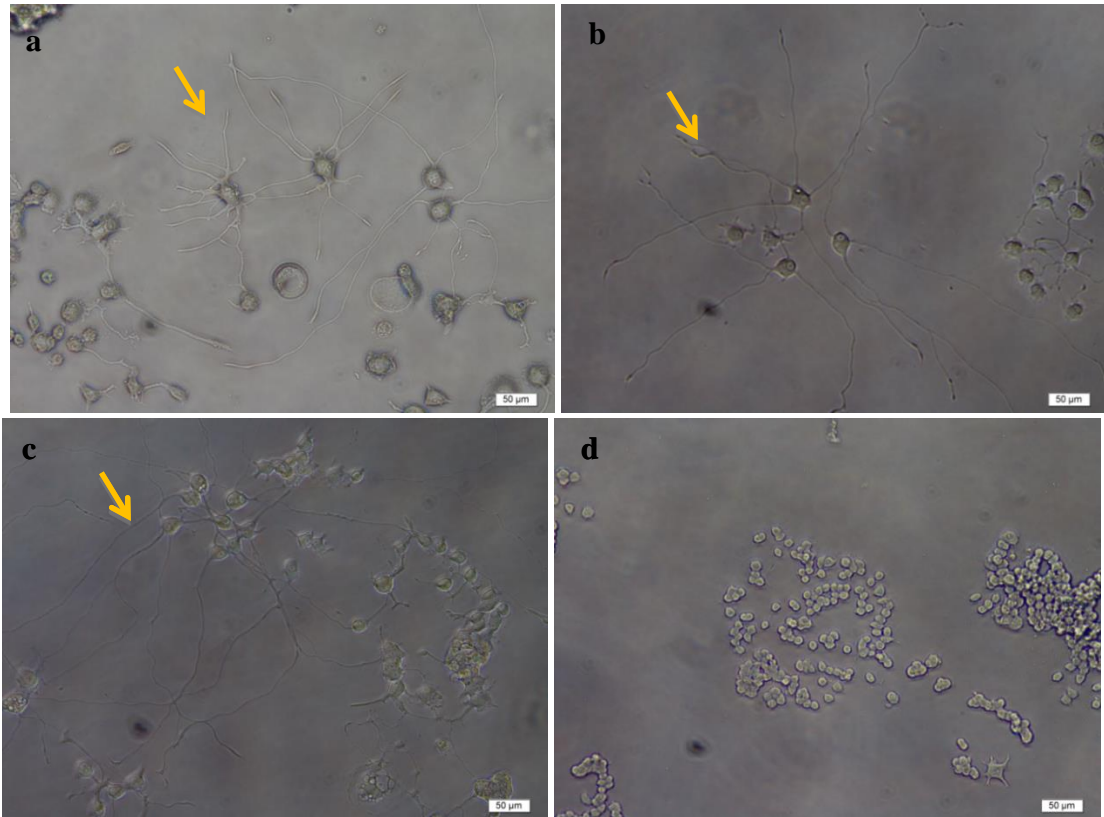


Figure 4.33. 10th day images of PC12 cells in SM with A; 25 ng/ml, B; 50 ng/ml, C;100 ng/ml, D; no NGF.

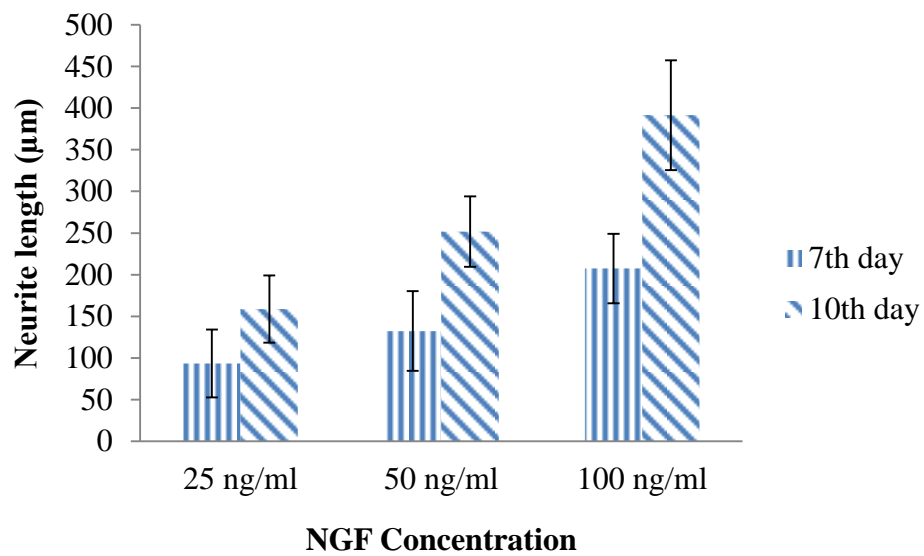


Figure 4.34. Measurement of neurite length of PC12 cells at 7th and 10th days after treatment of different concentrations of NGF.

4.4.3. Cell Attachment

Figure 4.27 shows the images of PC-12 cells attached on the NF and SW scaffolds. It was reported that coating of tissue culture plate with collagen increase the PC-12 cell attachment and growth (Turner et al. 1989). Since type B gelatin is a derivative of collagen, the attachment of PC12 cell onto the scaffolds was expected. Gelatin also has amino acid sequence, RGD, which allows cell attachment. As seen in the images, the cells attached and spreaded onto the NF scaffolds (Figure 4.35-a, b) while morphology of PC12 cells seeded into SW scaffolds was found smooth (Figure 4.35-c). *In vivo* basement membranes do not have smooth structures but, rather, are covered with grooves, ridges, pits, pores, and the fibrillar mesh work of the ECM, composed predominantly of interwined collagen and elastin fibers. With this experiment, the response of PC12 cells to the surface topography was observed.

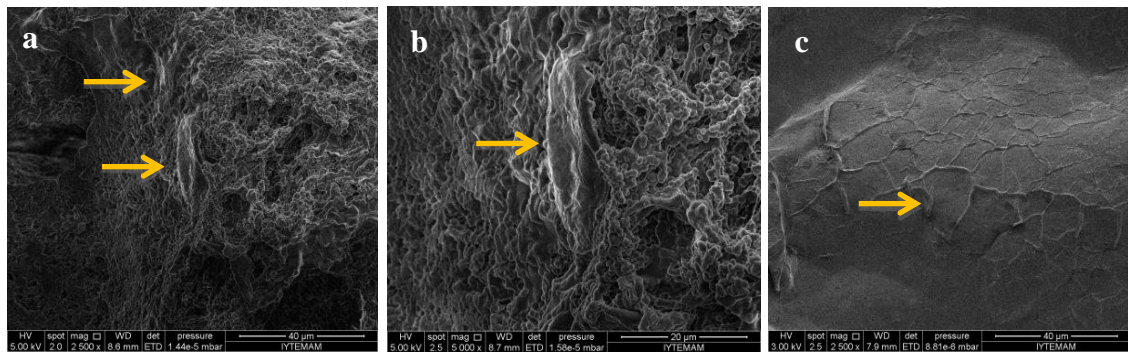


Figure 4.35. PC12 cells attached onto the cross-linked NF (a, b) and SW (c) scaffolds macropore size: 425-600 μm.

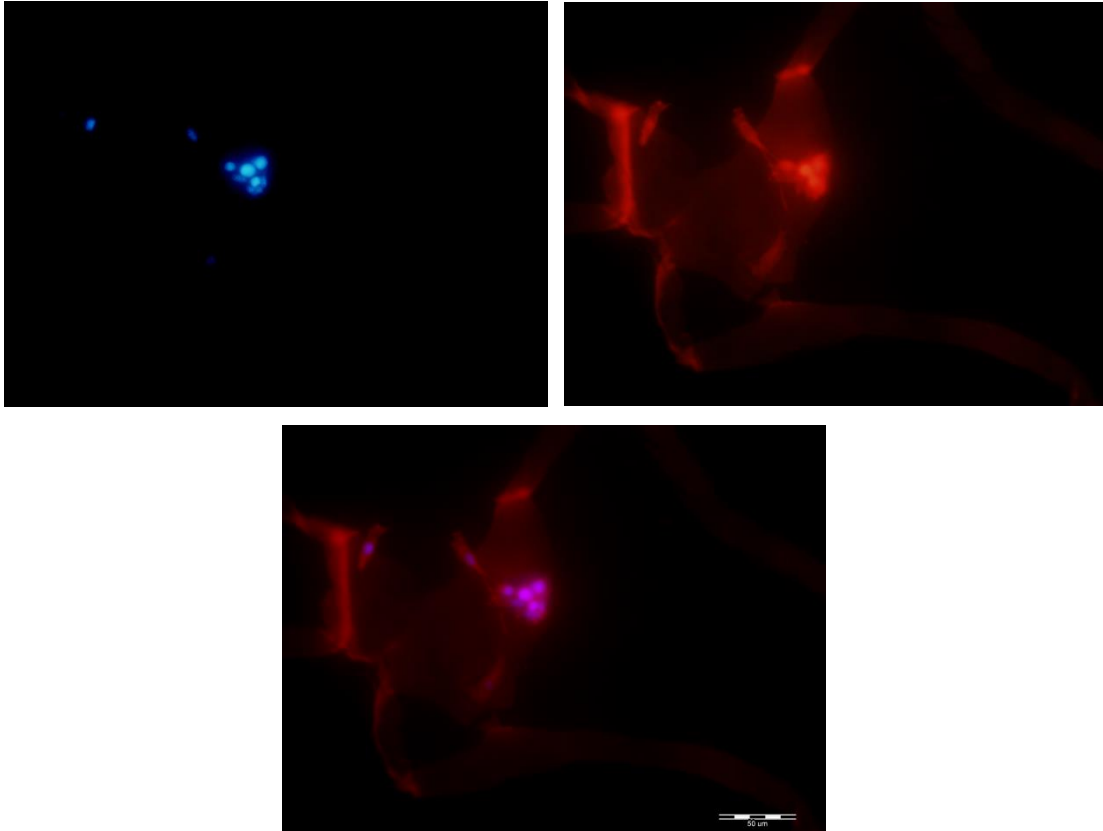


Figure 4.36. Fluorescent images of 50 ng/ml of NGF treated PC12 cells in gelatin NF scaffold dyed with a; DAPI (blue), b; Phalloidin (red), c; merged form of a and b.

Attachment of PC12 cells into the macroporous nanofibrous gelatin scaffold was also confirmed with the fluorescent microscope (Figure 4.36).

4.4.4. PC12 Cell Proliferation on the NF Gelatin Scaffolds Integrated with Alginate Microspheres

To observe proliferation of PC12 cell in the macroporous nanofibrous gelatin scaffolds in the presence of alginate particles, XTT assay was performed. First, gelatin scaffolds were placed into 96 well plate, kept overnight in complete medium for pre-wetting. Then, medium was removed and 2500 cells were seeded onto each scaffold. The scaffolds were kept at 37°C for 1 hour for cell attachment and then 100 μ l of CM was added into wells. As seen from Figure 4.37, proliferation behaviour of PC12 cells in 3D culture medium was similar to that in 2D culture medium. When NGF was added to the culture medium the cell number did not change between 6-8 days. This shows

that cells ceased the proliferation and the differentiation mechanism started as a response to NGF. On the 6th day, the proliferation of cells in the scaffolds in the presence of both alginate microspheres was found lower than in the empty scaffold (CM+Scaffold). At the end of the 10 days, the proliferation in the empty and 0.1% alginate spheres incorporated scaffolds (M+0.1% (A-MS)) was found similar whereas in the 1% alginate spheres attached scaffold (M+1% (A-MS)) proliferation was not different from the 6th day. The presence of 1% alginate microspheres decreased the pH of cell culture medium, hence, cells ceased the division and proliferation process. Since this effect may prevent differentiation mechanism of PC12 cells, further experiments continued with 0.1% alginate microspheres attached scaffolds.

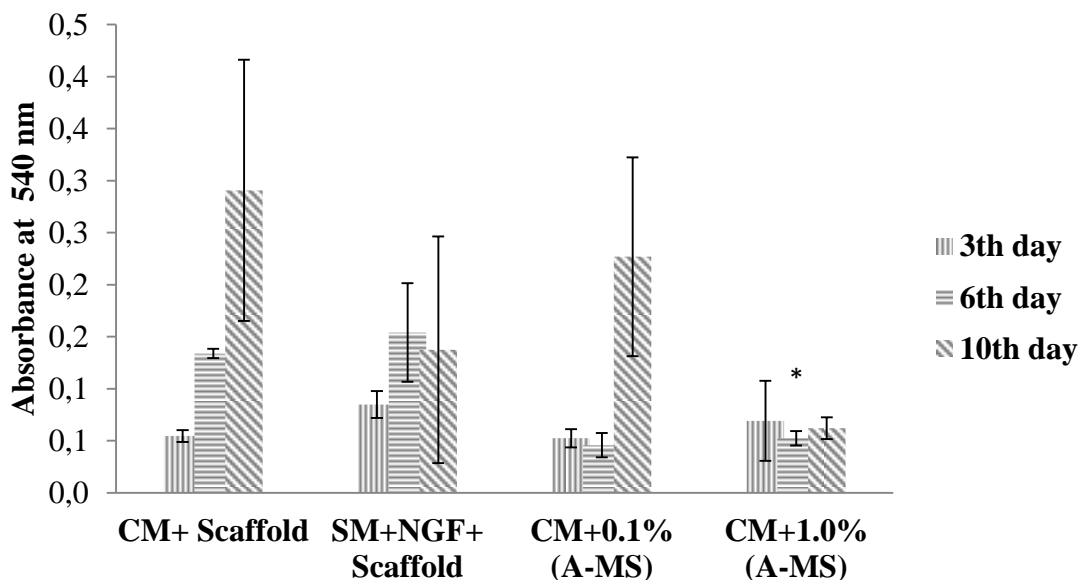


Figure 4.37. Absorbance value of PC12 cells cultured on macroporous nanofibrous gelatin scaffold with/without attached alginate microspheres (A-MS) measured by XTT proliferation assay.

4.4.5. Determination of NGF Bioactivity

To determine bioactivity of NGF loaded into alginate microspheres, 1 $\mu\text{g/ml}$ NGF loaded alginate microspheres were destroyed in PBS and the solution was added to cell culture medium of PC12 cells. On the 5th day, we observed neurite formation. (Figure 4.38). In our previous experiment, it was determined that free form of NGF (50 ng/ml/2 days) induced differentiation of PC12 cell at the end of the 7 days. It seems that

this is an expected result since amount of NGF loaded into the particles is more than the amount of directly added into the cells. On the other hand, it should be noted that NGF in the particles was exposed to harsh conditions during destroying the particles and all the NGF was immediately added into the cell culture medium. Based on this fact, it can be concluded that the method we used for encapsulating NGF did not significantly change its biological activity.

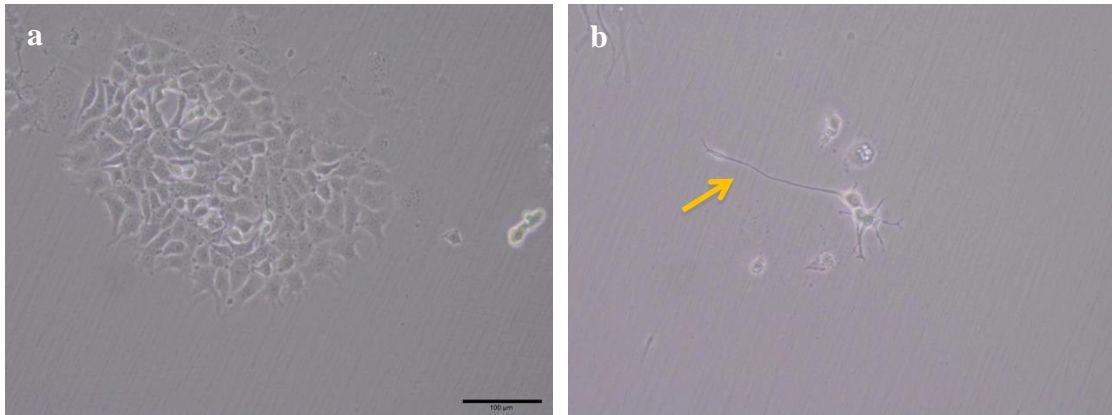


Figure 4.38. Appearance of PC12 cells at the 5th day in a; SM, b; NGF loaded alginate microspheres destroyed medium and SM.

4.4.6. PC12 Cell Differentiation on the Nanofibrous Gelatin Scaffold Integrated with NGF Loaded Alginate Microspheres

Figure 4.39-a shows that PC12 cells attached to the gelatin scaffold have spherical shape. When 50 ng/ml of free NGF was added to the scaffold, the shape of PC12 was no longer spherical but it was flatter (Figure 4.39-b). At the end of the four days, NGF encapsulated in 1% alginate particles did not initiate differentiation of PC12 cells (Figure 4.39-c). On the other hand, well organized neurite structure was obtained in the scaffold incorporated with 0.1% alginate particles (Figure 4.39-d through 4.39-f). Previously, we reported lower cell proliferation in the scaffold in the presence of 1% alginate particles compared to the proliferation level with 0.1% alginate particles. The negative effect of particles prepared with 1% alginate concentration was observed both on the proliferation and differentiation. At the end of 10 days, neurite extension was clearly observed through interconnected pores and a tissue like network formed in the scaffold integrated with 0.1% alginate particles (Figure 4.40-a and Figure 4.40-b). On

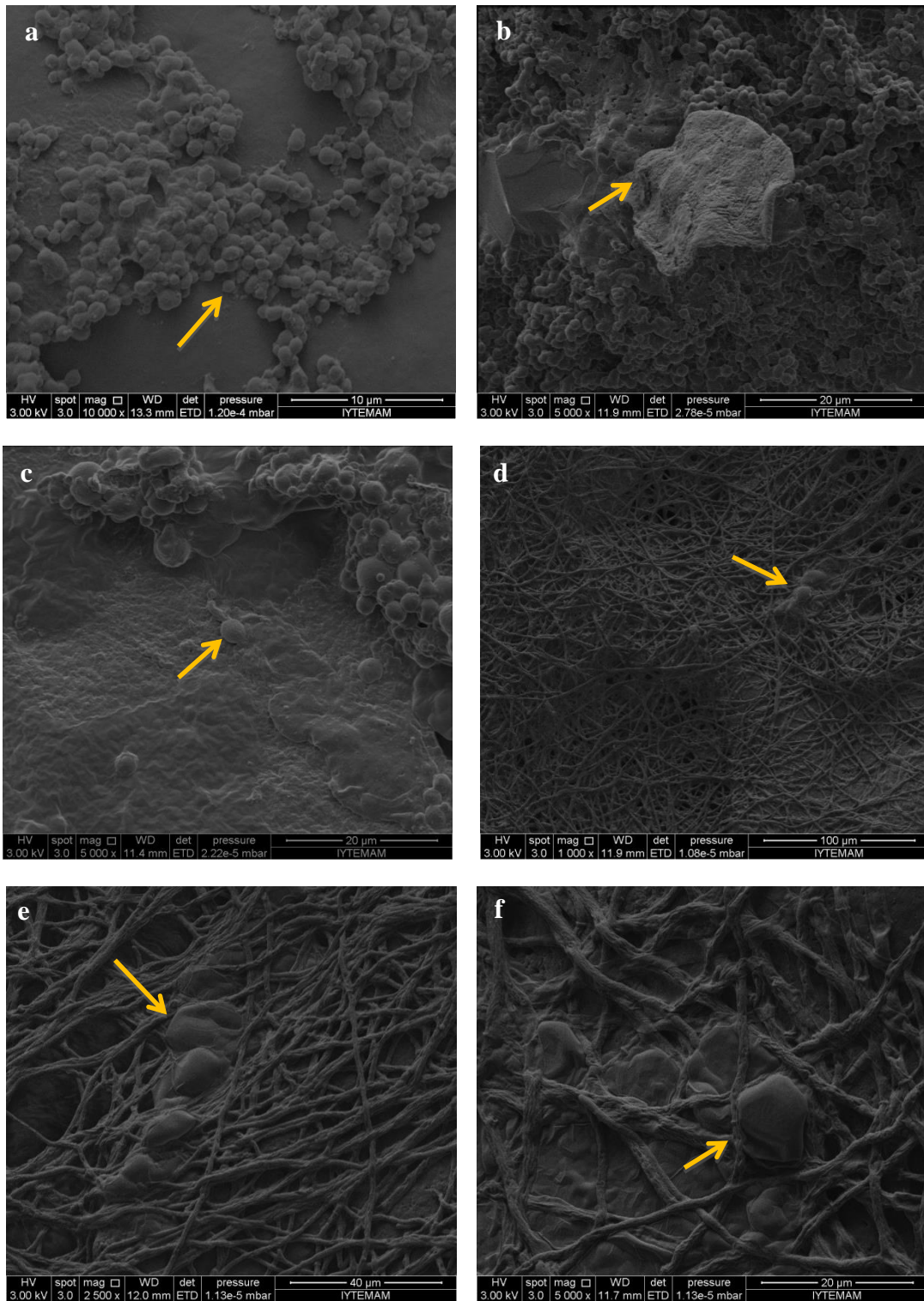


Figure 4.39. 4th day SEM images of PC12 cells seeded on a; gelatin scaffold b; gelatin scaffold and treated with 50 ng/ml of NGF, c; NGF loaded 1.0% alginate microspheres attached gelatin scaffold, d-f; NGF loaded 0.1% alginate microspheres attached nano-fibrous gelatin scaffold (Yellow arrow is indicate PC12 cells onto scaffolds).

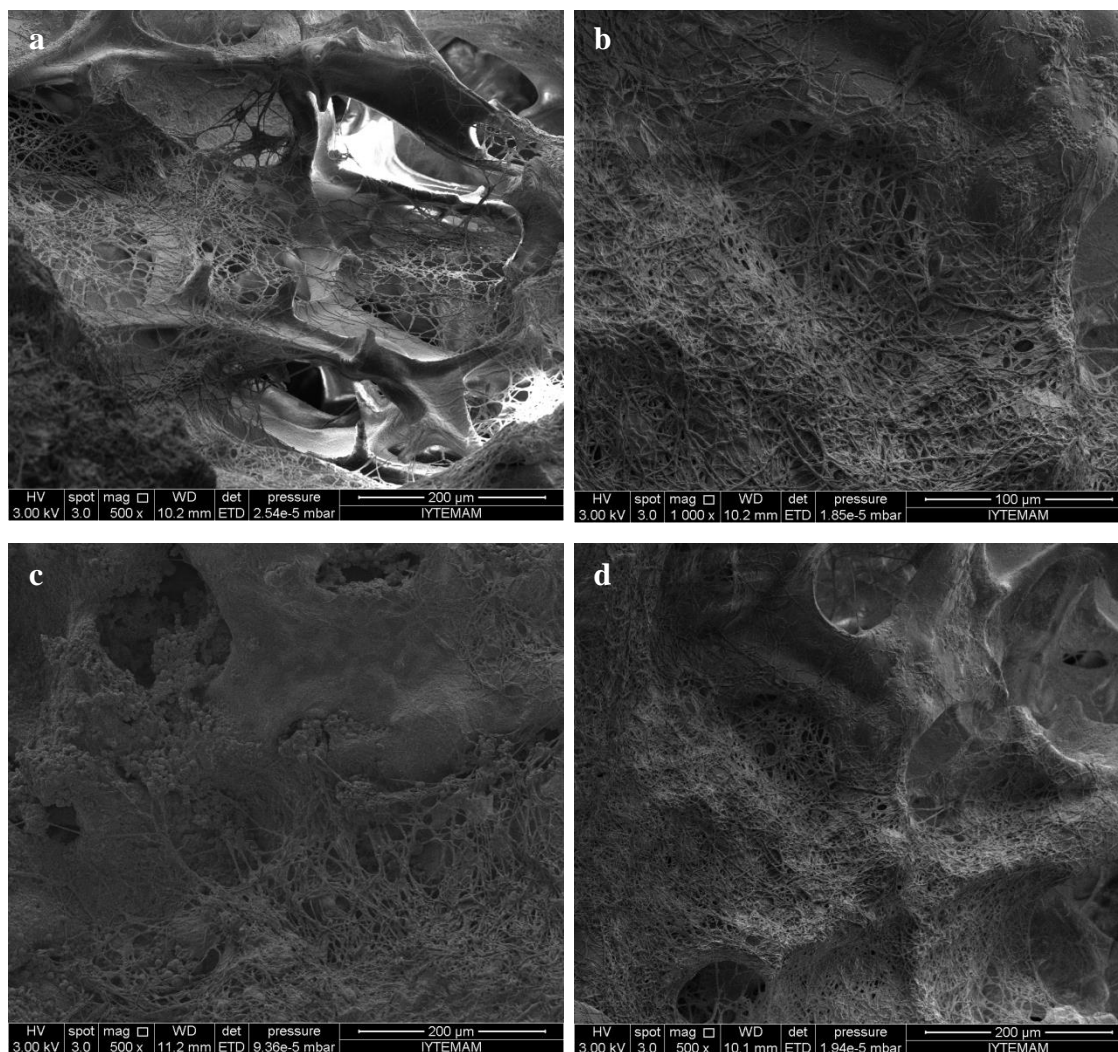


Figure 4.40. 10th day SEM images of PC12 cells seeded on a, b- 0.1% A-MS attached gelatin scaffold; c, d- 1.0% A-MS attached gelatin scaffold.

the 10th day, NGF in 1% alginate particles also started to induce differentiation of cells in the scaffold (Figure 4.40 c-d). The images show that neurite structure on 3D network was much more complex and intense than that observed in 2D cell culture medium. It should be noted that significant neurite extension in 2D culture was observed at the end of 7 days, but in the 3D scaffold including NGF loaded 0.1% alginate particles, neurites were observed on the 4th day. Although we added more NGF into much less number of cells in 2D culture environment (Table 4.9). These results indicate that use of an appropriate delivery carrier which can protect NGF from enzymatic degradation and provide control release of NGF is critical for prolonged retention and biological activity.

Table 4.9. Amount of NGF required at the end of 10 days for the observation of PC12 cell differentiation in 2D and 3D cell culture environment.

Cell culture geometry	Number of cells	Total amount of NGF added (ng)
2D	1,250	400
3D	30,000	250

Macroporous gelatin scaffold integrated with 250 ng NGF loaded microspheres prepared from which 250 ng NGF is loaded was seen suitable for the differentiation of PC12 cells for 10 days. We have shown that when these particles were coated with 1 $\mu\text{g/ml}$ PLL, the release of NGF can be extended up to 30 days (Figure 4.29). It is possible to further extend the release of NGF by increasing the concentration of PLL, loading amount of NGF and the number of layers coated on the particles.

In this study, a new “biomimetic nanoscaffold” with the interconnected macropores, nanofiber matrix structure and growth factor loaded microspheres was fabricated for nerve tissue engineering applications. This scaffold carries all the desirable structural features of a biomimetic nanoscaffold system as can be seen from comparison shown in Figure 4.41a and 41b. Biomimetic nanoscaffolds were developed for bone tissue regeneration (Wei et al. 2006, Wei et al. 2007) and wound healing application (Wei et al. 2008) as shown in Table 4.10. However, the concept is new in nerve tissue regeneration especially in brain tissue engineering.

Table 4.10. The prepared microsphere(MS)/nanosphere(NS) incorporated macroporous nanofibrous scaffold in literature.

Reference	Method	Polymer of Scaffold	Polymer of MS/NS	Active factor	Application
Wei 2006	TIPS	PLLA	PLGA/MS	PDGF-BB	Bone regeneration
Wei 2007	TIPS	PLLA	PLGA/NS	rhBMP	Bone regeneration
Wei 2008	TIPS	PLLA	PLGA/MS	PDGF-BB	Wound repair in multiple tissues
Current study	TIPS	Gelatin	Alginate/MS	NGF	Nerve tissue engineering

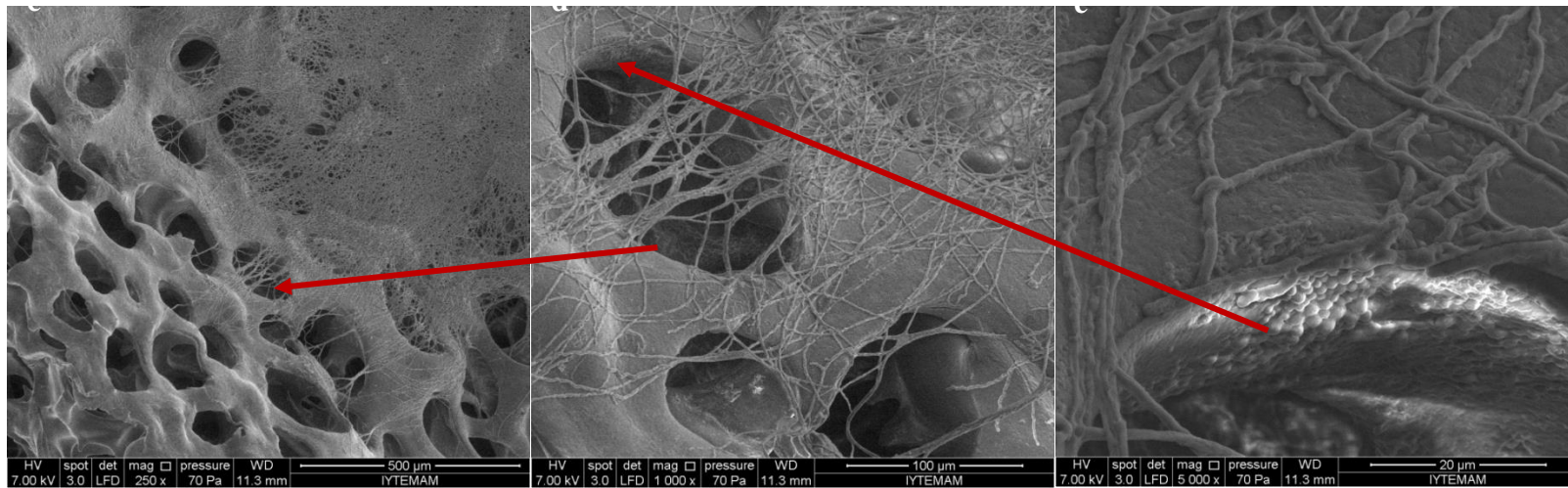
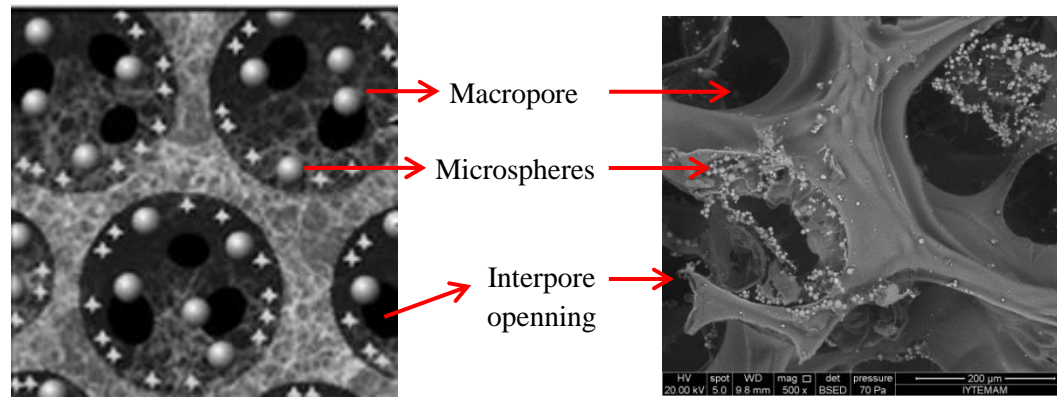


Figure 4.41. a- Model of biomimetic nanoscaffold system with interconnected macropores and growth factor loaded microspheres, b- NGF loaded alginate microspheres attached gelatin scaffold, c- 0.1% NGF loaded alginate microspheres attached gelatin scaffold with PC12 cells cultured for 10 days x250, d- x1000, e- x 5000.

CHAPTER 5

CONCLUSION

In living organisms most of the tissues have the capability of regeneration; on the other hand, this situation is different in mammalian adult neural cells since they lose their ability of proliferation. Compared to peripheral nervous system, central nervous system has restricted regeneration capability which results in trauma, stroke and neuropathology etc. In recent years, tissue engineering became a promising approach for the regeneration of nervous system. An ideal scaffold in tissue engineering should have high porosity and interconnectivity for tissue integration, vascularization and the transfer of nutrient and waste product, adequate mechanical properties suitable with targeted tissue, made from biodegradable material compatible with regenerated tissue and should mimic the natural extracellular matrix surface properties for the cell attachment, proliferation and differentiation. In this study, two different types of gelatin based scaffolds were prepared, one is in disc shape intended for brain tissue engineering and the other one has channeled structure proposed for peripheral nerve tissue engineering application.

Macroporous and nanofibrous scaffolds in disc shape have been prepared by thermally induced phase separation (TIPS) and porogen-leaching technique. The method allows controlling porosity, pore size, interpore connectivity, mechanical properties as well as pore morphologies of the scaffolds. The pore size of the scaffolds was controlled by the size of the paraffin spheres and the connectivity between the pores was provided by the heat treatment time of the paraffin assembly. The results have shown that not only the phase separation temperature but also polymer concentration plays an important role on the structure of the scaffold. Desirable nanofibrous biomimetic scaffolds can be obtained when the phase separation occurs in spinodal region. The dimensional stability of the scaffolds has been provided through chemical crosslinking. By changing the degree of crosslinking, it is possible to control the degradation rate of the scaffolds. Optimum preparation conditions (paraffin sizes, heat treatment time and gelatin concentration) have been selected based on the mechanical properties. Simply, the scaffold with a modulus value similar to that of the

brain tissue has been used for cell attachment. Single and multichanneled scaffolds for peripheral nerve tissue engineering applications have been fabricated by a combination of thermally induced phase separation and injection molding technique. Different surface morphologies have been produced in the form of nerve conduit by changing phase separation temperature and solvent-nonsolvent ratio.

Nanofibrous scaffolds have been integrated with nerve growth factor (NGF) loaded microspheres. A natural biopolymer, alginate, has been used as NGF carrier due to its inherent capability of encapsulating high isoelectric point proteins. Microspheres have been produced in water in oil emulsion through crosslinking of alginate with calcium ions. Homogeneous particles with smooth surface have been obtained using a mixture of lyophilic and hydrophilic surfactants. Carbodiimide reaction has been utilized efficiently for both crosslinking of the scaffold and attaching the alginate microspheres to the scaffold. High encapsulation efficiency of NGF has been achieved by mixing NGF with alginate before the emulsification process. The release rate of NGF from the microspheres has been controlled by the alginate concentration and by coating the particles with poly(L-lysine).

Nanofibrous scaffold provided better environment for cell attachment than the solid walled scaffolds. In addition, the differentiation of PC12 cells on the nanofibrous scaffolds integrated with NGF loaded microspheres has been observed in a shorter time than in the 2 dimensional cell culture medium. In order to induce differentiation, amount of NGF in the scaffold was smaller than the amount of added into cell culture.

In this study, a new biomimetic gelatin based nanofibrous scaffold has been prepared for the first time for brain tissue engineering application. With similar topologic and mechanical properties of brain tissue and capability of controlled release of growth factor, this scaffold has the great potential for the regeneration of destroyed tissues derived from traumatic brain injuries. It can also function as a model tissue for the pharmacological investigations and other treatment strategies for neurodegenerative diseases. Gelatin based channeled conduit with nanofibrous and ladder-like microstructure has also been prepared for the first time for peripheral nerve tissue engineering application. For the future work, the *in vivo* performance of biomimetic nanofibrous scaffolds and conduits integrated with NGF loaded microspheres should be investigated.

REFERENCES

- Abbott, A. 2003. "Cell culture: Biology's new dimension." *Nature*, 424: 870-872.
- Ahmed, S. 2009. "The culture of neural stem cells." *Journal of Cellular Biochemistry*, 106: 1-6.
- Aletta, J.M. 1996. "Phosphorylation of type III beta-tubulin PC12 cell neurites during NGF-induced process outgrowth." *J Neurobiol.*, 4: 61-75.
- Alnaief, M., M.A. Alzaitoun, C.A. García-González. 2011. "Preparation of biodegradable nanoporous microspherical aerogel based on alginate.", *Carbohydrate Polymers* 84: 1011–1018.
- Babensee, J.E., L.V. McIntire, A.G. Mikos. 2000. "Growth Factor Delivery for Tissue Engineering." *Pharmaceutical Research*, 17 (5): 497-504.
- Badami, A.S., M.R. Kreke, M.S. Thompson, J.S. Riffle, A.S. Goldstein. 2006. "Effect of fiber diameter on spreading, proliferation, and differentiation of osteoblastic cells on electrospun poly(lactic acid) substrates." *Biomaterials*, 27: 596-606.
- Binan, L., C. Tendey, G. De Crescenzo, R. El Ayoubi, A. Ajji, M. Jolicoeur. 2014. "Differentiation of neuro-nal stem cells into motor neurons using electrospun poly-L-lactic acid/gelatin scaffold." *Biomaterials*, 35: 664–667.
- Bini, T.B., S. Gao, T.C. Tan, S. Wang, A. Lim, L.B. Hai, S. Ramakrishna. 2004. "Electrospun poly(l-lactide-co-glycolide) biodegradable polymer nanofibre tubes for peripheral nerve regeneration," *Nanotechnology*, 15: 1459–1464.
- Bozkurt, A., G.A. Brook, S. Moellers, F. Lassner, B. Sellhaus, J. Weis, M. Woeltje, J. Tank, C. Beckmann, P. Fuchs, L.O. Damink, F. Schügner, I. Heschel, N. Pallua. 2007. "In vitro assessment of axonal growth using dorsal root ganglia explants in a novel three-dimensional collagen matrix." *Tissue Engineering*, 13: 2971–2979.
- Bozkurt, A., R. Deumens, C. Beckmann, D.L. Olde, F. Schügner, I. Heschel, B. Sellhaus, J. Weis, W. Jahnen-Dechent, G.A. Brook, N. Pallua. 2009. "In vitro cell alignment obtained with a Schwann cell enriched microstructured nerve guide with longitudinal guidance channels." *Biomaterials*, 30: 169–179.
- Bradbury, E.J., L.D.F. Moon, R.J. Popat. 2002. "Chondroitinase ABC promotes functional recovery after spinal cord injury." *Nature*, 416: 636–640.
- Chai, C., K.W. Leong. 2007. "Biomaterials Approach to Expand and Direct Differentiation of Stem Cells." *Molecular Therapy*, 15: 467–480.
- Chang, J-Y., J-H. Lin, C-H. Yao, J-H. Chen, T-Y. Lai, and Y-S. Chen. 2007. "In vivo evaluation of a biodegradable EDC/NHS-cross-linked gelatin peripheral nerve guide conduit material." *Macromolecular Bioscience*, 7: 500–507.

- Chen, R., S.J. Curran, J.M. Curran, J.A. Hunt. 2006. "The use of poly(l-lactide) and RGD modified microspheres as cell carriers in a flow intermittency bioreactor for tissue engineering cartilage." *Biomaterials*, 27: 4453–4460.
- Chen, V.J., P.X. Ma. 2004. "Nano-fibrous poly(L-lactic acid) scaffolds with interconnected spherical macropores", *Biomaterials*, 25: 2065-2073.
- Chen, V.J., P.X. Ma. 2006. "Polymer phase separation." In *Scaffolding in Tissue Engineering*. Ma P.X., J. Elisseeff (eds.) Taylor & Francis Group, 125-139.
- Chen, Y-S., J-Y. Chang, C-Y. Cheng, F-J. Tsai, C-H. Yao, and B-S. Liu. 2005. "An *in vivo* evaluation of a biodegradable genipin-cross-linked gelatin peripheral nerve guide conduit material." *Biomaterials*, 26: 3911–3918.
- Chiono, V., G. Ciardelli, G. Vozzi, J. Cortez, N. Barbani, P. Gentile, P. Giusti. 2008. "Enzymatically-modified melt-extruded guides for peripheral nerve repair." *Engineering in Life Sciences*, 8: 226–237.
- Chung, H.J., T.G. Park. 2007. "Surface engineered and drug releasing pre-fabricated scaffolds for tissue engineering." *Advanced Drug Delivery Reviews*, 59: 249–262.
- Ciofani, G., V. Raffa, A. Menciassi, P. Dario. 2008. "Alginate and chitosan particles as drug delivery system for cell therapy." *Biomed Microdevices*, 10: 131-40.
- Clements, I.P., Y.T. Kim, A.W. English, X. Lu, A. Chung, R.V. Bellamkonda. 2009. "Thin-film enhanced nerve guidance channels for peripheral nerve repair." *Biomaterials*, 30: 3834–3846.
- Cui, F.Z., W.M. Tian, S.P. Hou, Q.Y. Xu, I-S. Lee. 2006. "Hyaluronic acid hydrogel immobilized with RGD peptides for brain tissue engineering." *J Mater Sci Mater Med.*, 17: 1393-1401.
- Daly, W., L. Yao, D. Zeugolis, A. Windebank, A. Pandit. 2012. "A biomaterials approach to peripheral nerve regeneration: bridging the peripheral nerve gap and enhancing functional recovery." *J. R. Soc. Interface*, 9: 202-21.
- Das, K.P., T.M. Freudenrich, W.R. Mundy. 2004. "Assessment of PC12 cell differentiation and neurite growth: a comparison of morphological and neurochemical measures." *Neurotoxicology and Teratology*, 26: 397–406.
- Ellis-Behnke, R.G., Y.X. Liang, S.W. You, D.K. Tay, S. Zhang, K.F. So. 2006. "Nano neuro knitting: peptide nanofiber scaffold for brain repair and axon regeneration with functional return of vision." *Proc Natl Acad Sci USA*, 103: 5054–5059.
- Evans, G.R.D., K. Brandt, M.S. Widmer, L. Lu, R.K. Meszlenyi, P.K. Gupta, A.G. Mikos, J. Hodges, J. Williams, A. Gürlek, A. Nabawi, R. Lohman, C.W. Patrick Jr. 1999. "*In vivo* evaluation of poly(l-lactic acid) porous conduits for peripheral nerve regeneration." *Biomaterials*, 20: 1109–1115.

- Evans, N.D., E. Gentleman, J.M. Polak. 2006. "Scaffolds for stem cells." *Materials Today*, 9: 26-33.
- Ferguson, T.A., Y-J. Son. 2011. "Extrinsic and intrinsic determinants of nerve regeneration." *J Tissue Eng.* 2: 1-12.
- Fong, E.L.S., S-E. L-C. E. Burdett, V. Ramamoorthy, A.J. Lazar, F.K. Kasper, M.C. Farach-Carson, D. Vishwamitr, E.G. Demicco, B.A. Menegaz, H.M. Amin, A.G. Mikos, J. A. Ludwig. 2013. "Modeling Ewing sarcoma tumors *in vitro* with 3D scaffolds." *PNAS*, 110: 6500–6505.
- Greene,L.A. (1978) *J. Cell Biol.*, 78. 747-755.
- Greene.L.A. and Tischler,A.S. (1976) *Proc. Nald. Acad. Sci. USA*, 73. 2424-2428.
- Gu F., B. Amsden, R. Neufeld. 2004. "Sustained delivery of vascular endothelial growth factor with alginate beads." *Journal of Controlled Release*, 96: 463–472.
- Guan J., K.L. Fujimoto, W.R. Wagner. 2008. "Elastase-Sensitive Elastomeric Scaffolds with Variable Anisotropy for Soft Tissue Engineering.", *Pharmaceutical Research*, 25: 2400-2412.
- Härmä, V, J. Virtanen, R. Mäkelä, A. Happonen, J.P. Mpindi, M. Knuuttila, P. Kohonen, J. Lötjönen, O. Kallioniemi, M. Nees. 2010. "A comprehensive panel of three-dimensional models for studies of prostate cancer growth, invasion and drug responses." *PLoS One*. 5: e10431, 1-17.
- Hermanson G.T. 1996. "Protein Crosslinking Method." In *Bioconjugate Technique*. Hermanson G.T. (eds). Elsevier Inc. 144-148.
- Horning, J.L., S.K. Sahoo, S. Vijayaraghavalu, S. Dimitrijevic, J.K. Vasir, T.K. Jain, A.K. Panda, V. Labhasetwar. 2008. "3-D tumor model for *in vitro* evaluation of anticancer drugs." *Mol Pharm.* 5: 849-62.
- Höke, A. 2011. "A (heat) shock to the system promotes peripheral nerve regeneration." *J Clin Invest.* 121: 4231–4234.
- Hu, J., P.X. Ma. 2011. "Nano-fibrous tissue engineering scaffolds capable of growth factor delivery." *Pharm Res.* 28: 1273-1281.
- Hu, X., J. Huang, Z. Ye, L. Xia, M. Li, B. Lv, X. Shen, Z. Luo. 2009. "A novel scaffold with longitudinally oriented microchannels promotes peripheral nerve regeneration." *Tissue Engineering Part A*, 15: 3297–3308.
- Hutmacher, D., T. Woodfield, P. Dalton, J. Lewis. 2008. "Scaffold design and fabrication." In *Tissue Engineering*, Clemens van Blitterswijk (Ed), Elsevier Inc. 428.
- Ikada, Y. 2006. "Scope of tissue engineering." In *Tissue engineering fundamentals and applications*. Elsevier Inc. 1-89.

- Jay, S.M., W.M. Saltzman. 2009. "Controlled Delivery of VEGF Via Modulation of Alginate Microparticle Ionic Crosslinking." *Journal of Controlled Release*, 134: 26-34.
- Jia, L., M.P. Prabhakaran, X. Qin, S. Ramakrishna. 2013. "Stem cell differentiation on electrospun nanofibrous substrates for vascular tissue engineering." *Mater Sci Eng C Mater Biol Appl*, 33: 4640–4650.
- Khang, G., M.S. Kim, H.B. Lee. 2007. "A manual for biomaterial scaffold technology." 103.
- Kievit, F.M., S.J. Florczyk, M.C. Leung, O. Veiseh, J.O. Park, M.L. Disis, M. Zhang. 2010. "Chitosan-alginate 3D scaffolds as a mimic of the glioma tumor microenvironment." *Biomaterials*, 31: 5903-10.
- Kim, H., C.H. Tator, M.S. Shoichet. 2008. "Design of protein-releasing chitosan channels." *Biotechnol. Prog.* 24, 932–937.
- Kim, S.E., J.H., Park, Y.W. Cho, H. Chung, S.Y. Jeong, E.B. Lee, I.C. Kwon. 2003. "Porous chitosan scaffold containing microspheres loaded with transforming growth factor-beta1: implications for cartilage tissue engineering." *J Control Release*, 91: 365-74.
- Kroehne, V., I. Heschel, F. Schügner, D. Lasrich, J.W. Bartsch, H. Jockusch. 2008. "Use of a novel collagen matrix with oriented pore structure for muscle cell differentiation in cell culture and in grafts." *Journal of Cellular and Molecular Medicine*, 12: 1640–1648.
- Kuijpers, A.J., G.H.M. Engbers, J. Krijgsveld, S.A.J. Zaat, J. Dankert, J. Feijen. 2000. "Cross-linking and characterisation of gelatin matrices for biomedical applications." *J. Biomaterial Science Polymer Edition*, 11: 225-243.
- Lee J.E., S.E. Kim, I.C. Kwon, H.J. Ahn, H. Cho, S.H. Lee, H.J. Kim, S.C. Seong, M.C. Lee. 2004. "Effects of a chitosan scaffold containing TGF-beta1 encapsulated chitosan microspheres on *in vitro* chondrocyte culture." *Artif Organs*, 28: 829-39.
- Lee, J.K., C.G. Geoffroy, A.F. Chan. 2010. "Assessing spinal axon regeneration and sprouting in Nogo-, MAG-, and OMgp-deficient mice." *Neuron*, 66: 663–670.
- Lee, J.K., R. Chow, F. Xie, S.Y. Chow, K.E. Tolentino, B. Zheng. 2010. "Combined genetic attenuation of myelin and semaphorin-mediated growth inhibition is insufficient to promote serotonergic axon regeneration." *J Neurosci*, 30: 10899–10904.
- Lee, K.Y., S.H. Yuk. 2007. "Polymeric protein delivery systems." *Progress in Polymer Science*, 32: 669-697.
- Lemoine, D., F. Wauters, S. Bouchend'homme, V. Preat. 1998. "Preparation and characterization of alginate microspheres containing a model antigen." *International Journal of Pharmaceutics*, 176: 9–19.

- Leung, V., R. Hartwell, S.S. Elizei, H. Yang, A. Ghahary, F. Ko. 2014. "Postelectrospinning modifications for alginate nanofiber-based wound dressings." *J Biomed Mater Res Part B*, 102: 508-515.
- Li X-K., S-X. Cai, B. Liu, Z.L. Xu, X.Z. Dai, K.W. Ma, S.Q. Lin, L. Yang, K.L. Sung, X.B. Fu. 2007. "Characteristics of PLGA-gelatin complex as potential artificial nerve scaffold." *Colloids and Surfaces B*, 57: 198–203.
- Li, W-J., R. Tuli, C. Okafor, A. Derfoul, K.G. Danielson, D.J. Hall, R.S. Tuan. 2005. "A three-dimensional nanofibrous scaffold for cartilage tissue engineering using human mesenchymal stem cells." *Biomaterials*, 26: 599–609.
- Li, X., Z. Yang, A. Zhang. 2009. "The effect of neurotrophin-3/chitosan carriers on the proliferation and differentiation of neural stem cells." *Biomaterials*, 30: 4978–4985.
- Lim, S.H., H-Q. Mao. 2009. "Electrospun scaffolds for stem cell engineering." *Advanced Drug Delivery Reviews*, 61: 1084–1096.
- Liu X, P.X. Ma. 2004. "Polymeric scaffolds for bone tissue engineering." *Ann Biomed Eng*. 32: 477-86.
- Liu, X., P.X. Ma. 2009. "Phase separation, pore structure, and properties of nanofibrous gelatin scaffolds." *Biomaterials*, 30: 4094–4103.
- Lu, L., S. Peter, M. Lyman, H. Lai, S. Leite, J. Tamada, S. Uyama, J. Vacanti, R. Langer, A. Mikos. 2000. "In vitro and in vivo degradation of porous poly (DL-lactic-co-glycolic acid) foams." *Biomaterials*, 21: 1595-1605.
- Lu, M-C., S-W. Hsiang, T-Y. Lai, C-H. Yao, L-Y. Lin, and Y-S. Chen. 2007. "Influence of cross-linking degree of a biodegradable genipin-cross-linked gelatin guide on peripheral nerve regeneration." *Journal of Biomaterials Science, Polymer Edition*, 18: 843–863.
- Lutolf, M.P., P.M. Gilbert, H.M. Blau. 2009. "Designing materials to direct stem-cell fate" *Nature*, 26: 433–441.
- Ma P.X., R. Zhang. 1999. "Synthetic nano-scale fibrous extracellular matrix." *J Biomed Mater Res*. 46: 60-72.
- Ma, P.X. 2004. "Scaffolds for tissue fabrication." *Materials Today*, 7: 30–40.
- Ma, P.X. 2008. "Biomimetic materials for tissue engineering." *Adv Drug Del Rev*, 60: 184-198.
- Ma, P.X., J.W. Choi. 2001. "Biodegradable Polymer Scaffolds with Well-Defined Interconnected Spherical Pore Network." *Tissue Engineering*, 7: 23-33.
- Ma, P.X., R. Langer. 1999. "Fabrication of biodegradable polymer foams for cell transplantation and tissue engineering." In *Tissue Engineering Methods and Protocols*, Morgan, J., and Yarmush, M. (eds.) Humana Press, NJ, 47.

- Morlock, M., H. Koll, G. Winter, T. Kissel. 1997. "Microencapsulation of erythropoietin, using biodegradable poly(D,L-lactide-co-glycolide): protein stability and the effects of stabilizing excipients." *Eur. J. Pharm. Biopharm.* 43: 29-36.
- Nam, Y.S., T.G. Park. 1999. "Biodegradable polymeric microcellular foams by modified thermally induced phase separation method." *Biomaterials*, 20: 1783–1790.
- Nam, Y.S., T.G. Park. 1999. "Porous biodegradable polymeric scaffolds prepared by thermally induced phase separation." *J. Biomed.Mater. Res.*, 47, 8–17.
- Niu, X., Q. Feng, M. Wang, X. Guo, Q. Zheng. 2009. "Porous nano-HA/collagen/PLLA scaffold containing chitosan microspheres for controlled delivery of synthetic peptide derived from BMP-2." *J. Control Release*, 134: 111-117.
- O'Brien, F.J. 2011. "Biomaterials & scaffolds for tissue engineering" *Materials Today* 14: 88–95.
- Pabari, A., S.Y. Yang, A.M. Seifalian, A. Mosahebi. 2010. "Modern surgical management of peripheral nerve gap." *J. Plast. Reconstr. Aesthet. Surg.* 63: 1941–1948.
- Park, K.I., Y.D. Teng, E.Y. Snyder. 2002. "The injured brain interacts reciprocally with neural stem cells supported by scaffolds to reconstitute lost tissue." *Nat Biotechnol*, 20: 1111–1117.
- Pettikiriarachchi, J.T.S., C.L. Parish, M.S. Shoichet, J.S. Forsythe, D.R. Nisbet. 2010. "Biomaterials for Brain Tissue Engineering." *Aust. J. Chem.* 63: 1143–1154.
- Pfister, L.A., M. Papaloizos, H.P. Merkle, B. Gander. 2007. "Hydrogel nerve conduits produced from alginate/chitosan complexes." *Journal of Biomedical Materials Research Part A*, 80: 932–937.
- Plikk, P., S. Målberg, A.C. Albertsson. 2009. "Design of resorbable porous tubular copolyester scaffolds for use in nerve regeneration." *Biomacromolecules*, 10: 1259-1264.
- Porras, M., C. Solans, C. González, J.M. Gutiérrez. 2008. "Properties of water-in-oil (W/O) nano-emulsions prepared by a low-energy emulsification method." *Colloids and Surfaces A: Physicochemical and Engineering Aspects*, 324: 181–188.
- Porras, M., C. Solans, C. González, A. Martínez, A. Guinarta, J.M. Gutiérrez. 2004. "Studies of formation of W/O nano-emulsions." *Colloids and Surfaces A: Physicochemical and Engineering Aspects*, 249: 115–118.

- Premnath, P., B. Tan, K. Venkatakrishnan. 2013. "Direct patterning of free standing three dimensional silicon nanofibrous network to facilitate multi-dimensional growth of fibroblasts and osteoblasts." *J Biomed Nanotechnol*, 911: 1875–1881.
- Ravichandran, R., J.R. Venugopal, S. Sundarrajan, S. Mukherjee, S. Ramakrishna. 2012. "Precipitation of nanohydroxyapatite on PLLA/PBLG/Collagen nanofibrous structures for the differentiation of adipose derived stem cells to osteogenic lineage." *Biomaterials*, 33: 846–855.
- Rich, K.M., J.R. Luszczynski, P.A. Osborne, E.M. Johnson Jr. 1987. "Nerve growth factor protects adult sensory neurons from cell death and atrophy caused by nerve injury", *J. Neurocytol*, 16: 261–268.
- Rudkin, B.B., P. Lazarovici, B-Z. Levi, Y. Abe, K. Fujita, G. Guroff. 1989. "Cell cycle-specific action of nerve growth factor in PC12 cells: differentiation without proliferation." *The EMBO Journal*, 8: 3319 – 3325.
- Ruoslaht, E., 1996. "Brain extracellular matrix." *Glycobiology*, 6: 489-492.
- Sah, H. 1999. "Stabilization of proteins against methylene chloride/water interface-induced denaturation and aggregation." *J. Controlled Release*, 58: 143-151.
- Sarkar, S.D., B.L. Farrugia, T.R. Dargaville, S. Dhara. 2013. "Chitosan-collagen scaffolds with nano/microfibrous architecture for skin tissue engineering." *J Biomed Mater Res A*, 101: 3482–3492.
- Schmeichel, K.L., M.J. Bissell. 2003. "Modeling tissue-specific signaling and organ function in three dimensions." *J Cell Sci.*, 116: 2377–2388.
- Schugens, C., V. Maquet, C. Grandfils, R. Jerome, P. Teyssie. 1996. "Polylactide macroporous biodegradable implants for cell transplantation. II. Preparation of polylactide foams by liquid-liquid phase separation." *J Biomed Mater Res*. 30: 449-61.
- Schultz, S., G. Wagner, K. Urban, J. Ulrich. 2004. "High-Pressure Homogenization as a Process for Emulsion Formation." *Chemical Engineering & Technology* 27: 361–368.
- Shao, J., C. Chen, Y. Wang, X. Chen, C. Du. 2012. "Early stage evolution of structure and nanoscale property of nanofibers in thermally induced phase separation process." *Reactive and Functional Polymers*, 72: 765-772.
- Sofroniew, M.V., C.L. Howe, W.C. Mobley. 2001. "Nerve growth factor signaling, neuroprotection, and neural repair." *Annu Rev Neurosci*. 24:1217-81.
- Stamatialis, D.F., B.J. Papenburg, M. Gironés, S. Saiful, S.N.M. Bettahalli, S. Schmitmeier, M. Wessling. 2008. "Medical applications of membranes: Drug delivery, artificial organs and tissue engineering." *Journal of Membrane Science*, 308: 1–34.
- Starcher, B. 2001. "A Ninhydrin-Based Assay to Quantitate the Total Protein Content of Tissue Samples." *Analytical Biochemistry*, 292: 125-129.

- Sturesson, C., J. Carlfos. 2000. "Incorporation of protein in PLG-microspheres with retention of bioactivity." *J. Controlled Release*, 67: 171-178.
- Subramanian, A., U.M. Krishnan, S. Sethuraman. 2009. "Development of biomaterial scaffold for nerve tissue engineering: Biomaterial mediated neural regeneration." *Journal of Biomedical Science*, 16: 1-11.
- Sun, C., X. Jin, J.M. Holzwarth, X. Liu, J. Hu, M.J. Gupte, Y. Zhao, P.X. Ma. 2012. "Development of channeled nanofibrous scaffolds for oriented tissue engineering." *Macromol Biosci.*, 12: 761-9.
- Sun, P, Y. Xu, X. Du, N. Ning, H. Sun, W. Liang, R. Li. 2013. "An engineered three-dimensional gastric tumor culture model for evaluating the antitumor activity of immune cells in vitro." *Oncol Lett.* 5: 489-494.
- Tan, H, J. Wu, L. Lao, C. Gao. 2009. "Gelatin/chitosan/hyaluronan scaffold integrated with PLGA microspheres for cartilage tissue engineering." *Acta Biomater.* 5: 328-37.
- Tanaka, S., T. Takigawa, S. Ichihara, T. Nakamura. 2006. "Mechanical properties of the bioabsorbable polyglycolic acid-collagen nerve guide tube," *Polymer Engineering and Science*, 46: 1461-1467.
- Tang-Schomera, M.D., J.D. White, L.W. Tien, L.I. Schmitt, T.M. Valentina, D.J. Graziano, A.M. Hopkins, F.G. Omenetto, P.G. Haydon, D.L. Kaplan. 2014. "Bioengineered functional brain-like cortical tissue." *PNAS*, 111: 13811-13816.
- Teng, Y.D., E.B. Lavik, X. Qu, K.I. Park, J. Ourednik, D. Zurakowski, R. Langer, E.Y. Snyder. 2002. "Functional recovery following traumatic spinal cord injury mediated by a unique polymer scaffold seeded with neural stem cells." *Proc Natl Acad Sci USA*, 99: 3024-3029.
- Thomson, H.A., A.J. Treharne, P. Walker, M.C. Grossel, A.J. Lotery. 2011. "Optimisation of polymer scaffolds for retinal pigment epithelium (RPE) cell transplantation." *Br J Ophthalmol.* 95: 563-568.
- Tomita, M., E. Lavik, H. Klassen, T. Zahir, R. Langer, M. J. Younga. 2005. "Biodegradable Polymer Composite Grafts Promote the Survival and Differentiation of Retinal Progenitor Cells." *Stem Cells*, 23: 1579-1588.
- Turner, D.C., L.A. Flier, S. Carbonetto. 1989. "Identification of a cell-surface protein involved in PC12 cell-substratum adhesion and neurite outgrowth on laminin and collagen." *J Neurosci.* 9(9): 3287-3296.
- Valmikinathan, C.M., J. Tian, J. Wang, X. Yu. 2008. "Novel nanofibrous spiral scaffolds for neural tissue engineering." *J. Neural Eng.* 5: 422-432.
- Venugopal, J., Y.Z. Zhang, S. Ramakrishna. 2005. "Fabrication of modified and functionalized polycaprolactone nanofiber scaffolds for vascular tissue engineering." *Nanotechnology*, 16: 2138-2142.

- Wang T.W., M. Spector. 2009. "Development of hyaluronic acid-based scaffolds for brain tissue engineering." *Acta Biomaterialia*, 5: 2371-2384.
- Wang Y., H. Deng, Z-H. Zu, X-C. Shen, H. Liang, F-Z. Cui, Q-Y. Xu, I-S. Lee. 2010. "Interactions between neural stem cells and biomaterials combined with biomolecules." *Front. Mater. Sci. China*, 4: 325-331.
- Wang, L., Y. Tingyuan, G. Ma. 2013. Microspheres and microcapsules for protein drug delivery. In Guanghui Ma, Zhi-Guo Su (Eds), *Microspheres and Microcapsules in Biotechnology: Design, Preparation, and Applications*, 246-300.
- Wang, S., Q. Cai, J. Hou, J. Bei, T. Zhang, J. Yang, Y. Wan. 2003. "Acceleration effect of basic fibroblast growth factor on the regeneration of peripheral nerve through a 15-mm gap." *Journal of Biomedical Materials Research Part A*, 66: 522-531.
- Wang, W, S. Itoh, A. Matsuda, T. Aizawa, M. Demura, S. Ichinose, K. Shinomiya, J. Tanaka. 2008. "Enhanced nerve regeneration through a bilayered chitosan tube: the effect of introduction of glycine spacer into the CYIGSR sequence." *J Biomed Mater Res A*, 85: 919-928.
- Wang, X., W. Hu, Y. Cao, J. Yao, J. Wu, X. Gu. 2005. "Dog sciatic nerve regeneration across a 30-mm defect bridged by a chitosan/PGA artificial nerve graft." *Brain*, 128: 1897-1910.
- WEB_1 <http://www.applichem.com/en/literature/applications/no-12-cell-proliferation-assay-xtt/>.
- Wei, G., P.X. Ma. 2008. "Nanostructured Biomaterials for Regeneration." *Adv. Funct. Mater.* 18: 3568-3582.
- Wei, G., Q. Jin, W.V. Giannobile, P.X. Ma. 2007. "The enhancement of osteogenesis by nano-fibrous scaffolds incorporating rhBMP-7 nanospheres." *Biomaterials*. 28: 2087-2096.
- Wei, G., Q. Qiming Jin, W.V. Giannobile, P.X. Ma. 2006. "Nano-fibrous scaffold for controlled delivery of recombinant human PDGF-BB." *J Control Release*, 112: 103-110.
- Wells, L.A., H. Sheardown. 2007. "Extended release of high pI proteins from alginate microspheres via a novel encapsulation technique." *European Journal of Pharmaceutics and Biopharmaceutics*, 65: 329-335.
- Widmer, M.S., P.K. Gupta, L. Lu, R.K. Meszlenyi, G.R. Evans, K. Brandt, T. Savel, A. Gurlek, C.W. Patrick Jr, A.G. Mikos. 1998. "Manufacture of porous biodegradable polymer conduits by an extrusion process for guided tissue regeneration." *Biomaterials*, 19: 1945-1955.
- Williams, D.F. 2008. "On the mechanisms of biocompatibility." *Biomaterials*, 29: 2941-2953.

- Woo, K.M., V.J. Chen, P.X. Ma. 2003. "Nano-fibrous scaffolding architecture selectively enhances protein adsorption contributing to cell attachment." *J Biomed Mater Res A*, 67: 531-537.
- Wu J., C. Liao, J. Zhang, W. Cheng, N. Zhou, S. Wang, Y. Wan. 2011. "Incorporation of protein-loaded microspheres into chitosan-polycaprolactone scaffolds for controlled release." *Carbohydrate Polymers*, 86: 1048–1054.
- Xin, X., M. Hussain, J.J. Mao. 2007. "Continuing differentiation of human mesenchymal stem cells and induced chondrogenic and osteogenic lineages in electrospun PLGA nanofiber scaffold." *Biomaterials*, 28: 316–325.
- Xu, X-Y., X-T. Li, S-W. Peng, J-F. Xiao, C. Liu, G. Fang, K.C. Chen, G-Q. Chen. 2010. "The behaviour of neural stem cells on polyhydroxyalkanoate nanofiber scaffolds." *Biomaterials*, 31: 3967–3975.
- Yang, F., R. Murugan, S. Ramakrishna, X. Wang, Y.X. Ma, S. Wang. 2004. "Fabrication of nano-structured porous PLLAscaffold intended for nerve tissue engineering" *Biomaterials*, 25: 1891–1900.
- Yang, Y., L.D. Laporte, C.B. Rives, J-H. Jang, W-C. Lin, K.R. Shull, L.D. Shea. 2005. "Neurotrophin releasing single and multiple lumen nerve conduits." *Journal of Controlled Release*, 104: 433–446.
- Yang, Z., X. Zhao. 2011. "A 3D model of ovarian cancer cell lines on peptide nanofiber scaffold to explore the cell-scaffold interaction and chemotherapeutic resistance of anticancer drugs." *Int J Nanomedicine*, 6: 303-310.
- Yao, L., G.C.W. Ruiter, H. Wang, M.A. Knight, R.J. Spinner, M.J. Yaszemskid, A.J. Windebank, A. Pandit. 2010. "Controlling dispersion of axonal regeneration using a multichannel collagen nerve conduit." *Biomaterials*, 31, 5789-5797.
- Yeo, Y., N. Baek, K. Park. 2001. "Microencapsulation Methods for Delivery of Protein Drugs" *Biotechnol. Bioprocess Eng*, 6: 213-230.
- Zeng, W., M. Rong, X. Hu, W. Xiao, F. Qi, J. Huang, Z. Luo, 2014. "Incorporation of Chitosan Microspheres into Collagen-Chitosan Scaffolds for the Controlled Release of Nerve Growth Factor." *J Plos One*, 9: 1-9.
- Zhang, M., P. Boughton, B. Rose, C.S. Lee, A.M. Hong. 2013. "The Use of Porous Scaffold as a Tumor Model." *International Journal of Biomaterials*,
- Zhang, R., P.X. Ma, 1999. "Poly(a-hydroxyl acids)/hydroxyapatite porous composites for bone-tissue engineering. I. Preparation and morphology." *J Biomed Mater Res.*, 1: 446-55.
- Zhang, Y.Z., H.W. Ouyang, C.T. Lim, S. Ramakrishna, Z.M. Huang. 2005. "Electrospinning of gelatin fibers and Gelatin/PCL composite fibrous scaffolds." *J Biomed Mater Res B*, 72: 156–165.

APPENDIX A

CALCULATION OF EDC, NHS, COOH_{FREE} AND ACETONE AMOUNTS REQUIRED FOR CROSSLINKING REACTION

Calculation based on 0.025 g gelatin scaffold.

- Type B gelatin (Sigma) has 110 millimoles of free carboxyl groups per 100 g of protein. Then 0.025 g gelatin contains 0.0275 mmol COOH_{free} groups.

$$\begin{array}{r} 100 \text{ g gelatin} \quad 110 \text{ mmol COOH}_{\text{free}} \\ 0.025 \text{ g gelatin} \quad \quad \quad X \\ \hline X = 0.0275 \text{ mmol COOH}_{\text{free}} \end{array}$$

- For the EDC/COOH_{free} ratio of 2:1 (mole/mole)

$$n_{\text{EDC}} = 0.055 \text{ mmol}$$

$$n_{\text{EDC}} = \frac{m}{M_A}, \quad 0.055 \text{ mmol} = \frac{m}{191 \text{ g/mol}}, \quad m_{\text{EDC}} = 0.011 \text{ g}$$

- For the NHS/EDC ratio of 0.2 (mole/mole)

$$n_{\text{NHS}} = 0.011 \text{ mmol}$$

$$n_{\text{NHS}} = \frac{m}{M_A}, \quad 0.011 \text{ mmol} = \frac{m}{111.09 \text{ g/mol}}, \quad m_{\text{NHS}} = 0.0012 \text{ g}$$

- For the acetone/water ratio of 90/10 (v/v) and the EDC concentration of 5 mM.

Amount of acetone required for crosslinking is

$$5 \text{ mM} = \frac{n_{\text{EDC}}}{V}, \quad 5 \text{ mM} = \frac{0.055 \text{ mmol}}{V}, \quad V = 11 \text{ ml}$$

$$V_{\text{acetone}} = 9.9 \text{ ml and } V_{\text{water}} = 1.1 \text{ ml.}$$

- For the crosslinking reaction MES Hydrate Buffer was used. The concentration of MES Hydrate was 0.05 M (Liu and Ma 2009). Required amount of MES Hydrate can be calculated as;

$$0.05 \text{ M} = \frac{n_{\text{MES Hydrate}}}{V}, \quad 0.05 \text{ M} = \frac{n_{\text{MES Hydrate}}}{1.1 \text{ ml}}, \quad n_{\text{MES Hydrate}} = 0.055 \times 10^{-3} \text{ mol},$$

$$m_{\text{MES Hydrate}} = 0.055 \times 10^{-3} \text{ mol} \times 195 \text{ g/mol}, \quad m_{\text{MES Hydrate}} = 0.011 \text{ g}.$$

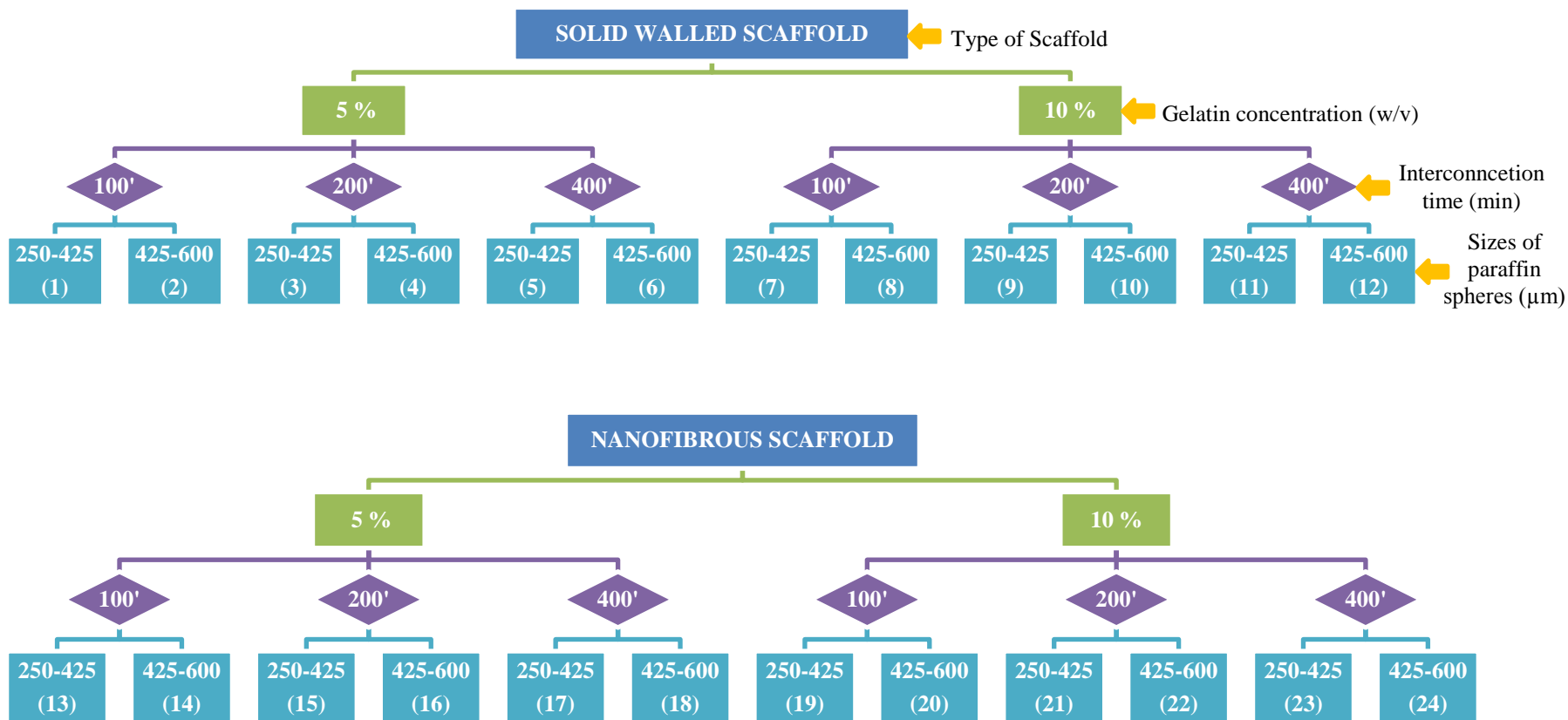


Figure A.1. List of solid walled and nanofibrous scaffolds prepared to determine optimum preparation conditions.

Table A.1. Compressive modulus value (kpa) of solid walled gelatin scaffolds.

Code of scaffold	1	2	3	4	5	6	7	8	9	10	11	12
Average compressive modulus (kPa)	3.84	2.94	4.09	3.08	3.42	5.14	7.31	8.37	7.08	4.38	4.36	4.87
Standart Deviation	0.73	0.22	0.09	0.37	0.77	0.86	1.37	0.94	3.29	0.89	0.80	0.26

Table A.2. Compressive modulus value (kpa) of nanofibrous gelatin scaffolds.

Code of scaffold	13	14	15	16	17	18	19	20	21	22	23	24
Average compressive modulus (kPa)	5.40	9.45	8.43	4.60	14.07	3.56	6.75	4.78	9.00	11.79	6.17	5.69
Standart Deviation	2.02	2.53	2.41	0.32	3.82	0.74	0.75	0.33	2.50	1.41	0.40	0.30

APPENDIX B

PROCEDURE FOR COATING CA-ALGINATE MICROSPHERES WITH POLY(L-LYSINE)

1. 1ml of 100 μ g/ml poly(L-lysine) was added onto Ca-alginate microspheres in 15 ml falcon tube.
2. Tubes were shaken for 30 minutes at 300 rpm.
3. Samples were centrifuged at 10,000 rpm for 5 min and supernatant was discharged.
4. 1 ml of 0.1% alginate solution was added to tubes and shaken at 300 rpm for 30 minutes.
5. Samples were centrifuged at 10,000 rpm for 5 min and supernatant was discharged.
6. Pellet was washed with 5 ml of water.
7. 1 ml of 20% CaCl₂ was added onto particles and shaken at 300 rpm for 10 min for crosslinking of alginate.
8. Samples were centrifuged at 10,000 rpm for 5 min and supernatant was discharged.
9. Pellet was washed with 5 ml of water.
10. These steps (step 1 through 9) were repeated until desired number of layers were obtained.

VITA

Melda BÜYÜKÖZ

Education

2014 Philosophy of Doctorate (Ph.D.) İzmir Institute of Technology, Department of Bioengineering

2008 Master of Science (M.Sc.) Kocaeli University, Department of Medical Biology

2004 Bachelor of Science (B.S.) Ege University, Department of Biology

Presentation

Büyüköz M., Erdal E., Altinkaya S.A., Nanofibrous and Oriented Gelatin Scaffolds for Nerve Tissue Engineering, World Conference on Regenerative Medicine, October 23-25, 2013, Leipzig, Germany.